University of South Bohemia

Faculty of Science

Department of Molecular Biology

Master thesis

Functional analysis of Ssc1 and Iba57 proteins in *Trypanosoma brucei*

Tomáš Skalický

Supervisor: Prof. RNDr. Julius Lukeš Csc.

České Budějovice, 2011

Skalický T. (2011). Functional analysis of Ssc1 and Iba57 proteins in *Trypanosoma brucei*. Msc. thesis, in English – 91 p., Faculty of Science, University of South Bohemia, České Budějovice

Annotation:
Aim of this thesis was to shed light on the function(s) of Iba57 and Ssc1 proteins in both life cycle stages of *T. brucei* using RNA interference. Depletion of Ssc1 resulted in severe grow phenotype, decrease in activities of iron-sulphur cluster-containing enzyme aconitase but no increase in oxidative stress sensitivity or accumulation of ROS in mitochondrion. Down regulation of Iba57, specialized maturation factor of aconitase and homoaconitase, lead to depletion of aconitase, destabilization of Isa1 and increased sensitivity to oxidative stress and accumulation of ROS in both stages.

This work was supported by the Grant Agency of the Czech Republic204/09/17 and 206/09/H02, the Ministry of Education of the Czech Republic (2B06129, LC0032 and 6007665801), and the Praemium Academiae award to J.L..

I hereby declare that all the work summarized in this thesis was performed on my own and only using the cited literature.

Prohlašuji, že v souladu s § 47b zákona č. 111/1998 Sb. v platném znění souhlasím se zveřejněním své Magisterské práce, a to v nezkrácené podobě – v úpravě vzniklé vypuštěním vyznačených částí archivovaných Přírodovědeckou fakultou - elektronickou cestou ve veřejně přístupné části databáze STAG provozované Jihočeskou univerzitou v Českých Budějovicích na jejích internetových stránkách.

České Budějovice, April 28, 2010

.....

Tomáš Skalický

Acknowledgements

I would like to express my thanks to Prof. Julius Lukeš for the opportunity to work in his laboratory. I would like to thanks all members of Laboratory of Functional Biology of Protist and Laboratory of Molecular Biology of Protist for their suggestions, help and understanding, also I would like to thanks Zuzana Vávrová for her scientific guidance and invaluable advice, and our technicians Gabriela Ridvanová and Eva Černotíkova, without their work the everyday life in laboratory would be much more difficult.

My special thanks goes to Maruška for her moral support, patience and overall help and finally never enough thanks to my family because without their support I could never achieve in my life what I've achieved.

Content

1 Introduction

1.1 *Trypanosoma brucei*

Trypanosoma brucei is a parasitic protist a member of the order Kinetoplastida. This flagellate causes human African trypanosomiasis (HAT), commonly known as sleeping sickness, and nagana in many wild and domestic animal species. The disease is endemic in some regions of Sub-Saharan Africa, covering 36 African's countries (Barrett et al., 2003).

There are five sub-species of *T. brucei*, which cause different variants of trypanosomiasis. *T. brucei gambiense* causes slow onset chronic trypanosomiasis in humans. It is most common in central and western Africa, where humans are thought to be the primary reservoir. Second sub-specie is *T. brucei rhodesiense* that causes fast onset acute trypanosomiasis in humans. It is most common in southern and eastern Africa, where wild animals and livestock are thought to be the primary reservoir. Another two sub-species *T. equiperdum* and *T. evansi* are responsible for causing serious diseases called dourine and surra in horses, camels and water buffaloes. These two have partially [dyskinetoplastidy (Dk)] or totally [akinetoplastidy (Ak)] lost their kinetoplast DNA (Lai et al., 2008). The last sub-species is *T. brucei brucei* which causes animal African trypanosomiasis, also called nagana (Roberts and Janovy, 2004) is non-infectious for human Due to its susceptibility to lysis by human apolipoprotein L1 (Pays and Vanhollebeke, 2008).

These obligate parasites, except *T. equiperdum* and *T. evansi* that are locked in the bloodstream form and are transmitted mechanically (Brun et al., 1998), have two hosts – an insect vector (Tse-tse fly *Glossina* species) and a mammalian host. Due to large differences between these hosts trypanosome undergoes during its life cycle complex changes in morphology, metabolism and surface proteins (Fig. 1). Main stages are the bloodstream stage in mammalian blood, the procyclic stage in the tse-tse fly midgut and the infectious metacyclic stage in the tse-tse fly salivary glands (Vickerman, 1985). The bloodstream (BS) and procyclic (PS) stages can be easily cultivated in liquid media and together with a range of unique biological features like polycistronic transcription, absence of introns, trans-splicing of nuclear transcripts, RNA editing of mitochondrial transcripts (Lukeš et al., 2005) and massive kinetoplast DNA network composed of circular molecules, make the *Trypanosoma brucei* an excellent model organism for laboratory studies.

As stated above during its life cycle *T. brucei* undergoes complex changes including adaptation of its energy metabolism (Bringaud et al., 2006). When compared to the PS, which has metabolically fully active mitochondrion possessing complete enzymatic machinery for oxidative metabolism, the

mitochondrion of the BS has only minor role in the energy metabolism relying on glycolysis as the main metabolic source of ATP (Tielens and Hellemond, 2009). Mitochondrial electron transport chain and citric acid cycle activities are developmentally regulated in the life cycle of trypanosomes. These pathways involve proteins containing iron-sulfur (Fe–S) clusters such as aconitase, fumarase or respiratory complexes I, II and III.

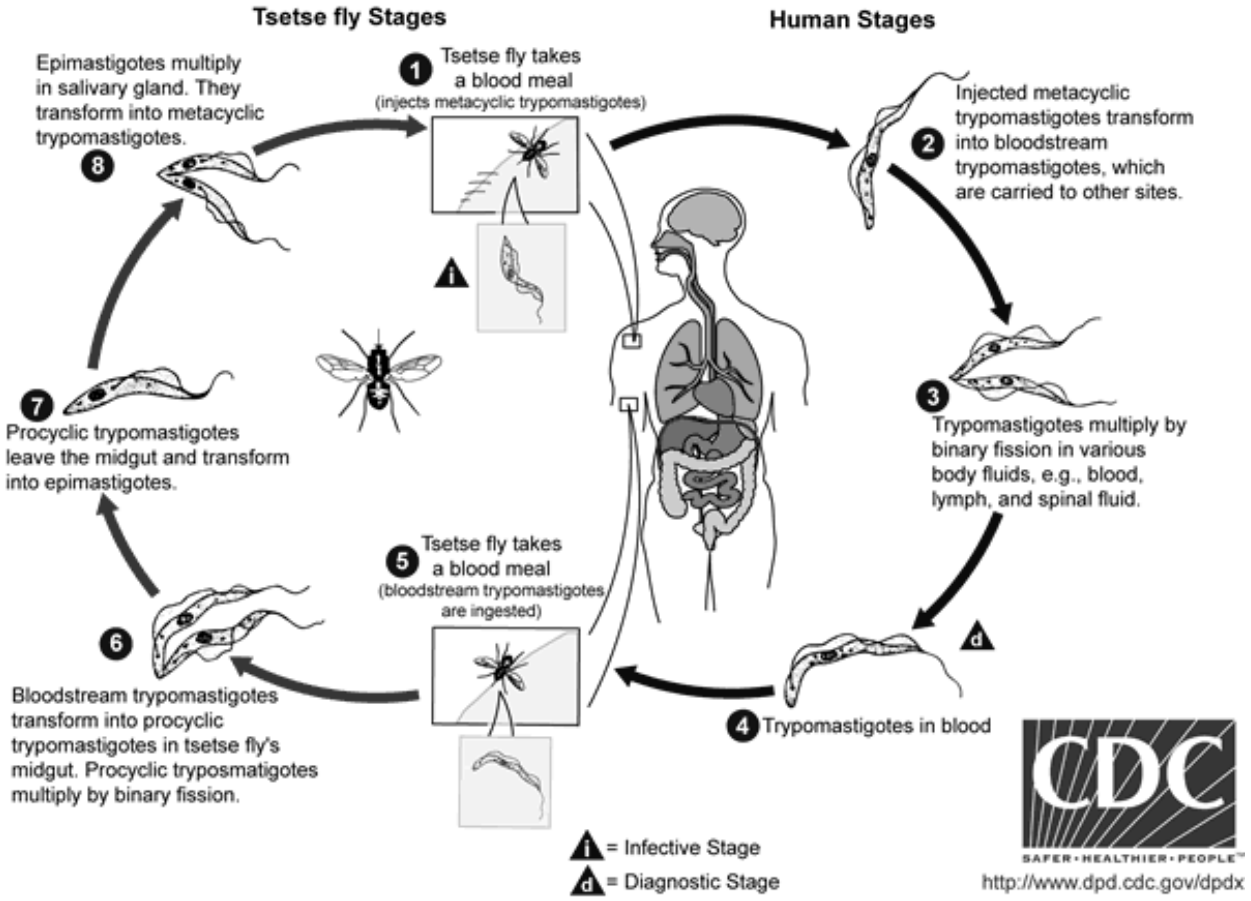

Figure 1: Life cycle of *T. brucei* (taken from http://dpd.cdc.gov/dpdx/HTML/TrypanosomiasisAfrican.htm)

1.2 Fe–S clusters and Fe–S proteins

Iron-sulfur (Fe–S) clusters are small inorganic cofactors, which are thought to be among the earliest catalysts in the evolution of biomolecules (Huber et al., 2003; Wächtershauser et al., 2007). Fe–S clusters are found in all kingdoms of life and are part of many proteins involved in electron transfer, catalysis and regulatory processes.

The chemically simplest Fe–S clusters are the rhombic [2Fe–2S] and the cubic [4Fe–4S] types, that

are composed of ferrous (Fe^{2+}) and/or ferric (Fe^{3+}) iron and sulphide (S^{2-}) ions (Fig. 2). These types of clusters are present in many proteins such as ferredoxin, Rieske Fe-S protein, biotin synthase, respiratory complex III, xanthine dehydrogenase and ferrochelatase, which contain [2Fe–2S] clusters. Aconitase and aconitase-like proteins, sulfite reductase, glutamate dehydrogenase, respiratory complexes I and II, and DNA glycosylase carry [4Fe–4S] clusters (Lill and Mühlenhoff, 2005). Fe–S clusters are usually incorporated into proteins through coordination of the iron ions by cysteine or histidine residues.

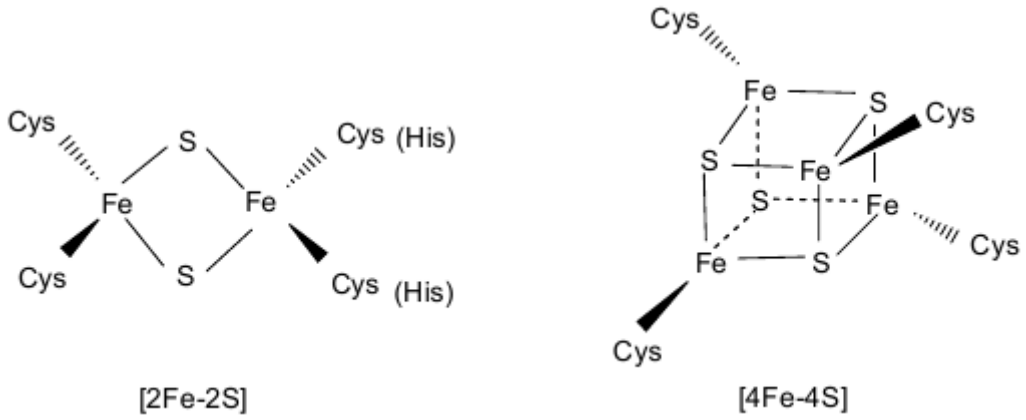

Figure 2: Two most common Fe-S clusters in nature.

The binding motifs for Fe–S clusters in proteins are not highly conserved but some consensus motifs have been recognized, including the $CX_4CX_2CX_{\sim 30}C$ motif in mammalian and plant [2Fe–2S] ferredoxins and the $CX_4CX_2CX_{20\text{-}40}C$ motif, which was originally defined in [4Fe–4S] ferredoxins (Lill and Mühlenhoff, 2008). Many Fe–S clusters are quite labile and can be destroyed under oxidative stress conditions.

1.3 Biogenesis of Fe-S proteins

Fe–S clusters were discovered in the early 1960s by purifying enzymes with characteristic electron paramagnetic resonance signals. In those days it was thought that these cofactors can assemble spontaneously on proteins (Malkin and Rabinowitz, 1966). This view was held until 1990s when it was found that Fe–S protein biogenesis in living cells is a catalyzed process with complex and coordinated reactions. In the past decade numerous biogenesis components were identified and extensive insights into the mechanisms of biogenesis was obtained (Johnson et al., 2005; Balk et al., 2005; Lill and Mühlenhoff, 2006; Vickery et al., 2007; Lil and Mühlenhoff, 2008; Ayala-Castro et

al., 2008; Roulant and Tong, 2008; Xu and Moller, 2008; Fontecave et al., 2008; Bandyopadhay et al., 2008).

Three different systems for the biogenesis of Fe–S proteins have been identified in bacteria; the NIF, ISC and SUF systems. The NIF (nitrogen fixation) system is required for specific maturation of nitrogenase in azototrophic bacterium *Azotobacter vinelandii* (Dos Santos et al., 2004; Rubio and Ludden, 2005); while the ISC (iron-sulfur cluster) assembly and SUF (sulfur mobilization) systems are required for generation of housekeeping Fe-S proteins under normal and oxidative-stress conditions (Zheng et al. 1998; Patzer and Hantke 1999, Takahashi and Tokumoto 2002; Fontecave et al., 2008).

Maturation of cytosolic and nuclear Fe-S proteins in the yeast *Saccharomyces cerevisiae* is dependent on the mitochondrial ISC assembly machinery, mitochondrial ISC export system and cytosolic Fe-S protein assembly pathway (CIA) (Kispal et al., 1999; Lil and Mühlenhoff, 2008). The central role in Fe-S protein maturation provides mitochondria and its ISC assembly machinery (Fig. 3) which was inherited from bacteria in the endosymbiotic event.

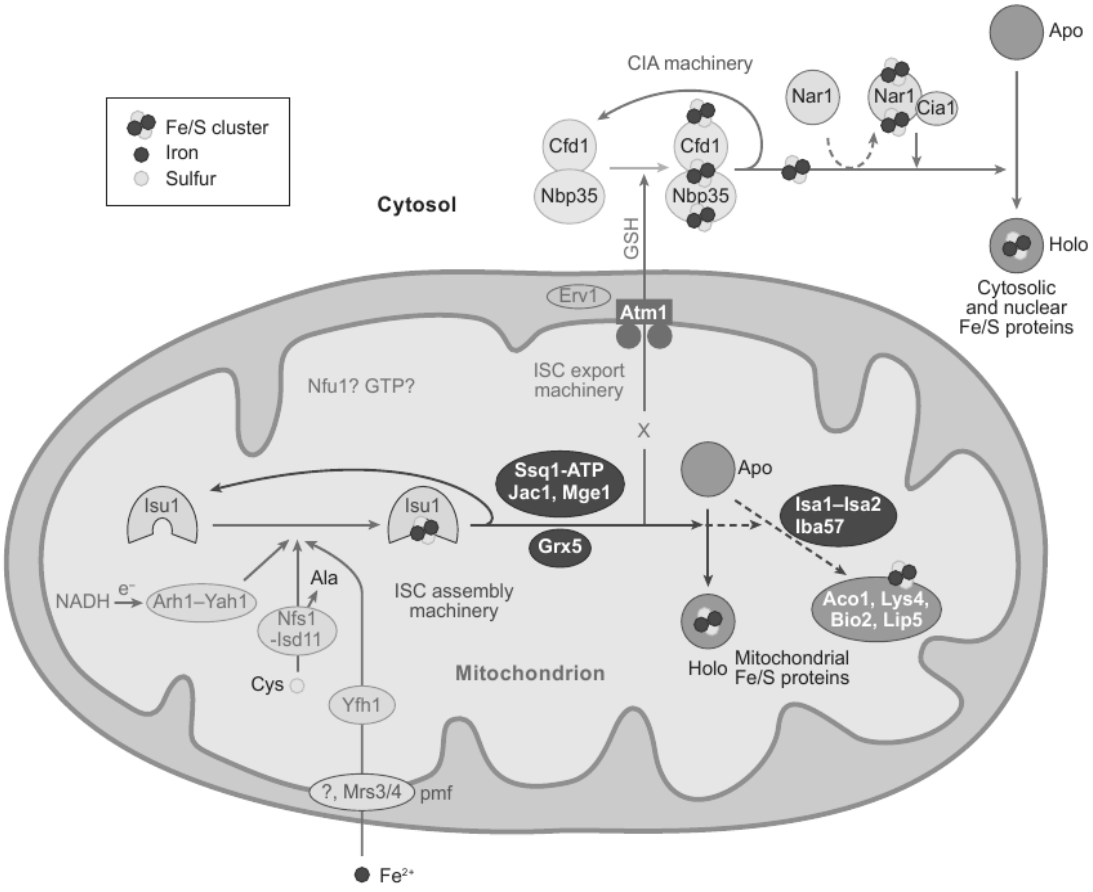

Figure 3: A model for the pathways of Fe-S protein biogenesis. (taken from Lill and Mühlenhoff, 2008)

This Fe-S protein maturation can be divided into two steps (Mühlenhoff et al. 2003; Dutkiewicz et al. 2006): the *de novo* assembly of a Fe-S cluster on the scaffold protein Isu1, and the transfer of the Fe-S cluster from the scaffold to target apoproteins and cofactors.

Sulphur for Fe-S cluster biosynthesis is obtained by the cysteine desulphurase complex Nfs1-Isd11 through conversion of cysteine into alanine (Zheng et al., 1994). Import of iron in to mitochondria from cytosol is most likely done by the inner membrane carriers Mrs3 and Mrs4 and other unknown factors (Lill and Mühlenhoff, 2008), and the delivery of iron to scaffold proteins is performed by the iron-binding protein frataxin Yfh1 (Cook et al., 2006; Long, et al., 2008). Electrons for the Fe-S cluster biogenesis on scaffold protein are provided by ferredoxin reductase Arh1 and ferredoxin Yah1. Fe-S cluster release from Isu1 is achieved by interaction of specialized Hsp70 chaperone Ssq1 (mtHsp70) with Isu1. It should be mentioned that chaperone Ssq1 is present only in some fungi and most eukaryotes have a common mtHsp70 called Ssc1 (Schilke et al., 2006). The DnaJ-like cochaperone Jac1 and the nucleotide exchange factor Mge1 assist the ATP-dependent function of Ssq1. Furthermore, the monothiol glutaredoxin Grx5 is also involved in this second major step. Finally the ISC proteins Isa1, Isa2, and Iba57 are specifically required for the insertion of Fe-S clusters into aconitase-type (Aco1, Lys4) and SAM-dependent (Bio2, Lip5) enzymes. Extramitochondrial Fe-S protein biogenesis requires the core ISC assembly machinery and components of the mitochondrial ISC export machinery (Lill and Mühlenhoff, 2008). After export of the mitochondrially formed Fe-S clusters, further maturation steps take place in the cytosol via the CIA machinery, where Fe-S clusters are transiently assembled on the soluble p-loop NTPase Cfd1 and Nbp32, which form a complex and serve as a scaffold (Netz et al., 2007). After that the Fe-S clusters are transferred to apoproteins by CIA proteins Nar1 and Cia1 (Balk et al., 2005).

1.4 The Iba57 protein

Iba57 is a novel member of the mitochondrial ISC assembly system which belongs to the COG0354 protein family, occurring in all domains of life. It is a specific maturation factor of the Fe-S clusters of aconitase and homoaconitace, and is also needed for the catalytic function of the radical-SAM Fe-S proteins lipoic acid synthase and biotin synthase, which catalyzes the insertion of sulphur into desthiobiotin (Mühlenhoff et al., 2007). Iba57 is localized in the mitochondrial matrix and is required for mitochondrial DNA (mtDNA) maintenance (Gelling et al., 2008). Depletion of Iba57 in *S. cerevisiae* also impairs oxidative stress resistance (Waller et al., 2010). Subsequently, it was shown that Iba57 physically interacts with the ISC proteins Isa1 and Isa2 and forms a complex that

represents the first example of a specialized Fe-S protein maturation system in eukaryotes (Gelling et al., 2008).

1.5 The Ssc1 protein

The Ssc1 protein is a member of chaperon family Hsp70. Molecular chaperons of the 70 kDa family mediate many important cellular processes in prokaryotes and eukaryotes, such as the translocation and prevention of aggregation of proteins (Bukau et al., 2006; Hartl et al., 2002; Mayer et al., 2005). They also promote protein folding and assembly by binding to unfolded or partially folded polypeptide chains. They are highly conserved in amino acid sequence and structure and have two functional domains (Bukau and Horwich, 1998). A highly conserved 44kDa N-terminal domain exhibits ATPase activity (ATPase domain) and is together with a less conserved C-terminal peptide binding domain (PBD) connected by a short hydrophobic interdomain linker. The C-terminal part can be divided into the 18 kDa peptide-binding domain and a small 10 kDa variable domain at the extreme C-terminus. In some types of eukaryotic Hsp70 proteins the variable domain has been shown to act as a binding domain site for co-factors that modulate their activity (Demand et al., 1998; Horton et al., 2001). The tertiary structure of the ATPase domain is similar to that of hexokinase and actin (Flaherty et al., 1990, 1991; Bork et al., 1992) whereas the C-terminal peptide binding domain has a unique ß-sandwich structure followed by extended α-helices (Zhu et al., 1996). The conserved sequence LPPVK near the third conserved cysteine is responsible for stimulation of ATPase activity (Hoff et al., 2003)

The interaction between the two domains is critical for the function of Hsp70s (Buchberger et al., 1994b, 1995). The PBD binds unfolded polypeptides in cooperation with the ATPase domain, which binds and hydrolyzes ATP. In the ATP state the PBD has low affinity for substrates and binds and releases substrates rapidly. Hydrolysis leads to the ADP-bound state of the ATPase domain, in which the PBD adopts a closed conformation and binds substrates with high affinity. The substrate binding to the PBD stimulates the hydrolysis rate of the ATPase domain (Buchberger et al., 1995; Laufen et al., 1999; Mayer et al., 2000; Moro et al., 2003). In the ATP state the interdomain linker binds to a hydrophobic cleft present in the ATPase domain and stimulates the ATPase activity (Swain et al., 2007).

Two types of co-factors stimulate the cellular activity of Hsp70 family members. Members of the J co-chaperone family stimulate the ATPase activity, which leads to more efficient binding; whereas nucleotide exchange factors like Mge1 accelerate the exchange of ADP to ATP, followed by the release of substrates.

The most abundant member of the Hsp70 chaperone family, Ssc1, mediates protein folding in the matrix space and drives translocation of proteins across the mitochondrial inner membrane together with Jac1 and Mge1 (Schilke et al., 1996; Baumann et al., 2000; Matouschek et al., 2000; Strub et al., 2000). These three proteins are well known for their role in the biogenesis of Fe-S cluster proteins, where they transfer the clusters from the scaffold to the target proteins (Dutkiewicz et al., 2004; Schilke et al., 2006). Jac1 interacts with the scaffold Isu protein, targeting it to Hsp70, where its conserved PVK tripeptide binds in the peptide binding cleft of Hsp70. Simultaneously, the J domain of Jac1 (conserved HPD motif) interacts with Hsp70's ATPase domain, stimulating conversion to ADP and stabilizing the Isu:Hsp70 interaction. Subsequently, the Fe-S cluster is transferred to the recipient apoprotein (Schilke et al., 2006) (Fig. 4).

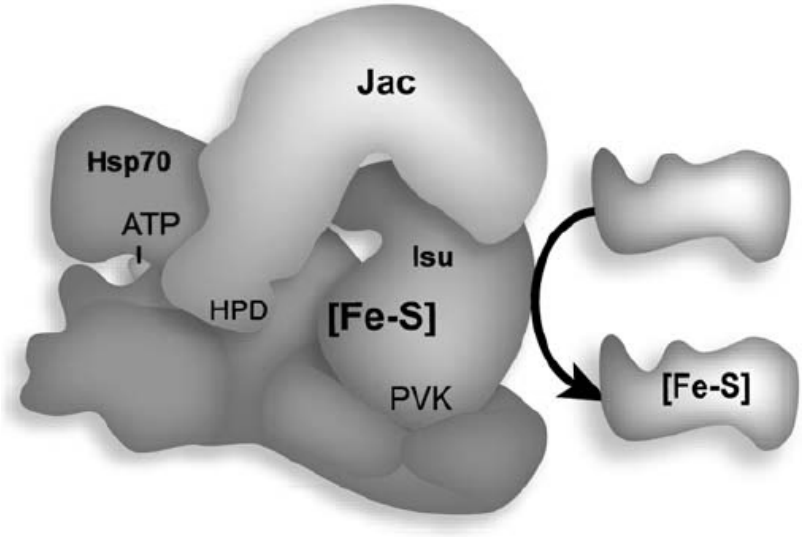

Figure 4: Model of chaperone function in Fe-S cluster biogenesis. (Taken from Schilke *et al.*, 2006)

The Ssc1 chaperon and its nucleotide exchange factor Mge1 are also required for normal import and maturation of nuclear-encoded mitochondrial proteins (Laloraya et al., 1995; Westerman et al., 1995). Mutations of genes encoding these proteins result in decreased activities of mitochondrial proteins containing Fe-S clusters, such as aconitase and succinate dehydrogenase. It also leads to significant increase in mitochondrial iron levels and reduced growth rates (Voisine et al., 2001; Lutz et al., 2001; Schilke et al., 1999). The Ssc1 has one more binding partner, the co-chaperone Hep1 that is required to prevent the aggregation of Ssc1 (Sichting et al., 2005). The Hep1 specifically binds to the ATPase domain and interdomain linker and prevents its aggregation (Blamowska, 2010). In this work, I decided to shed light on the function(s) of Iba57 and Ssc1 in both life cycle stages of *T. brucei*.

2 Materials and methods

2.1 RNAi silencing

2.1.1 Preparation of primers and Polymerase Chain reaction (PCR)

A 447-nt long region of the Iba57 gene and 559-nt long region of the Ssc1 gene were PCR amplified using primers with added HindIII restriction site to the 5'-end of the Iba57 forward (Iba-Fw) primer, BamHI restriction site was added to the reverse (Iba-Rv) primer, XhoI restriction site to the 5'-end of the Ssc1 forward (Ssc-Fw) primer and BamhI site was added to the reverse (Ssc-Rv) primer (Tab.1; sites are underlined).

	Tb927.8.6480 (Iba57)	Tb927.6.3740 (Ssc1)
Fw	CTCGAGATGCGCAAGAAGTTAG	CCTCGAGGATGGCACTGCA
Rv	GGATCCATGAGTACGGTGAGTGAG	CGGATCCCTTTGATTCCGAC

Table 1: Primers for the PCR amplification of the Iba57 and Ssc1 fragment. Underlined are the sequences recognized by restriction endonucleases HindIII, BamHI and XhoI

PCR reaction program

1. denaturation 96°C 5 minutes
2. denaturation 94°C 1 minute
3. primers extension 55°C 1 minute
4. polymerase 72°C 1,5 minutes

(steps 2–4: 30x)

5. polymerase 72°C 10 minutes
6. hold at 4°C

4µl of the PCR product was checked on agarose gel and the rest was cleaned by GenElute PCR clean-up kit (Sigma-Aldrich) according to manufacturer's instruction.

2.1.2 PCR - pGEM cloning and *E. coli* transformation

The pGEM®-T Easy Vector System (Promega) was used according to the manufacturer's instruction (plasmid map in Fig. 5).

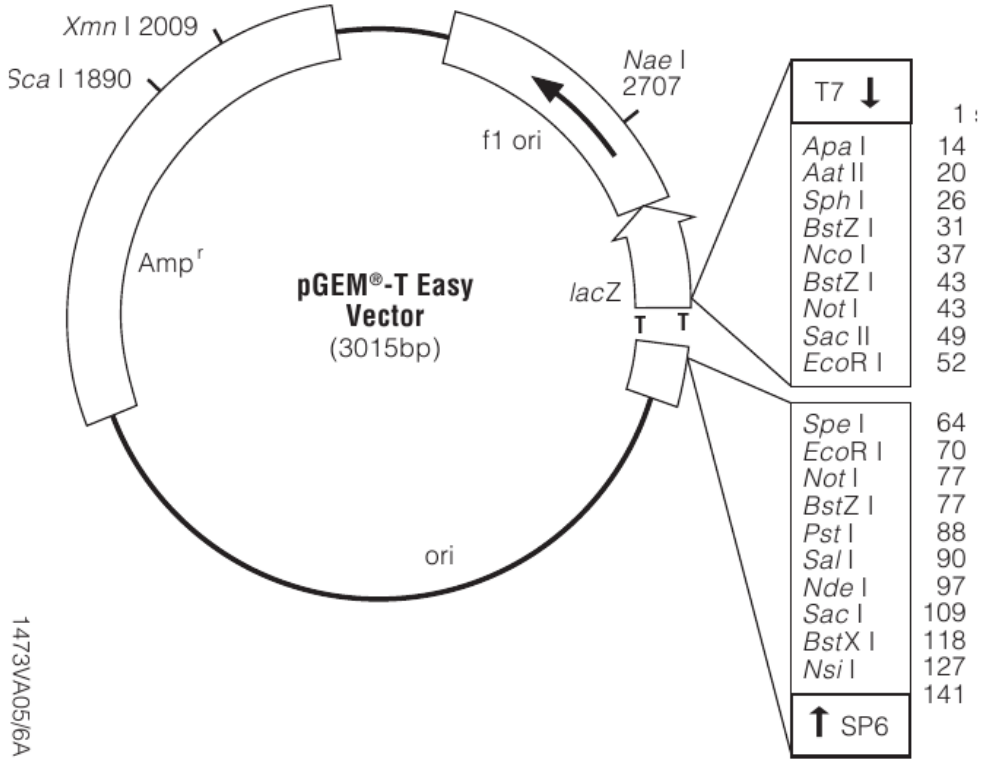

Figure 5: Map of the pGEM®-T Easy Vector System (Promega).

- Transformation of *E. coli* (add 50µl of *E. coli* strain XL1 blue and leave them 5-30 minutes on ice, heat shock 1 minute 42°C, leave 2 min on ice, add 250 µl SOC and shake 1 hour at 37°C)
- Add 4 µl of IPTG (final concentration 0,1 mM) and 40 µl X-gal (final concentration 40mg/ml) to the agarose plates because blue-white selection
- After 16-18 hours of transformed *E. coli* XL1 incubation on agarose plates pick up only white colonies for plasmid isolation
- Verify the cloning by restriction reaction with proper restriction enzymes and separate the fragments on an agarose gel

2.1.3 Gel extraction

Performed according to the QIAquick Gel Extraction Kit (QIAGEN) protocol.

2.1.4 Ligation to p2T7-177 plasmid (Fig. 6) and transformation of *E. coli*

a) Preparation of p2T7-177 plasmid

- Multiplication of circular p2T7-177 plasmid in *E. coli* followed by its isolation by QIAprep Spin Miniprep Kit (QIAGEN) performed according manufacturer's instruction
- Restriction of circular p2T7-177 plasmid with restriction enzymes used above
- Separation of the plasmid fragments on agarose gel and isolation of the proper linear p2T7-177 plasmid from the using the QIAquick Gel Extraction Kit (QIAGEN) protocol

b) Ligation of construct to linear p2T7-177 plasmid

- Mix ligation reaction: 5µl 10x ligation buffer, 1 µl T4 DNA ligase (3 Units/ µl), 2 µl linear P2T7-177 plasmid, 8 µl construct
- Run the ligation reaction at 4°C over night

c) Transformation of *E.coli*

- See step 2.1.2, selection on ampicilin plates

2.1.5 Isolation of plasmid DNA for transfection

This procedure was performed the Midi-prep Kit (QIAGEN) kit according manufacturer's protocol.

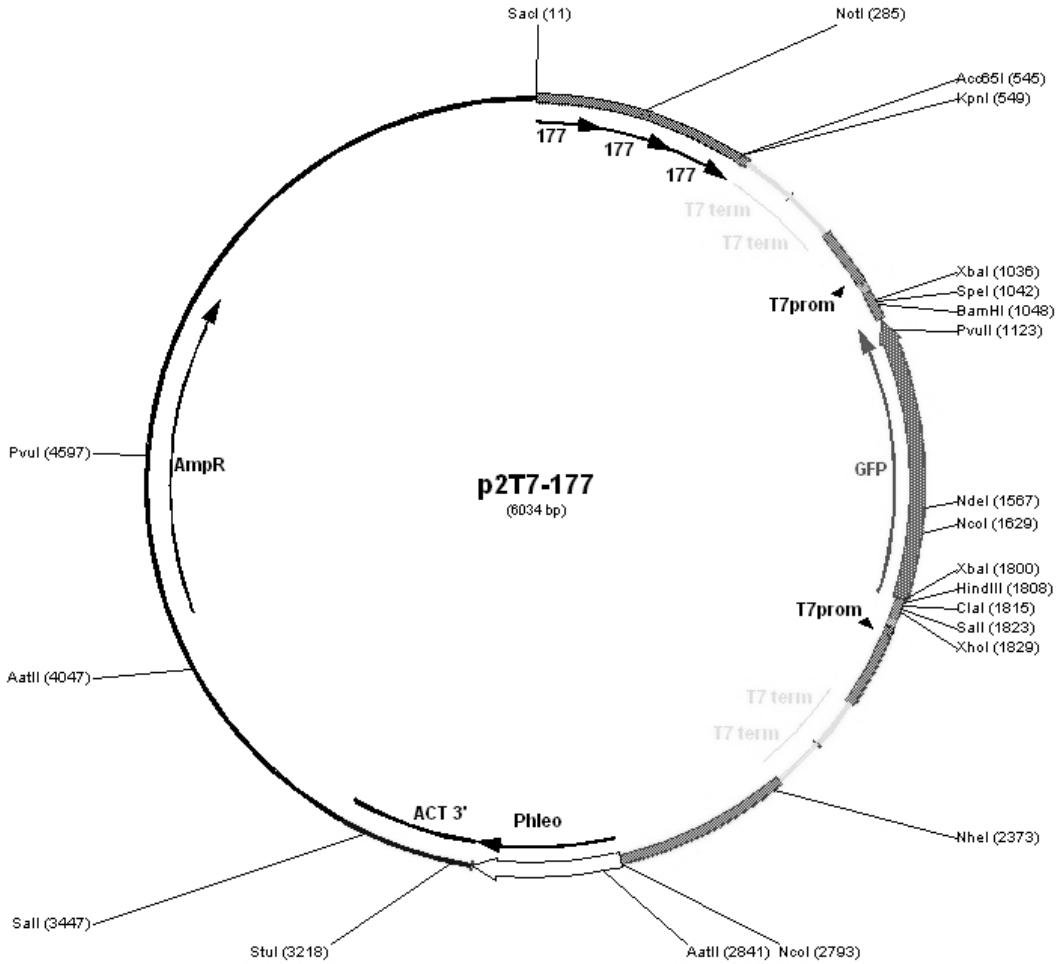

Figure 6: Map of p2T7-177 vector (Wickstead et al., 2002)

2.1.6 Linearise plasmid for transfection

- 20 µg DNA
- 20 µl 10x buffer
- 20 U (units) Enzyme Not I
- Final volume - 100 µl
- Incubate at 37°C for 2 hours
- To isolate the linearized plasmid add ½ volume of phenol and ½ volume of chloroform supplemented with isoamyl alcohol in a ratio (1:20)
- Vortex 1 minute

- Centrifuge at 4°C and 16100 g 10 minutes and take the upper aqueous phase to a new tube
- Precipitate with 1/10 volume Na Acetate and 2.5 X volume Ethanol (100%)
- Incubate at - 80°C for at least 30 min
- Spin down 30 min at 16100 g and 4°C
- Wash with 180µl ice cold 70% ethanol
- Air dry for 10 min in TC hood and resuspend in 50 µl of sterile dH_2O

Cytomix 50 ml:

- 6 ml 1 M KCl
- 6 ml 1 M $CaCl_2$
- 433 µl 1 M K_2HPO_4
- 134 µl 1 M KH_2PO_4
- 1 ml 0,1 M EDTA
- 54 mg glucose
- 250 µl 1 M $MgCl_2$
- 6,25 ml 200 mM HEPES pH= 7,6

2.1.7 Transfection of procyclic *T.brucei*

- Harvest 10 ml of mid-log culture (1 - 2 x 10^7 cells per ml) by centrifugation at 3000 RPM, 10 minutes, 4°C
- Wash the cell pellet once with 10 ml ice cold cytomix buffer
- Resuspend cells in 1 ml of ice cold cytomix
- Load cuvettes (0.2 cm gap) with 10 µg of linearized sterile DNA, cool on ice
- Add 0,5 ml cell suspension to the cuvettes and mix by pipetting up and down
- Electroporate with ECM650 (BTX) machine with two pulses using the followed settings
- BTX settings: 1600 V, 25 Ω, 50 µF

- Resuspend electroporated cells in 5 ml of medium supplemented with hygromycin (H) final concentration 50 mg/ml and G418 (G) to final 15 mg/ml, and incubate for about 18 hours
- Add 2,5 µg/ml phleomycin into flask and then distribute into plate for semi-cloning of transformants by limiting dilution in SDM-79 in 24-well plates
    A. Load the first row of wells with 1.5 ml of your culture
    B. Load the second and third rows with 1 ml fresh SDM-79 (10% FBS, with drug)
    C. Load the third row with 0.5 ml fresh SDM-79 (10% FBS, with drug)
    D. Starting in the fourth column, transfer 0.5 ml of the first well into the second, pipette up and down, transfer 0.5 ml to the third well, and so on (Fig. 7)
- Keep the plate at 27°C until mock transformants are eliminated by phleomycin selection (takes 7-10 days). Don't dilute wells until they are teeming with transfectants. Start with 1:2 dilutions.

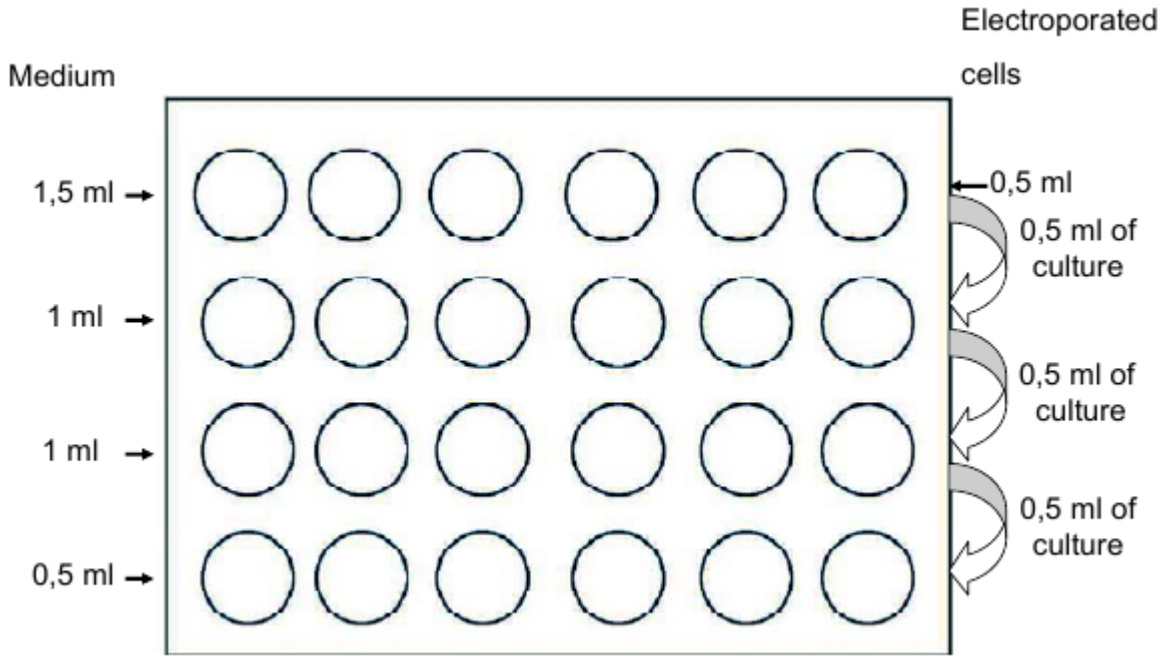

Figure 7: Dilution of electroporated cells (taken from Novotná, 2010)

2.1.8 Transfection of bloodstream *T. brucei*

- Prepare 90 ml HMI-9 medium with appropriate drugs for parental cell growth. Distribute among three falcon tubes as following: 30 ml in Tube A, 27 ml in Tube B and C.
- Harvest 30 million cells by centrifugation at 1 500 RPM for 10 minutes at RT.
- Resuspend in 100 µl amaxa Human T-cell solution at 4°C.
- Add 10 µg of DNA (in 5 µl) to the cuvette, immediately add 100 µl cells, replace the cap of the cuvette and transfect.
- Transfer the entire cell-DNA mixture to Tube A, containing 30 ml of the prepared medium (cell density 10 millions cells/ml). Invert several times to mix well.
- Transfer 3 ml of the cells from Tube A to Tube B. Invert several times to mix well (cell density = 1 million cells/ml). Repeat procedure for Tube C (cell density = 0,1 million cells/ml).
- Distribute 1 ml aliquots of each dilution to three 24-well plates and incubate under 5% CO_2 at 37°C over night.
- Prepare 75 ml HMI-9 medium with the selective drug at double the normal concentration. Aliquot 1 ml to each well of the three 24-well plates.
- Transformed cells are easily seen on the 5^{th} or the 6^{th} day after transfection.

2.2 *T. brucei* cultivation

- Procyclic stage T. brucei are grown in SDM-79 medium (Brun and Schonenberger, 1979) at 27°C

  A. Hygromycin (50 µg/ml), neomycin (G418) (15 µg/ml) - (H, G) for wild type (WT 29-13)

  B. Hygromycin, neomycin, phleomycin (2,5 µg/ml) – (H,G,P) for stable cell line (non-induced cells)

  C. Hygromycin, neomycin, phleomycin, tetracyclin (1 µg/ml) – (H, G, P, tet) for stable cell line (induced cells)

- Bloodstream stage are grown in HMI-9 medium at 37°C and under 5% CO_2
  A. Neomycin and phleomycin (1,25 µg/ml) for stable cell line (non-induced cells)
  B. Neomycin (G418) (2,5 µg/ml) for wild type (WT 427)
  C. Neomycin, phleomycin and tetracyclin (1 µg/ml) for stable cell line (induced cells)
- Density of the culture is measured by the Beckman Coulter Z2 Particle Counter

2.3 Isolation of RNA

- Spin down the cells at 2000 RPM 10 minutes, discard supernatant
- Resuspend cells in 1 ml of RNA Blue and store the cells in -80°C freezer
- Take cells out of -80°C freezer and thaw them on ice, then keep at RT (room temperature) 5 minutes
- Add 200 µl chloroform and vortex 15 sec, keep 2 min at RT to settle down
- Spin 15 minutes at 4°C, 13 200 RPM, suck out upper layer and put into a new tube
- Add 500 µl of isopropanol, vortex 15 sec, keep at RT 10 min to settle down
- Spin 10 minutes at 4°C, 13 200 RPM, discard supernatant
- Add 1 ml ice cold 75% EtOH, spin 10 min at 4°C, 13 200 RPM
- Suck out EtOH, air dry pellet
- Resuspend pellet in 50 µl water (according to pellet size) and keep on ice
- Incubate 10 minutes at 60°C water bath
- Measure concentration of RNA using NanoDrop (Thermo SCIENTIFIC)

2.4 Northern blot analysis

2.4.1 Gel preparation and solutions

Prepare 100 ml, 1% agarose gel in MOPS (Tab. 2) buffer with formaldehyde; Running buffer (Tab. 4) and 1,5x Sample buffer (Tab. 3).

RNA gel (1%) 100ml:

- 10 ml 10x MOPS
- 1 g Agarose
- 72 ml dd H_2O
- After cooling down add 18 ml of formaldehyde

10x MOPS 100 ml	
0,5 M MOPS	40 ml
3 M Sodium Acetate	1,67 ml
0,5 EDTA pH 8	2 ml
miliQ water	53,33 ml
Keep at RT	

Table 2: 10x MOPS preparation

1,5x Sample Buffer	
Formamid	600 µl
Formaldehyde 37%	210 µl
10x MOPS	156 µl
Ethidium bromide	5 µl
Wrap into Aluminium foil and keep at 4°C	

Table 3: 1,5x Sample buffer preparation

Running buffer 500 ml	
10 x MOPS	**55 ml**
miliQ water	**445 ml**
37% formaldehyde	**50 ml**

Table 4: Running buffer preparation

2.4.2 RNA sample preparation

- Take 15 µg of RNA, add appropriate volume of 1,5x Sample buffer to get 1x final concentration
- Incubate 10 min at 65°C water bath
- 3 minutes on ice, add 2 µl of Loading Solution
- Run samples at 90 V, 3 hours, shake buffer every 30 minutes
- Check gel under UV, take picture

2.4.3 RNA blotting

- Assemble blotting apparatus as shown on Fig. 8
- Pour 10x SSC buffer on filter papers and into bath, after each layer get rid of the bubbles by rolling with a glass stick
- Let blot for 24 hours
- Immobilize the RNA on membrane by UV crosslinking (UV Stratalinker, Stratagene)
- Check membrane under UV and mark small arrows according to the ladder, keep wrapped at 4°C

2.4.4 Pre-hybridization

- Pre-incubate the membrane in NaPi (sodium phosphate buffer) in cylinder
- Rotate at 55°C over night

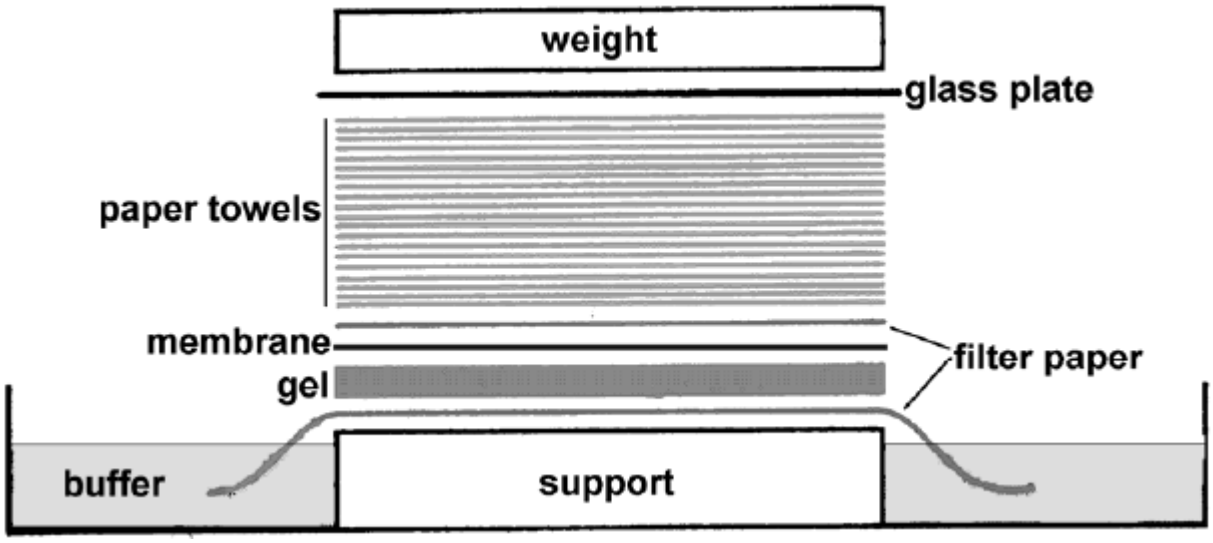

Figure 8: Blotting apparatus (taken from Novotná, 2010)

2.4.5 Radioactive labeling

Labeling by random priming, using the HexaLabel DNA labeling Kit or DecaLabel (MBI Fermentas), according to manufaccturer's protocol using 100 ng (in 20µl MiliQ water) of purified PCR product as a template.

- Purify the probe in spin column (MicroSpin G-50 Sephadex-GE Healthcare) according to the manufacturer's protocol
- Heat the probe at 100°C 3 min, put on ice and then add to 5 ml of NaPi and pour into the cylinder with the pre-hybridized membrane
- Rotate at 60°C O/N

2.4.6 Membrane washing

- Take cylinder with membrane out of 60°C, pour probe into a 50 ml Falcon tube and keep in freezer
- Add 5 ml of 2x SSC buffer + 1% SDS into cylinder and keep moving at RT 20 min
- Pour liquid into radioactive waste container and add 5 ml of 0,2x SSC buffer + 0,1% SDS, keep moving at 55°C for 20 minutes

- Pour liquid into radioactive waste container, place the membrane on a filter paper and measure radioactivity, in case of strong signal repeat the previous step
- Discard washing liquid, take membrane out of the cylinder, wrap into foil and place into phosphoimager cassette, RNA on top, over night
- View in a Typhoon Phosphoimager (Amersham)

2.5 Growth curves

The goal is to monitor a growth of cell cultures upon induction of RNAi to see if RNAi silencing of the target gene results in growth inhibition. For measuring the cell culture was used Beckman Coulter Z2 Particle Counter.

2.5.1 Growth curves for procyclic stage of *T. brucei*

Cells were grown in 10 ml media SDM-79 with appropriate antibiotics and their density was measured every 24 hours using the Beckman Coulter Z2 Particle Counter for 12 days. Starting cell density was $2x10^6$ cells/ml and the cells were diluted every day to the starting concentration $2x10^6$ cells/ml.

2.5.2 Growth curves for bloodstream stage of *T. brucei*

Cells were grown in 10 ml media HMI-9 with appropriate antibiotics and their density was measured every 24 hours using the Beckman Coulter Z2 Particle Counter for 10 days. Starting cell density was $2x10^5$ cells/ml and the cells were diluted every day to the starting concentration $2x10^5$ cells/ml.

2.6 Quantitative real time PCR

This method is very sensitive so it is important to work only with gloves, use only new filtered pipette tips for each manipulation to avoid contamination with foreign DNA, RNases, PCR products etc. Also is very important to pay attention to be precise, use dedicated water and reagents only for qPCR.

2.6.1 Designing primers

Design primers using primer design tool on http://frodo.wi.mit.edu/primer3/input.htm

General rules:

- Shorter amplicons work most efficiently, 80- to 150-bp sequences yielding the most consistent results.
- Do not overlap primer and probe sequences. The optimal primer length is 20 bases.
- Keep the GC content in the 40 to 70% range.
- Avoid runs of identical nucleotides. If repeats are present, there must be fewer than four consecutive G residues.
- Keep the Tm between 58 to 60 °C
- Make sure the last five nucleotides at the 3´ end contain no more than two G and/or C bases.

2.6.2 Cell harvest

- Harvest 10^9 cells at a concentration of 1-2x10^7 cells/ml

2.6.3 DNase treatment of RNA using DNA-free Kit (Ambion)

- Digest 15 µg of RNA in a total of 50 µl reaction volume
- Add 5 µl of 10x buffer and 1 µl DNA-free enzyme
- Incubate for ½ hour at 37 degrees
- Add 0.5 µl DNA-free enzyme
- Incubate for ½ hour at 37 degrees
- Add 5 µl of 10x Inactivation buffer
- Incubate for 2 minutes at RT, flicking tube every 30 seconds
- Centrifuge for 90 second at 10,000x g
- Transfer 44 µl to fresh eppendorf tube (Make sure not to come to close to the inactivation resin)

2.6.4 Precipitation of RNA

Add:

5µl 3M NaOAc

1 µl glycogen

150 µl EtOH

- Mix well
- Incubate at -80°C for 1 hour
- Spin down max speed at 4°C for 30 minutes
- Wash with 1 ml 70% EtOH
- Air dry for no more than 5-10 minutes
- Resuspend in 10 µl MilliQ (prewarmed to 65°C)
- Measure RNA concentration in Nanodrop

2.6.5 cDNA / Reverse Transcription

- Used kits:
  Superscript III Reverse Transcriptase (10,000U) (Invitrogen)
  RNaseOUT™ Recombinant Ribonuclease Inhibitor (5,000U) (Invitrogen)
- The following 20 µl reaction volume can be used for 5 µg of total RNA.
- For the following reactions use the 0.5ml eppendorf tubes used for PCR reactions

Reagent	[Stock]	Dilution	[Final]	Amount	4.5xMM
Random Primers	3µg/ µl	1:12	250ng	1 µl	4.5 µl
Total RNA			~5 µg	4.5 µl	
dNTP Mix, pH 7	10mM each			1 µl	4.5 µl
MilliQ water			13 µl total	6.5 µl	29.25 µl
Total				13 µl each	38.25 µl

Table 5: Reactions preparation for reverse transcription

- Heat mixture to 65°C for 5 minutes and incubate on ice for at least 1 minute
- Collect the contents of the tube by brief centrifugation and add:

Reagent	[Stock]	Amount	4.5xMM
First Strand Buffer	5x	4 µl	18 µl
DTT	0.1M	1 µl	4.5 µl
RNaseOUT rRNase Inhibitor	40U/ul	1 µl	4.5 µl
SuperScript III RT	200U/ul	1 µl	4.5 µl
Total		7 µl each	31,5 µl

Table 6: Reactions for RNase inhibition and reverse transcription

- Mix by pipetting gently up and down
- Incubate tube at 25°C for 5 minutes
- Incubate at 50°C for 60 minutes
- Inactivate the reaction by heating at 70°C for 15 minutes
- Keep sample at 4°C

- Always include a –RT control for each RNA sample, so follow the same protocol for the RT reaction but leave out the RT.
- After the RT reaction, add 180 µl water to the 20 µl RT for a total of 200 µl. A further 1:50 dilution is then done for the high abundance internal controls like β-tubulin and 18S rRNA.

2.6.6 Real-Time PCR

- Used kit: Power SYBR Green PCR Master Mix (Applied Biosystems)
- Label tubes and place into metal rack kept in the fridge upstairs
- Pipet all the PCR reagents in the qPCR room with the provided pipets and filtered tips

Reagent	[Stock]	Amount
Power SYBR Green PCR Master Mix	2x	10 µl
Primer Mix	1.5 µM	8 µl
cDNA Template		2 µl
Total		20 µl

Table 7: Reaction mix for qPCR

Primer	[Stock]	Amount	MilliQ	[Final]	1xRxn	20xMM
For	100 µM	7.5 µl	492.5 µl	10 µM	4 µl	80 µl
Rev	100 µM	7.5 µl	492.5 µl	10 µM	4 µl	80 µl
Total					8 µl	160 µl

Table 8: Primer Master Mix (MM)

- Dilute primers to 10 µM as described above, [Final] = 300 nM each primer
- Make Primer pair master mix for each set of primers
- Add 2 µl cDNA to each appropriate tube
- Add 8 µl of appropriate primer pair to each tube
- Add 10 µl of SYBR Green to each tube
- Beware the SYBR Green MM is soapy, and difficult to pipette accurately
- Pipette up and down 5x to mix thoroughly, be careful not to introduce any bubbles
- Use Rotor-Gene RG300 (Corbett research)

qPCR reaction program:

Reaction Step	Temperature	Time	Comments
	50°C	2 min	
Denaturation	95°C	10 min	required to activate the AmpliTaq Gold® DNA Pol.
Denaturation	95°C	15 sec	X40 cycles
Annealing/Extension	60°C	1 min	

Table 9: qPCR reaction program

Melting curve: control to determine the presence of a single amplicon according to the melting temp

- Heat from 60°C → 95°C, set ramp from 60°C to 95°C
- Rising by 1 degree/ step
- Wait for 45 sec on first step
- Wait for 5 sec for each step afterwards

- Data taken from Rotor Gene Application Software version 6.1 71 were analyzed by Pfaffl method (Pfaffl, 2001) - principle of which is a relative quantification of transcripts based on the relative expression of a target gene versus an unaffected reference gene.
- If using new primers for the first time, it is a good idea to run out 15ul of the amplified DNA from one of each +RT triplicate and its corresponding –RT sample on a 2% agarose gel.

2.6.7 Primers for qPCR

Gene	Forward	Reverse
Iba57	TTGAACCACGTGGACATCAC	CTTTGCGTAGCTCCTTTTCG
Ssc1	GGACGCTGAGAAGGAGAATG	TGCCTTTTGCAGTTTGTCAG
β-tubulin	GCAGAGTCCAACATGAACGA	AGCCGCGACATAGAAAAAGA
18S rRNA	GCGAAACGCCAAGCTAATAC	CGTCCGCGTCTAGTATTGCT

Table 10: Sequences of used primers for qPCR

2.7 Digitonin fractionation

Procedure optimized for procyclic stage of *T. brucei*

2.7.1 Cell harvesting

- Harvest at least $1x10^9$ cells/ ml
- Spin them down for 10 minutes at 3000 RPM, 4°C
- Rinse with cold SHE buffer (1 ml/ 10^8 cells)
- Centrifuge for 10 minutes at 3000 RPM, 4°C
- Remove SHE buffer
- Dilute to $5x10^9$/ ml with cold SHE buffer, keep on ice

2.7.2 Protein quantification (Bradford)

- 2 µl cells + 18 µl HBSS buffer → suspension of cells
- 5 µl suspension of cells + 245 µl water + 1 ml Bradford reagent
- Vortex for few seconds and keep at RT for 10 minutes
- Measure absorbance, determine concentration of proteins

2.7.3 Preparation of cytosolic and mitochondrial fraction

- Cells (1 mg of protein) add 200 µl HBSS buffer and 8 µl digitonin (10 mg/ ml)
- Immediately vortex for few seconds
- Incubate for 5 minutes at RT
- Centrifuge for 2 minutes at 13 000 RPM RT
- Pipette supernatant (Cytosolic fraction) to a new eppendorf tube and keep on ice
- Wash pellet in HBSS buffer
- Totally resuspend in 200 µl HBSS buffer
- Add 0,1% Triton X-100 (2 µl 10% TX-100)
- Incubate for 5 minutes on ice
- Centrifuge for 2 minutes at 13 000 RPM, RT
- Pipette supernatant (Mitochondrial fraction) to a new eppendorf tube and keep on ice

2.7.4 Preparation of whole cell lysate

- Cells (1 mg of protein) add 200 µl HBSS buffer and 2 µl 10% TX-100
- Incubate for 5 minutes on ice
- Centrifuge for 2 minutes at 13 000 RPM, RT
- Pipete supernatant (Total lysate) to a new eppendorf tube and keep on ice

2.7.5 Solutions for digitonin fractionation

HBSS with glucose (1 liter)	
NaCl	7,9999 g
KCl	0,4004 g
$MgSO_4$	0,1997 g
$CaCl_2$	0,1852 g
KH_2PO_4	0,0599 g
Na_2HPO_4	0,1182 g
$NaHCO_3$	0,3503 g
glucose	0,9999 g
MilliQ up to volume 1 liter	
adjust pH to 7,3 and store at RT	

Table 11: HBSS buffer preparation

10% Triton X-100 (50 ml)	
Triton X-100	5 ml
MiliQ water	45 ml
Store at RT	

Table 14: Dilution of Triton X-100

SHE buffer (2 liters)	
Sucrose	171,15 g
HEPES	11,915 g
EDTA	0,7445 g
MiliQ water	Up to volume of 2 liters
Store at 4°C	

Table 12: SHE buffer preparation

Digitonin (1 ml)	
Digitonin	10 mg
MiliQ water	1 ml
dissolve by heating (10 minutes at 96°C)	
Store at -20°C	

Table 13: Preparation of digitonin

2.8 Enzyme activity measurements

Measurements were performed on plate spectrophotometer Tecan S200 (Infinite).

2.8.1 Fumarase activities

- Pipette 5x 235 µl of fumarase buffer (250 mM TrisHcl pH 7.5) into 3 rows and 30 µl of cell lysate obtained by digitonin fractionation (Cyto, Mito and Total fraction) into 96 well UV transparent plate.
- Measure kinetic absorbance at 240 nm.
- Wait until signal is stable because of depletion of residual malate in sample.
- Add 5 µl of malate (1 M L-Malic acid) into each sample and measure fumarase activities at 240 nm.

2.8.2 Aconitase activities

- Pipette 5x 235 µl of aconitase buffer (90 mM TrisHcl pH 7.5) into 3 rows and 20 µl of cell lysate obtained by digitonin fractionation (Cyto, Mito and Total fraction) into 96 well UV transparent plate.
- Add 5 µl of isocitrate (0,5 M L-Isocitric acid trisodium salt) into each sample.
- Measure kinetic absorbance at 240 nm.

2.8.3 Threonine dehydrogenase activities

- Pipette 5x 235 µl of threonine dehydrogenase buffer (0,2 M TrisHcl pH= 8,6 and 0,25 M KCl) into 2 rows in 96 well UV transparent plate.
- Add 50 µl of 0,6 M L-Threonine into wells with buffer
- Add 15 µl of Cytosolic and Total fraction obtained by digitonin fractionation, each to different row.
- Add 5 µl of NAD (50 mg/ ml)
- Measure kinetic absorbance at 340 nm.

2.9 Alamar Blue assay

Alamar Blue, an indicator of metabolic cell function, is used in drug sensitivity assays as a fluorescent and colorimetric dye (Räz et al., 1997). In this particularly assay paraquat is used as a drug producing reactive oxygen species (ROS) inside living cells and thus exposing cells to oxidative stress. Goal of this assay is to monitor if the RNAi silenced cells are more susceptible to oxidative stress.

- Used chemicals:
    A. Resazurine sodium salt (Invitrogen)
    B. Paraquat dichloride PESTENAL® (Sigma-Aldrich)
    C. Pentamidine isethionate salt (Sigma-Aldrich) as a positive control

- Use 96 well plate.
- Prepare Paraquat drug stock at 400 mM and Pentamidine at 100 mM concentration.
- Pipette 10ul of the drug and 40ul of the media into the first well (first column).
- Pipette 50ul of cell media into the rest of the columns.
- Dilute the drug (10ul) across the plate (at the end you will have 10x dilution of the drug in each column)
- Count your cells and adjust the density to a desired concentration (for BS cells: $4x10^5$ cells/ml; for PS cells: $4x10^6$ cells/ml)
- Add 50ul cells to each well. Final concentration of your cells is:
    - BS cells $2x10^5$/ml = $2x10^4$/well
    - PS cells $2x10^6$/ml = $2x10^5$/well
- Incubate cells for 44 hours at the appropriate temperature
- Add 10ul of Resazurine (1.25mg/ 10 ml 1x PBS, pH 7.4, sterilized)
- Incubate for 4 hours and then read fluorescence (Tecan Infinite) using a fluorescence excitation wavelength of 540-570 nm (peak is 570 nm). Read fluorescence emission at 580-610 nm (peak emission is 585 nm).
- Analyze data using GraphPad Prism software using nonlinear regression (curve fit) and sigmoidal dose-response analysis.

2.10 ROS measurement

All measurements were performed on BD FACSCantoII flow cytometer (BD Biosciences)

- Use 24 well plates (4 rows x 6 wells)
- Count your cells and dilute them to a desired concentration ($4x10^6$ cells/ml for PS cells)
- Pipette 2 ml of diluted cells to each well - use different row for each cell line
- To the third and fourth well of each cell line add Paraquat to get final concentration of 40 µM and to the last two wells add Paraquat to get final concentration of 80 µM.
- Incubate cell for 48 hours at the appropriate temperature
- Count your cells and harvest them and centrifuge them at 3000 RPM for 10 minutes
- Resuspend cells in RT medium to get concentration of $5x10^6$ cells/ml.
- Pipette 1 ml of each cell line incubated with or without Paraquat into a new 24 well plates to get quadruplicates of each sample.
- Ad to the wells dihydrorhodamine 123 (DHR) for measuring ROS and Propidium iodide (PI) according to scheme on Figure 9 and incubate for 30 minutes
- Add 5 ml of Hemasol solution (BioPharma) to the cells and pipette 200 µl of each sample to the 96 U-shaped well plates for flow cytometry
- Insert the plate with samples into the High throughput sampler (HTS) in BD FACSCantoII flow cytometer and measure samples
- Export all acquired data as FCS files and evaluate them in FlowJo software, make overlays and statistics
- DHR have the highest excitation in FITC region (560 nm), PI in PE region (470 nm)

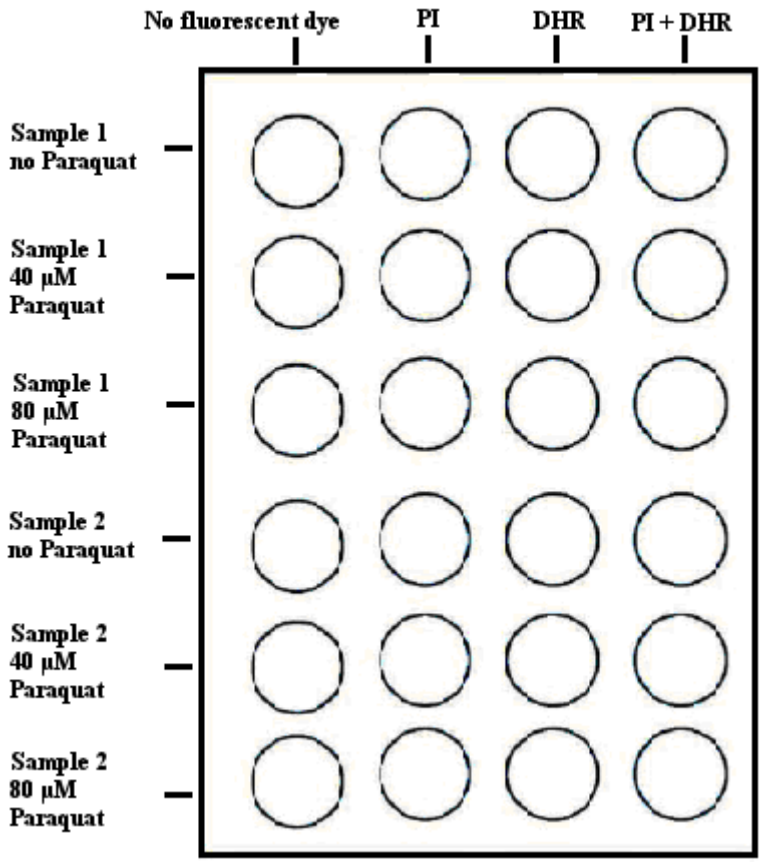

Figure 9: Scheme for applying fluorescent dyes

2.11 Western analysis

- Count the cells
- Centrifuge at 4°C 3000 RPM for 10 minutes
- Resuspend in 2x PBS and lyse by the addition of an equal volume 2 x Sample Buffer (125 mM Tris-HCl, 4% SDS, 20% glycerol, 10% 2-mercaptoethanol, 0.004% bromophenol blue), so that the concentration of the lysate corresponds to 1 x 10^6 cells/µl
- Boil the samples for 10 min at 100°C
- Run 12 µl of the lysate on a 12% SDS-PAGE for 80 minutes at 65 V
- Blot the proteins from gel to PVDF membrane
- Take the membrane to the 1x PBS + 5% milk + 0,04% Tween solution and keep at 4°C over night
- Transfer the membrane to 50 ml Falcon tube, add 5 ml of solution consist of 1x PBS + 5% milk + 0,04% Tween, apply primary antibody in proper concentrations, rotate the Falcon

- Pour out the milk with antibody, wash the membrane with 25 ml of 1xPBS + 0,04% Tween for 5 minutes, repeat five times
- Add 5 ml of a new solution with the same composition as used for primary antibody and apply secondary antibody, rotate for another 1 hour
- Discard the milk and wash the membrane with 25 ml of 1xPBS + 0,04% Tween for 5 minutes, repeat five times
- Use Pierce ECL Western Blotting Substrate (Thermo scientific) for chemiluminescence detection and LAS-3000 luminescent image analyzer (FujiFilm) for taking the picture of membrane

3 Results

3.1 Generation of Iba57 and Ssc1 PS and BS knockdown cell lines

The vector prepared as described in Materials and Methods was transfected into either BS (strain 427) and PS (strain 29-13) cells. After obtaining stable transformants by selection for phleomycin resistance, the cells were induced by tetracyclin (tet +) to a final concentration of 1 μg/ml and collected after four days for Northern blot analysis to verify the induction of dsRNA production and downregulation of Iba57 and Ssc1 mRNA. Non-induced cells (tet-) were grown and processed in parallel as a negative control (Fig. 10).

A

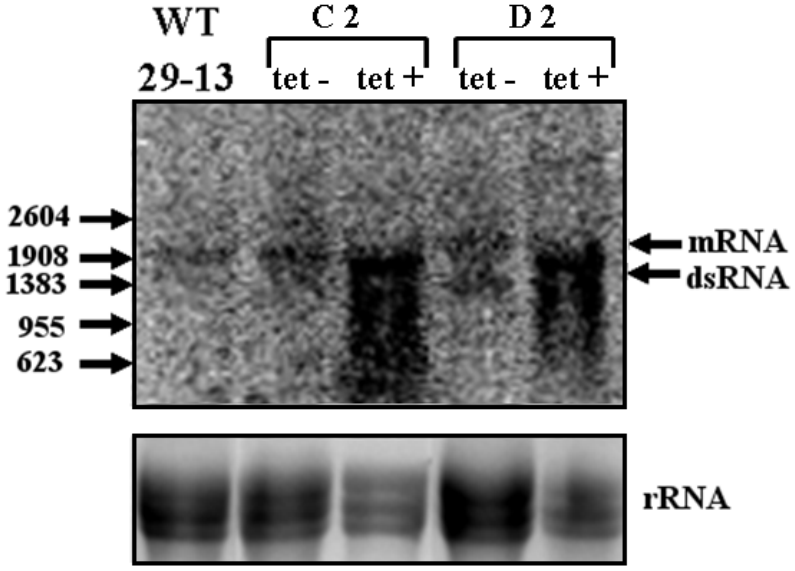

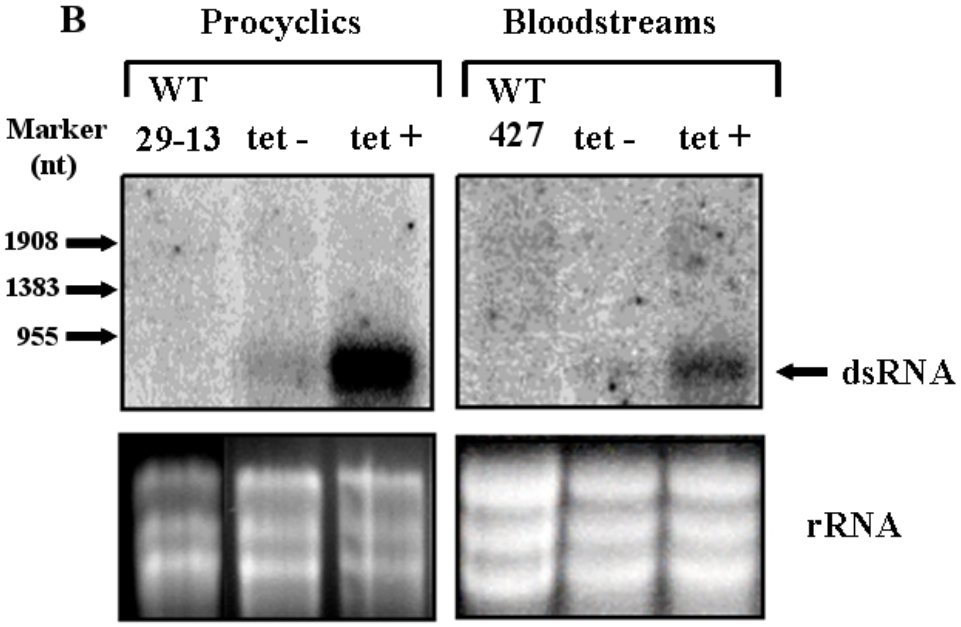

Figure 10: RNAi silencing of Ssc1 and Iba57. A) Cloned Ssc1 PS cell lines C2 and D2. Ssc1 mRNA (predicted size 1974 bp) is present in PS wild-types and non-induced cells (tet-) and the band around 1118 bp in induced cells (tet +) corresponds to the anti-Ssc1 dsRNA, but due to a short time of running the RNA gel the Ssc1 mRNA and the anti-Ssc1 dsRNA are very close. Northern analysis of bloodstream form Ssc1 cell lines was unsuccessful. B) RNAi silencing of PS and BS Iba57 clones. The Iba57 mRNA at predicted size 1020 bp is not visible in both PS and BS non-induced cells (tet-) as well as in PS and BS wild-types. The anti-Iba57 dsRNA band at 894 bp is visible in both PS and BS induced cells (tet+).

3.2 Silencing of Ssc1 and Iba57 in PS and BS

Stable cell lines were grown for 12 days for PS and 10 days for BS in the presence or absence of tetracycline. The growth was measured by density (cells/ml) of the cell culture every 24 hours after tetracycline induction (Fig. 11). Strong inhibition of growth in tet+ cells was observed in both stages of Ssc1 cell lines after 4 days of induction although an escape from RNAi after day 6 post induction occurred. There was a mild inhibition of growth in the PS Iba57 cell line and no inhibition of growth in BS cell line for the same gene (Fig.11).

A

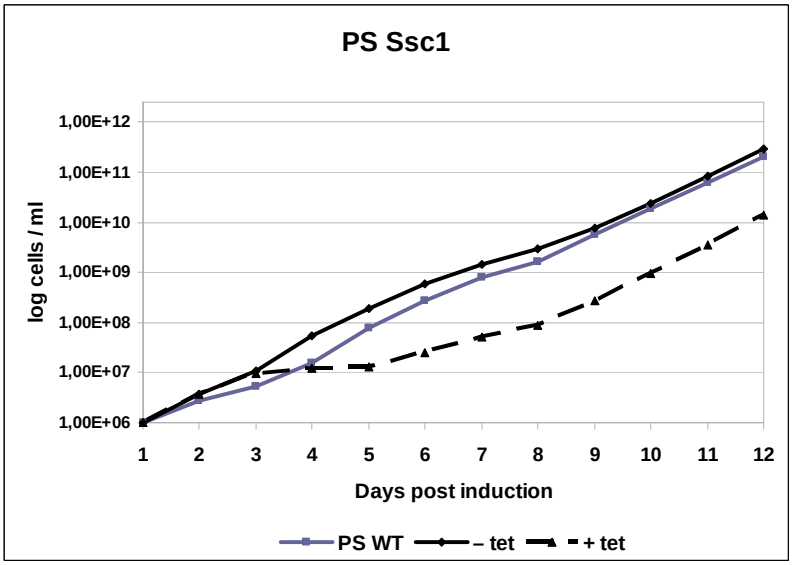
PS Ssc1
log cells / ml
1,00E+12
1,00E+11
1,00E+10
1,00E+09
1,00E+08
1,00E+07
1,00E+06
1 2 3 4 5 6 7 8 9 10 11 12
Days post induction
PS WT
– tet
+ tet

B

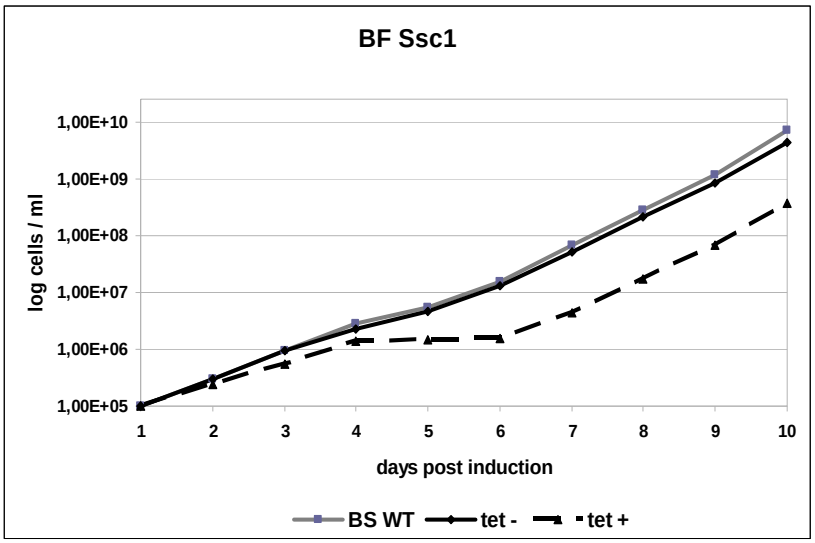
BF Ssc1
log cells / ml
1,00E+10
1,00E+09
1,00E+08
1,00E+07
1,00E+06
1,00E+05
1 2 3 4 5 6 7 8 9 10
days post induction
BS WT
tet -
tet +

C

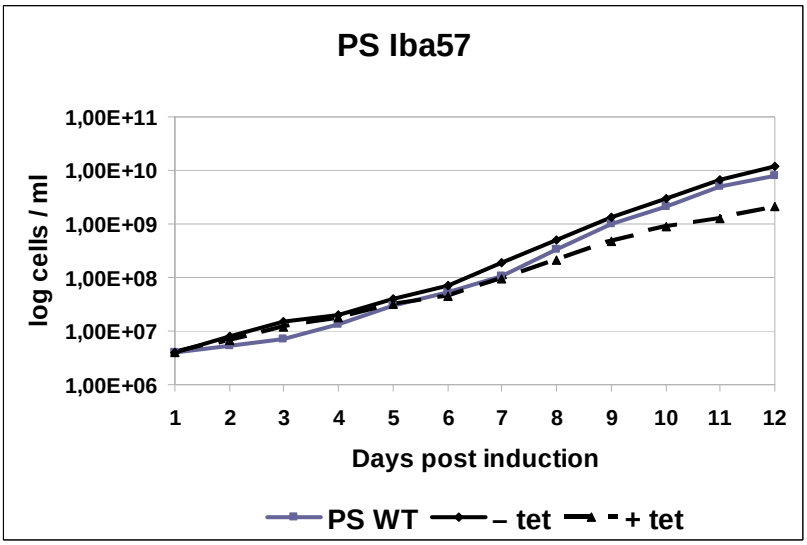
PS Iba57
log cells / ml
1,00E+11
1,00E+10
1,00E+09
1,00E+08
1,00E+07
1,00E+06
1 2 3 4 5 6 7 8 9 10 11 12
Days post induction
PS WT
– tet
+ tet

D

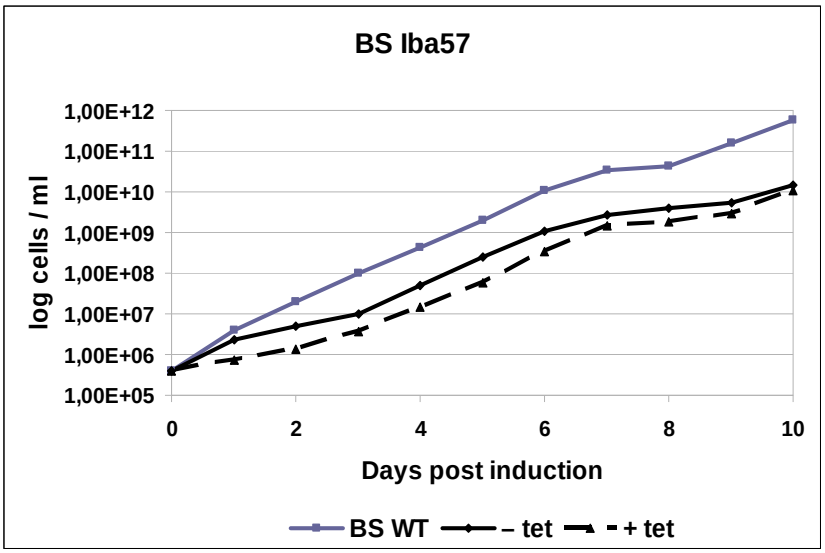

Figure 11: Downregulation of Ssc1 inhibits growth in both stages and Iba57.in procyclic stage. Logarithmic graph plotting the density of non-induced (tet-) and induced (tet+) cells (cells/ml) against days after tetracyclin induction (final concentration of 1µg/ml). Both procyclic stage and bloodstream stage cells were diluted every day, PS to a concentration $4x10^6$ and BS to $4x10^5$ cell/ml.

3.3 Quantitative real-time PCR

The template for qPCR was cDNA generated from the non-induced and RNAi-induced cells of both stages of *T. brucei*. This assay verified the RNAi silencing of Ssc1 and Iba57 in both PS and BS (Ssc1 and Iba57 amplicon, Fig. 12). The data were normalized to the measured level of cytoplasmic 18S rRNA, which it is not affected by RNAi, and calculated using the Pfaffl method (Pfaffl et al., 2001).

A

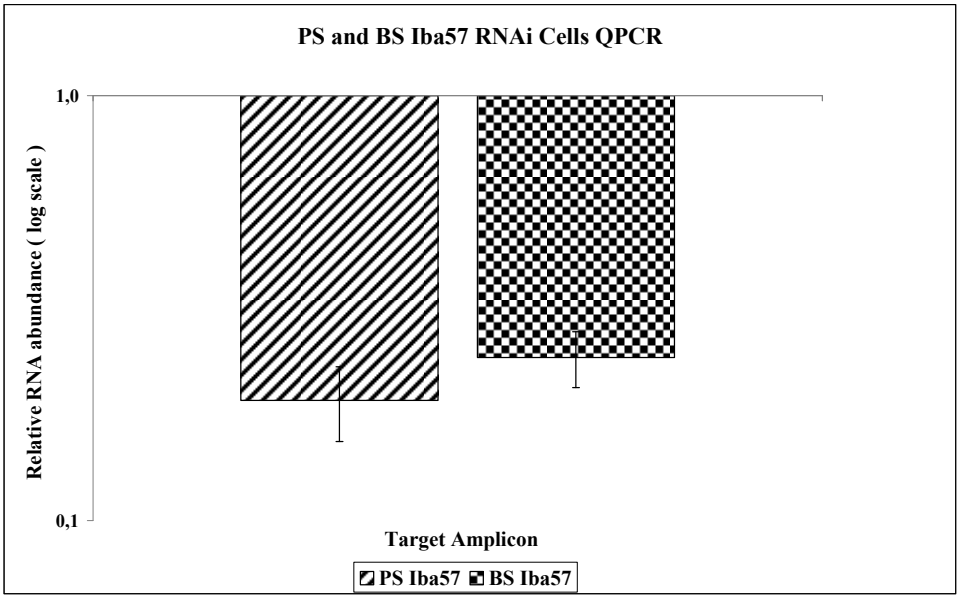

B

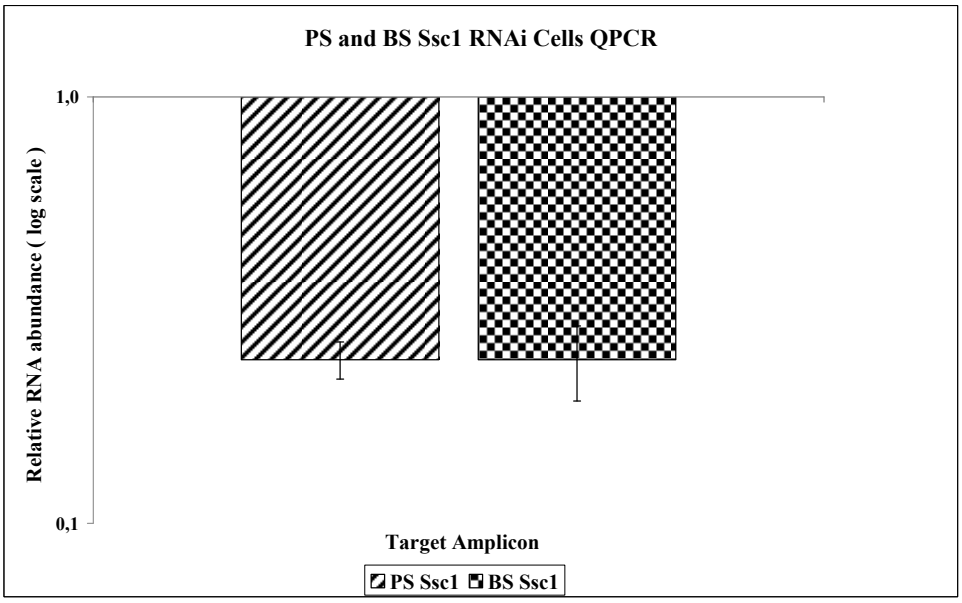

Figure 12: Quantitative real-time PCR analysis performed on knockdowns of Iba57 and Ssc1. The RNA levels from three replicates were normalized to 18s rRNA. The RNA abundance in logarithmic scale shows decrease of measured RNAs after RNAi silencing of A) Iba57 and B) Ssc1.

3.4 Western analysis

Whole cell lysates from induced (tet +) and non-induced (tet-) PS cells of Iba57 and Ssc1 knockdowns were loaded on a SDS-PAGE gel and analyzed by Western analysis with antibodies. A monoclonal antibody against the *T.brucei* mitochondrial hsp70 (Panigrahi et al., 2008) was used on the Ssc1 cell line (Fig. 13 A) with an enolase detected by specific polyclonal antibody serving as a loading control. No antibody against Iba57 but because Isa1 physically interacts with Iba57 in *S. cerevisiae* (Gelling et al., 2008) an anti-Isa1 antibody was used to monitor the presence of Iba57 in *T. brucei* (Fig. 13 B) Antibody recognizing MRP1 (Vondrušková, 2005) was used as a loading control furthermore to test if Iba57 is a special assembly factor for the maturation of aconitase, an aconitase antibody was tested against Iba57 cell line (Fig. 13 C).

A

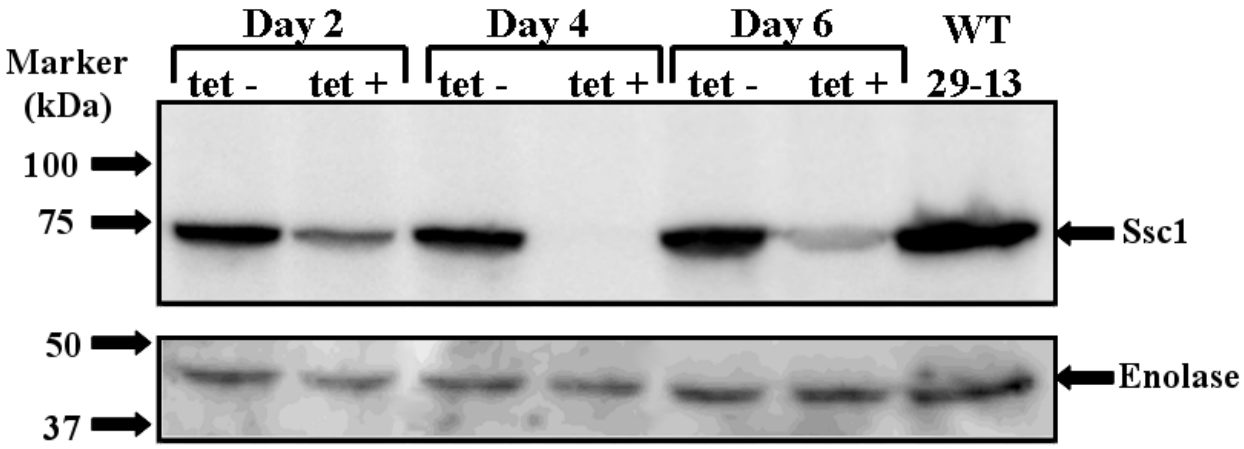

B

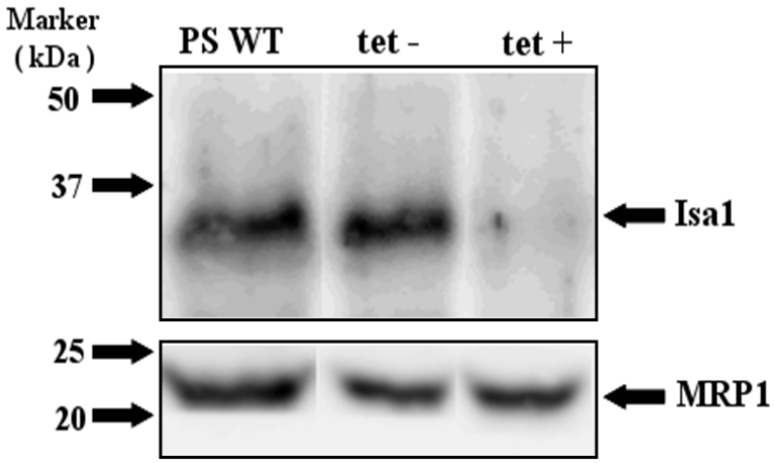

C

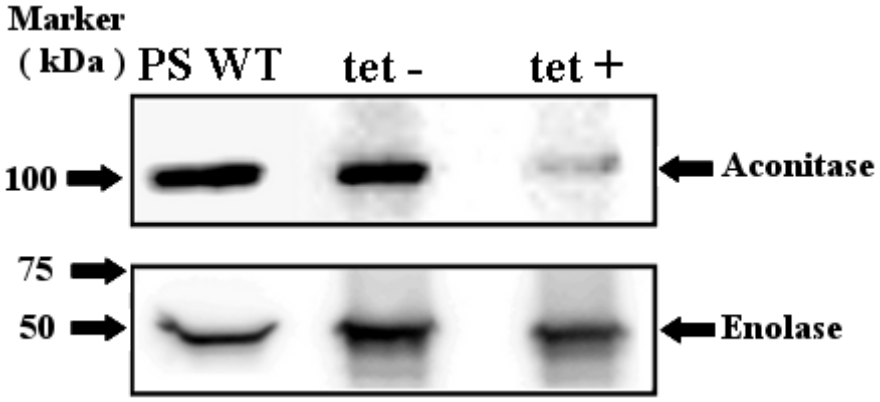

Figure 13: Western analysis of induced (tet+) and non-induced (tet-) Ssc1 and Iba57 knockdowns. A) A monoclonal antibody against mitochondrial hsp70 (~71 kDa) used on Ssc1 knockdowns proved expected depletion of Ssc1. Ssc1 was undetectable on day 4 after induction but reappeared on day 6. B) The antibody against Isa1 (~32 kDa) used on the Iba57 knockdowns confirmed the assumption that depletion of Iba57 also destabilizes Isa1. C) Similar result was also observed with antibody against aconitase (~99 kDa).

3.5 Enzyme activity measurements

Activities of aconitase and fumarase were measured in the mitochondrion and in the cytosol to check if the depletion of Iba57 or Ssc1 has influence on these Fe-S cluster-containing enzymes.

A

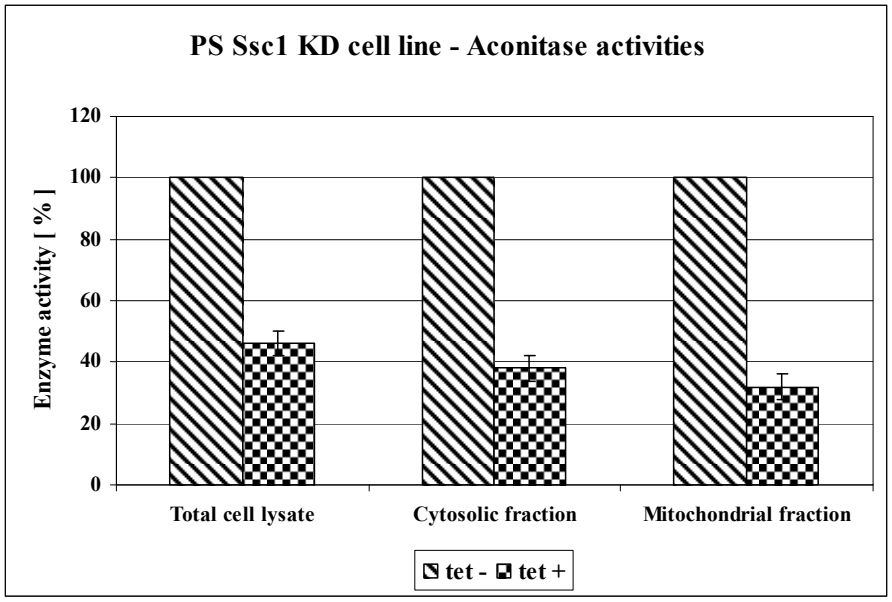

B

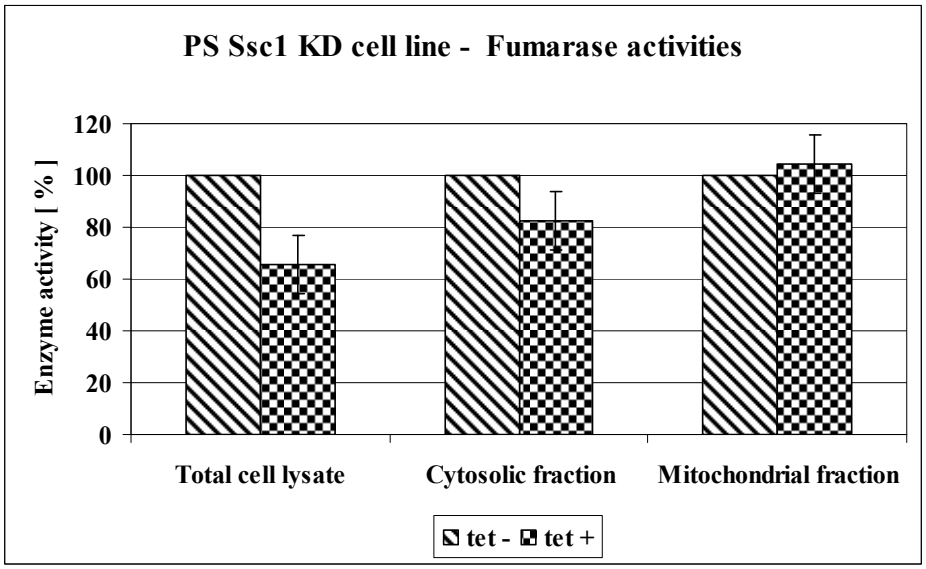

C

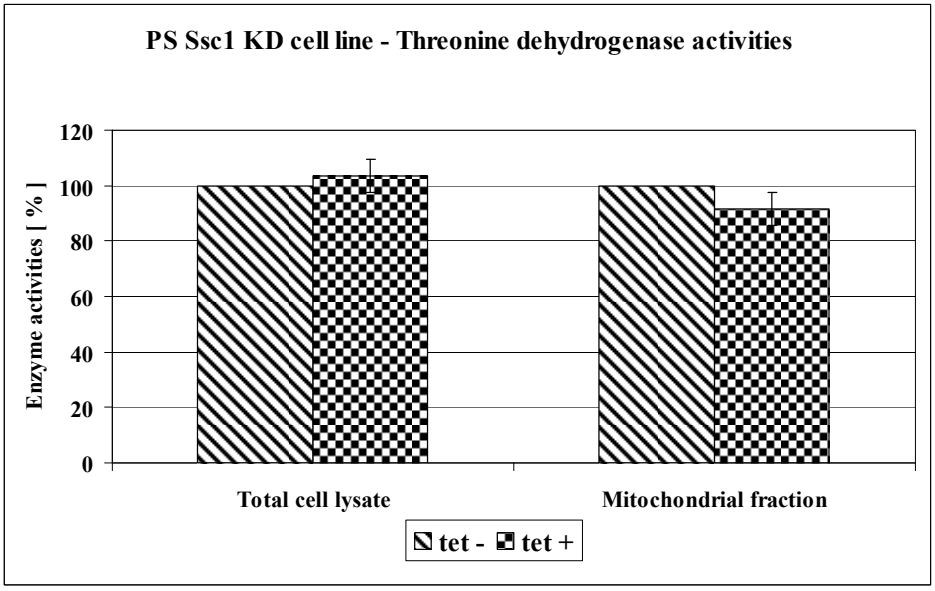

Figure 14: Comparative measurement of enzymatic activities in the Ssc1 cell lines showed that depletion of Ssc1 has severe effect on activity of aconitase (Fig. 14 A) but no effect on fumarase activity (Fig. 14 B). The threonine dehydrogenase activity (Fig 14 C) was used as a control because this protein has no Fe-S clusters. The values shown are the means from three independent measurements.

3.6 Oxidative stress

3.6.1 Alamar blue assay

Ssc1, a member of the chaperone family hsp70, is often upregulated under cell stress to help the cell to deal with any damage. It is also known that Iba57 helps to protect the cells against oxidative stress in *C. cerevisiae* and its depletion impairs resistance against oxidative stress. To test if Iba57 and Ssc1 RNAi cells are more sensitive to stress and oxidative stress in particular, alamar blue assays were performed.

A

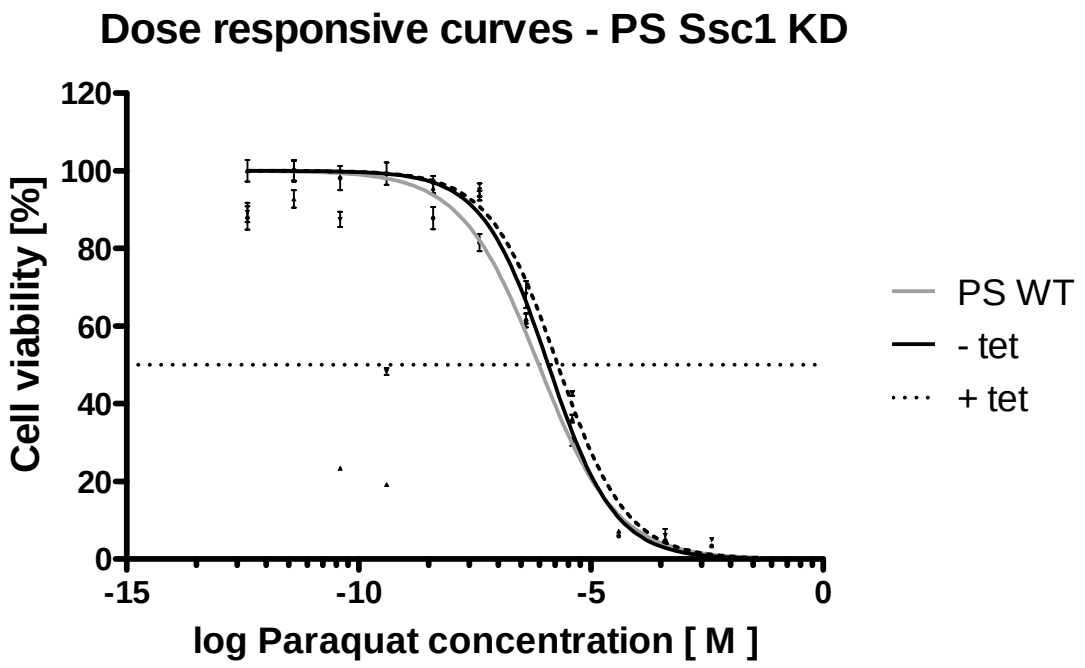

B

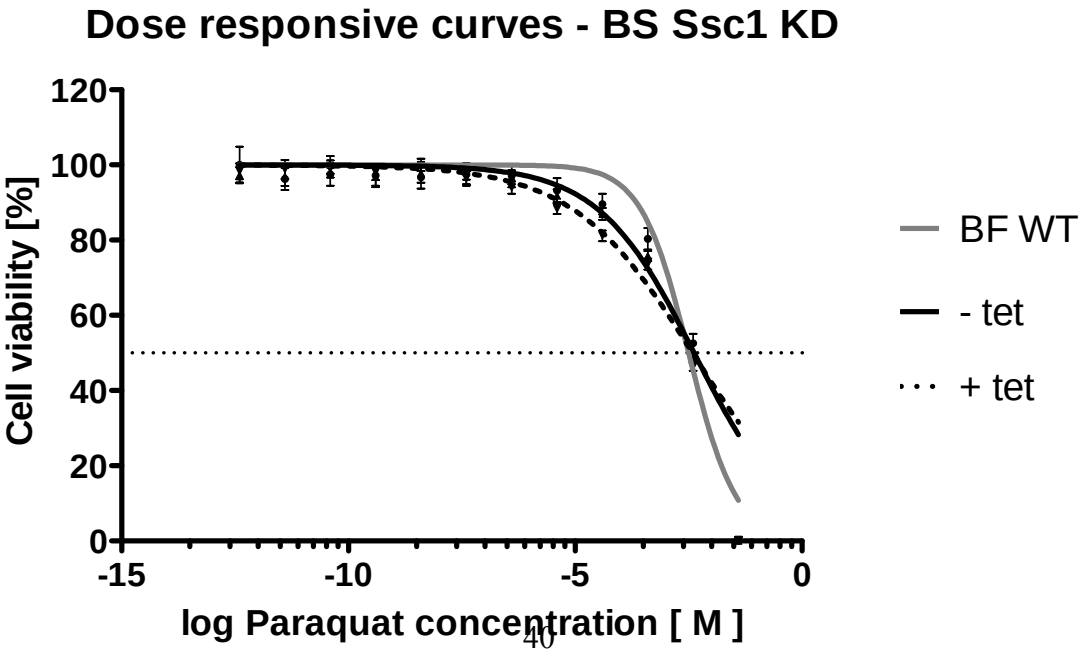

C

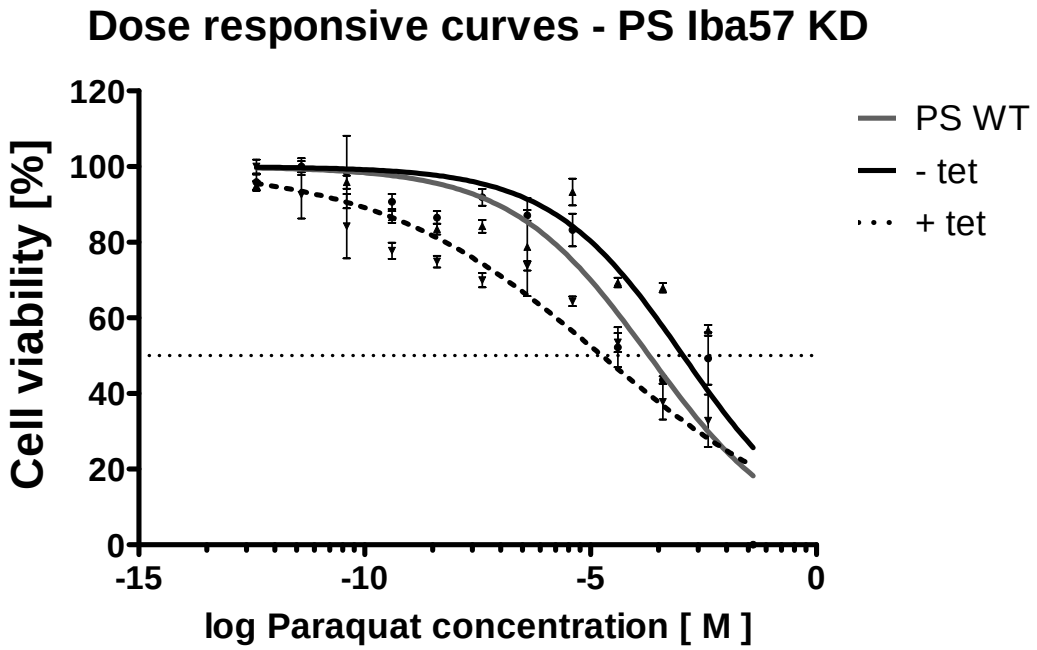

D

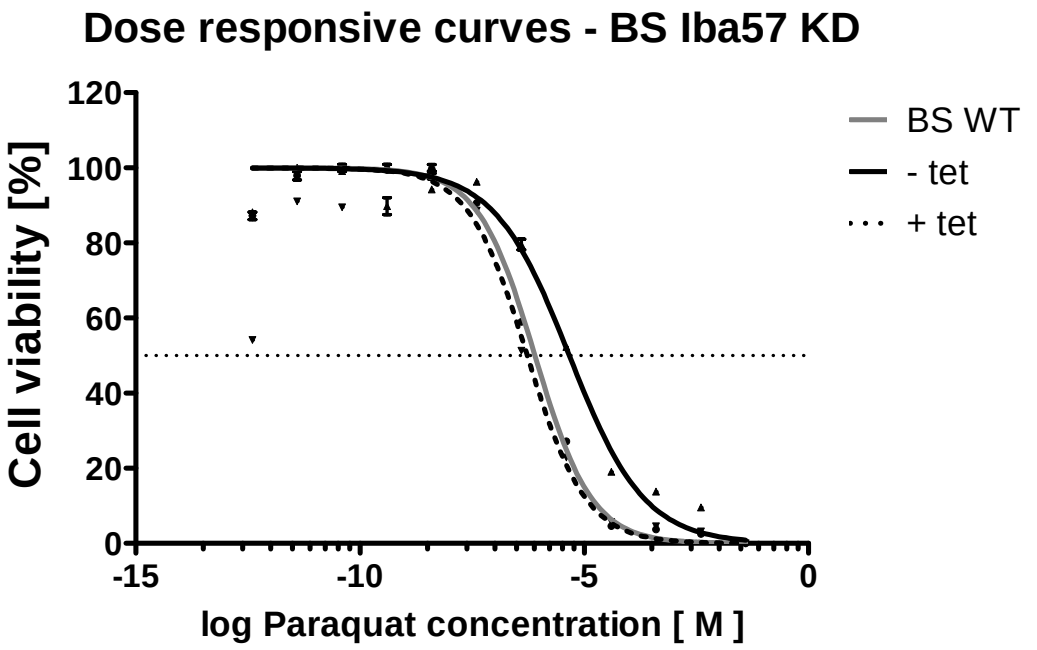

Figure 15: Alamar blue assays, using paraquat as a ROS inducing agent, performed on Ssc1 and Iba57 cell lines in both stages revealed elevated oxidative stress sensitivity in Iba57 RNAi cells and surprisingly no sensitivity alternation in Ssc1 RNAi cells. Non-induced and induced cells from Ssc1 and Iba57 cell line in both stages were exposed to various concentrations of paraquat (in the range from 4^{-10} to 40 mM) for 44 hours starting at the time when the grow phenotype appeared. The

values shown are the means from three independent inductions. A) Depletion of Ssc1 in PS surprisingly showed no increase of oxidative stress sensitivity (EC_{50} for noninduced cells = 1,212 µM and 1,951 µM for induced cells). B) Similar results provided measurements in BS (EC_{50} for noninduced cells = 4,182 mM and 3,869 mM for RNAi-induced cells). C) Down-regulation of Iba57 in PS leads to 62x higher sensitivity to paraquat (EC_{50} for noninduced cells = 1,126 mM and 17,930 µM for induced cells). D) In BS an increase to oxidative stress sensitivity was also observed but it was not as drastic as in PS (EC_{50} for noninduced cells = 3,287 µM and 0,416 µM for induced cells).

3.6.2 ROS measurement

A

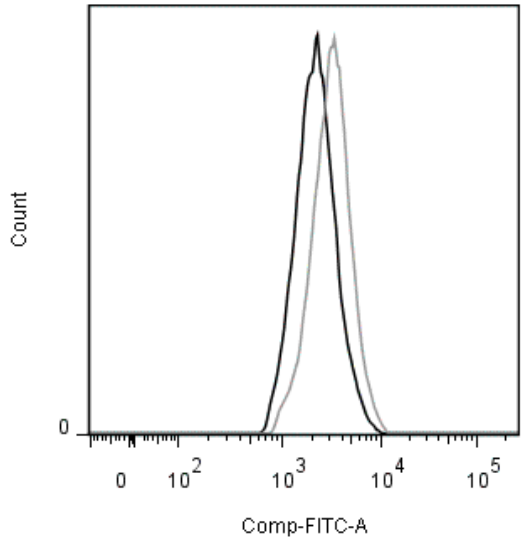

	Sample Name	Median , Comp-FITC-A	Freq. of Total
	PS Iba -tet	2951	93,6%
	PS Iba +tet	2029	93,9%

B

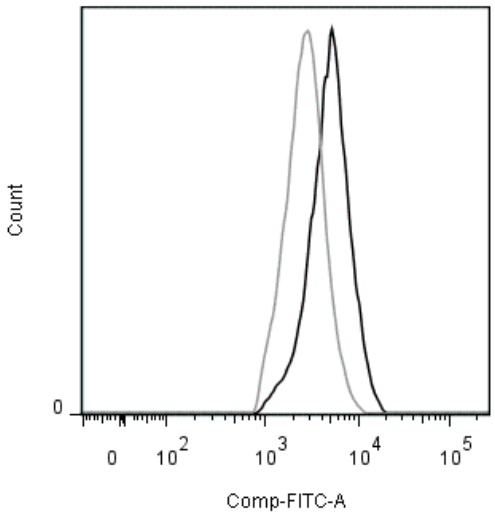

	Sample Name	Median , Comp-FITC-A	Freq. of Total
	PS Iba -tet	2509	91,3%
	PS Iba +tet	4660	95,1%

C

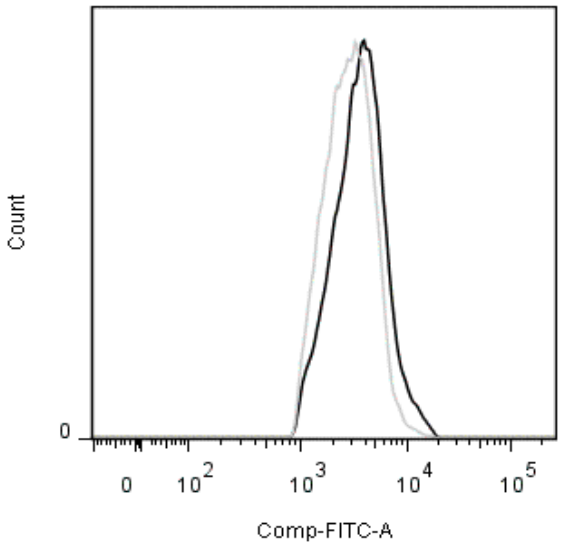

	Sample Name	Median , Comp-FITC-A	Freq. of Total
	PS Ssc -tet	2643	93,6%
	PS Ssc +tet	3369	92,3%

D

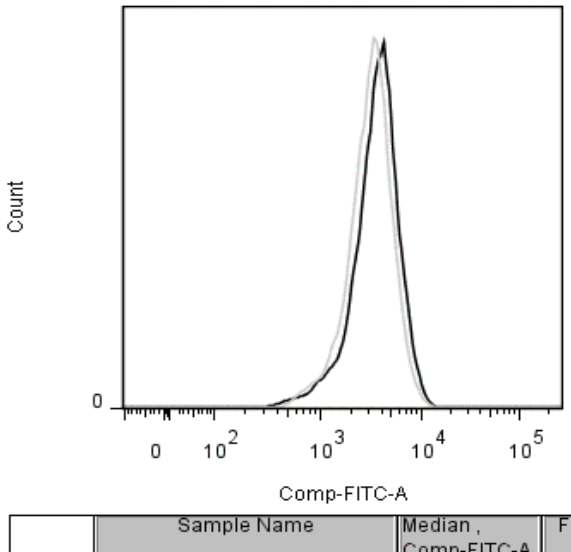

	Sample Name	Median , Comp-FITC-A	Freq. of Total
	PS Ssc1 -tet	3026	94,2%
	PS Ssc1 +tet	3474	96,2%

Figure 16: Reactive oxygen species (ROS) accumulation was measured in Iba57 and Ssc1 cell line cultivated with or without paraquat. A) The PS Iba57 knock-downs 6 days of RNAi induction (black line) grown without paraquat were compared to the respective non-induced cells (grey line). There was no ROS accumulation; RNAi-induced cells even exhibited slightly lower ROS accumulation. B) The PS Iba57 knock-down cells treated the same way but this time grown in presence of paraquat showed accumulation of ROS in RNAi induced cells. C) The PS Ssc1 knock-downs 4 days of RNAi induction grown without paraquat compared to the non-induced cells showed no difference in ROS accumulation. The same picture was observed in cells cultivated with paraquat (Fig. 16 D).

4 Discussion and conclusions

4.1 Iba57

Functional analysis of Iba57 in *T. brucei* was originally engaged as an addition to the study of Isa1 and Isa2 proteins in our laboratory (see Attachment). Iba57, a novel member of the mitochondrial ISC assembly system, is known as a specific maturation factor of the Fe-S clusters of aconitase (Mühlenhoff et al., 2007) that in *S. cerevisiae* physically interacts with the Isa1 and Isa2 proteins (Gelling et al., 2008). Furthermore its involvement in protection against oxidative stress in *E. coli*. was discovered (Waller et al., 2010). I have devoted part of my master thesis to investigation of the function and interactions of Iba57 in both stages of *T. brucei*.

Iba57 was RNAi silenced in the PS and BS stages of *T. brucei* and the RNA from induced and non-induced cells was analyzed by Northern blot analysis. Due to very low level of transcriptions, the down-regulation of Iba57 mRNA in both PS and BS was not clearly visible; however the detected synthesis of dsRNA in the tet-induced cells was indicative of functional RNAi. Moreover, efficient silencing of Iba57 in both stages was subsequently confirmed by real time qPCR.

The putative function of Iba57 implied likely essentiality for both life cycle stages. Growth curves verified mild essentiality with steady growth inhibition in PS but dispensability in BS. I have chosen day six after tet induction for the collection of cells for further analysis. It is known that PS cell have a fully developed mitochondrion, where active Krebs cycle enzymes and a respiratory chain are present while only rudimental mitochondrion is found in BS, which produce all their energy by glycolysis (Hannaert et al., 2003). Because Iba57 is a specific maturation factor of the Fe-S clusters-containing aconitase, an enzyme that is part of the Krebs cycle, differences in interstagial activity of aconitase may be responsible for the non-essentiality of Iba57 for the BS. This conclusion is further supported by functional study of Isa1 and Isa2, which are binding partners of Iba57. Both Isa1 and Isa2 proteins are essential only for the PS cells (see attachment).

Since in *S. cerevisiae* Iba57 physically interacts with Isa1 and Isa2 (Gelling et al., 2008) I have tried to test similar association in *T. brucei*, using western blot analysis of wild type PS and non-induced and RNAi-induced Iba57 knock-downs with a polyclonal antibody against TbIsa1 (see attachment). Indeed, ablation of Iba57 caused destabilization of TbIsa1, providing an indirect evidence of physical interaction of both proteins also in *T. brucei.*

Iba57 is also known as a specific maturation factor of the Fe-S clusters of aconitase and

homoaconitace, as well as for the catalytic function of the radical-SAM Fe-S proteins lipoic acid synthase and biotin synthase (Mühlenhoff et al., 2007). To test if down-regulation of Iba57 in *T. brucei* affects stability of some of these proteins I have performed western blot analysis with polyclonal antibody against aconitase of wild type PS, non-induced and RNAi-induced Iba57 knock-downs. Also in this case I have observed a destabilization of aconitase while the level of control enolase was unaltered. However, only a partial drop of activity of aconitase was measured (data not shown), perhaps caused by only limited decrease of the enzyme in cells depleted for Iba57. To test whether down-regulation of Iba57 impairs oxidative stress resistance as is the case in *E. coli* (Waller et al., 2010) Alamar blue assay using paraquat as oxidative stress inducer was performed. Data obtained from this assays revealed that indeed, down-regulation of Iba57 in PS leads to 62x higher sensitivity to paraquat. In BS an increase to oxidative stress sensitivity was also observed but it was not as drastic as in PS. This suggests that one of the functions of Iba57 serves in *T. brucei* is to protect the cell against oxidative stress.

To prove ROS accumulation in mitochondria, a measurement using flow cytometry and dihydrorhodamine 123 as a ROS visualization agent were conducted. ROS accumulation was measured in the PS cells six days after RNAi induction and two days with or without paraquat. There was no ROS accumulation in cells cultivated without paraquat; induced cells even exhibited slightly lower ROS accumulation. On the other hand the PS Iba57 knock-down cells cultivated in presence of paraquat showed accumulation of ROS upon RNAi-induction. These results together with Alamar blue assays provide clear evidence that in *T. brucei* Iba57 has a role in protection of the cells against oxidative stress.

4.2 Ssc1

The Ssc1 protein, a member of the chaperon Hsp70 family mediates many important cellular functions in all domains of life. Among its main function belongs translocation of proteins across the mitochondrial inner membrane (Schilke et al., 1996; Baumann et al., 2000; Matouschek et al., 2000; Strub et al., 2000), prevention of their aggregation (Bukau et al., 2006; Hartl et al., 2002; Mayer et al., 2005), promotion of protein folding (Bukau and Horwich, 1998) and transfer of Fe-S clusters from the scaffold to the target proteins (Dutkiewicz et al., 2004; Schilke et al., 2006). It is clear that Ssc1 is involved in many cell processes and cannot act alone. For example in Fe-S biogenesis Ssc1 cooperates with the co-chaperone Jac1, the nucleotide release factor Mge1 and the scaffold protein Isu (Schilke et al., 2006). Also the complex structure and function of Ssc1 requires maintenance, likely provided by the chaperone Hep1, without the presence of which Ssc1 has a high tendency to self-aggregation (Sichting et al., 2005).

In our laboratory we already study the function of Mge1 and Hep1 and have found that depletion of these proteins results in severe growth phenotype, strongly indicating their essentiality in *T. brucei* (Týč J., Basu S., Černotíková E., Lukeš J., unpublished data). To better understand what is their function and interactions in *T. brucei* I have investigated the function of Ssc1.

Ssc1 was RNAi silenced in PS and BS cells of *T. brucei* and while by Northern blot analysis the Ssc1 mRNA was visible in the wild type and non-induced cells, its decrease upon RNAi was clearly triggered by the dsRNA. However, Northern blot analysis of the BS failed to detect the target mRNA both in the non-induced and RNAi-induced cells. Possible explanation is that the very low amount of the Ssc1 transcript in this stage was below the detection limit. However, silencing of Ssc1 in both stages was ultimately confirmed by real time qPCR.

Based on the results obtained from Mge1 and Hep1 knock-downs in our laboratory, I expected Ssc1 essentiality in both stages. Indeed, growth curves verified essentiality with massive growth inhibition of both the PS ad BS followed by escape from RNAi after day six of induction. The eventual resistance to RNAi was not surprising; this phenomenon was observed in many cases (Lukeš, personal communication). For further analysis I have chosen day four after tet induction.

To detect the depletion of Ssc1 I have performed western blot analysis on the PS cells using a monoclonal antibody against *T. brucei* mitochondrial Hsp70 kindly provided by Alena Zíková (Panigrahi et al., 2008). I have used RNAi-induced cells from several time points to follow the dynamics of the Ssc1 protein. Efficient RNAi was confirmed by complete disappearance of the

Ssc1 protein on day four after induction followed by its reappearance on day six, which is in nice correlation with the grow curves.

It is known that depletion of Ssc1 results in a decrease of the activities of mitochondrial proteins containing Fe-S clusters, such as aconitase and succinate dehydrogenase (Voisine et al., 2001; Lutz et al., 2001; Schilke et al., 1999). To test whether similar mechanisms are at play in *T. brucei,* I have performed comparative measurements of aconitase and fumarase activities, using non-Fe-S threonine dehydrogenase as a control. As expected, depletion of Ssc1 had a severe effect on aconitase activity of which RNAi-induced cells was much lower than in the non-induced cells. Interestingly, the fumarase activity was not affected, however, with the accuracy of measurement confirmed by unaltered activity of threonine dehydrogenase. From these experiments it can be concluded that in *T. brucei* Ssc1 is required for proper biogenesis in some of these Fe-S clusters.

Hsp70 chaperons are known to be upregulated under stress conditions (Cohen et al., 1991; Zhao et al., 2007). To test if depletion of Ssc1 affects stress sensitivity also in trypanosomes Alamar blue assays using paraquat as ROS producing agent were performed. Data obtained from these experiments did not reveal any significant increase in sensitivity to stress in both the PS and BS cells of *T. brucei*.

In the light of these results I have further tested ROS accumulation in Ssc1 RNAi-induced cells using flow cytometry, with the results being also negative this leads to the conclusion that although essential in both stages, the Ssc1 is not involved in reaction to cell stress, and it is the indispensability of this protein an another presently unknown process that is responsible for the observed lethality of Ssc1-lacking flagellates.

5 Literature

Ayala-Castro C., Saini A., Outten F. W. (2008). Fe-S cluster assembly pathways in bacteria. **Microbiol. Mol. Biol. Rev**. 72:110–125.

Balk J., Aguilar Netz D.J., Tepper K., Pierik A.J., Lill R. (2005). The essential WD40 protein Cia1 is involved in a late step of cytosolic and nuclear iron-sulfur protein assembly. **Mol. Cell. Biol**. 25:10833–41.

Bandyopadhyay S., Chandramouli K., Johnson M. K. (2008) Iron-sulfur cluster biosynthesis. **Biochem. Soc. Trans.** 36:1112–1119.

Barrett M.P., Burchmore R.J., Stich A., Lazzari J.O., Frasch A.C., Lazuli J.J. and Krishna S. (2003). The trypanosomiases. **Lancet**. 362:1469-80.

Baumann F., Milisav I., Neupert W., Herrmann J.M. (2000). Ecm10, a novel hsp70 homolog in the mitochondrial matrix of the yeast Saccharomyces cerevisiae. **FEBS Lett**. 487:307-12.

Blamowska M., Sichting M., Mapa K., Mokranjac D., Neupert W., Hell K. (2010). ATPase domain and interdomain linker play a key role in aggregation of mitochondrial Hsp70 chaperone Ssc1**. J Biol Chem.** 285:4423-31.

Bork P., Sander C., Valencia A. (1992). An ATPase domain common to prokaryotic cell cycle proteins, sugar kinases, actin, and hsp70 heat shock proteins. **Proc Natl Acad Sci USA**. 89:7290-4.

Bringaud F., Rivière L., Coustou V. (2006). Energy metabolism of trypanosomatids: adaptation to available carbon sources. **Mol. Biochem. Parasitol**. 149:1-9.

Brun R, Hecker H, Lun Z-R (1998) *Trypanosoma evansi* and *T. equiperdum*: distribution, biology, treatment and phylogenetic relationship. **Vet Parasitol** 79:95–107.

Brun R. and Schonenberger M. (1979). Cultivation and in vitro cloning or procyclic culture forms of Trypanosoma brucei in a semi-defined medium. Short communication. **Acta Trop**. 36:289-292.

Buchberger A., Theyssen H., Schröder H., McCarty J.S., Virgallita G., Milkereit P., Reinstein J., Bukau B. (1995). Nucleotide-induced conformational changes in the ATPase and substrate binding domains of the DnaK chaperone provide evidence for interdomain communication. **J. Biol. Chem**. 270:16903-10.

Buchberger A., Valencia A., McMacken R., Sander C., Bukau B. (1994). The chaperone function of DnaK requires the coupling of ATPase activity with substrate binding through residue E171. **EMBO J.** 13:1687-95.

Bukau B., orwich A.L. (1998). The Hsp70 and Hsp60 chaperone machines. **Cell**. 92:351-66.

Bukau B., Weissman J., Horwich A. (2006). Molecular chaperons and protein quality control. **Cell**. 125:43-51.

Cohen D.M., Wasserman J.C., Gullans S.R. (1991). Immediate early gene and HSP70 expression

in hyperosmotic stress in MDCK cells. **Am J Physiol**. 261:C594-601.

Cook J.D., Bencze K.Z., Jankovic A.D., Crater A.K., Busch C.N., Bradley P.B., Stemmler A.J., Spaller M.R., Stemmler T.L., et al. (2006) Monomeric yeast frataxin is an iron binding protein. **Biochemistry** 45:7767–7777.

Demand J., Lüders J., Höhfeld J. (1998). The carboxy-terminal domain of Hsc70 provides binding sites for a distinct set of chaperone cofactors. **Mol. Cell. Biol**. 19:2023-8.

Dos Santos P.C., Dean D.R., Hu Y., Ribbe M.W. (2004). Formation and insertion of the nitrogenase iron-molybdenum cofactor. **Chem. Rev**. 104:1159–73.

Dutkiewicz R., Marszalek J., Schilke B., Craig E.A., Lill R., Mühlenhoff U. (2006). The Hsp70 chaperone Ssq1p is dispensable for iron-sulfur cluster formation on the scaffold protein Isu1p. **J. Biol. Chem.** 281:7801–8.

Dutkiewicz R., Schilke B., Cheng S., Knieszner H., Craig E.A., Marszalek J. (2004). Sequence-specific interaction between mitochondrial Fe-S scaffold protein Isu and Hsp70 Ssq1 is essential for their in vivo function. **J. Biol. Chem**. 279:29167-74.

Flaherty K.M., DeLuca-Flaherty C., McKay D.B. (1990). Three-dimensional structure of the ATPase fragment of a 70K heat-shock cognate protein. **Nature.** 346:623-8.

Flaherty K.M., McKay D.B., Kabsch W., Holmes K.C. (1991). Similarity of the three-dimensional structures of actin and the ATPase fragment of a 70-kDa heat shock cognate protein. **Proc Natl Acad Sci USA**. 88:5041-5.

Fontecave M. and Ollagnier-de-Choudens (2008). Iron-sulfur cluster biogenesis in bacteria: mechanisms of cluster assembly and transfer. **Arch. Biochem. Biophys**. 474:226-237.

Gelling C., Dawes I.W., Richhardt N., Lill R., Mühlenhoff U. (2008). Mitochondrial Iba57p is required for Fe/S cluster formation on aconitase and activation of radical SAM enzymes. **Mol. Cell. Biol.** 28:1851-61.

Hannaert V., Bringaud F., Opperdoes F.R., Michels P.A. (2003). Evolution of energy metabolism and its compartmentation in Kinetoplastida. **Kinetoplastid Biol Dis**. 2:11.

Hartl F.U. and Hayer-Hartl M. (2002). Molecular chaperones in the cytosol: from nascent chain to folded protein. **Science**. 295:182-8.

Hoff K.G., Cupp-Vickery J.R., Vickery L.E. (2003). Contributions of the LPPVK motif of the iron-sulfur template protein IscU to interactions with the Hsc66-Hsc20 chaperone system. **J. Biol. Chem**. 278:37582-9.

Horton L.E., James P, Craig E.A., Hensold J.O. (2001). The yeast hsp70 homologue Ssa is required for translation and interacts with Sis1 and Pab1 on translating ribosomes. **J. Biol. Chem**. 276:14426-33.

Huber C, Eisenreich W, Hecht S, Wächtershauser G. (2003). A possible primordial peptide cycle. **Science** 301:938–40.

Kispal G., Csere P., Prohl C., Lill, R. (1999). The mitochondrial proteins Atm1p and Nfs1p are required for biogenesis of cytosolic Fe/S proteins. **EMBO J**. 18:3981–3989.

Lai D.H., Hashimi H., Lun Z.R., Ayala F.J., Lukes J. (2008). Adaptations of Trypanosoma brucei to gradual loss of kinetoplast DNA: Trypanosoma equiperdum and Trypanosoma evansi are petite mutants of T. brucei. **Proc Natl Acad Sci U S A**. 105:1999-2004.

Laloraya S., Dekker P.J., Voos W., Craig E.A., Pfanner N. (1995). Mitochondrial GrpE modulates the function of matrix Hsp70 in translocation and maturation of preproteins. **Mol. Vell. Biol.** 15:7098-105.

Laufen T, Mayer MP, Beisel C, Klostermeier D, Mogk A, Reinstein J, Bukau B. (1999). Mechanism of regulation of hsp70 chaperones by DnaJ cochaperones. **Proc. Natl. Acad. Sci. USA** 96:5452-7

Lill R. And Mühlenhoff U. (2005). Iron-sulfur-protein biogenesis in eukaryotes. **Trend Biochem. Sci.** 30:133-141.

Lill R. and Mühlenhoff U. (2006). Iron-sulfur protein biogenesis in Eukaryotes: components and mechanisms. **Annu. Rev. Cell. Dev. Biol**. 22:457-486.

Lill R. and Mühlenhoff U. (2008). Maturation of Iron-Sulfur Proteins in Eukaryotes: Mechanisms, Connected Processes, and Diseases**. Annu. Rev. Biochem**. 77:669-700.

Lill R. and Mühlenhoff U. (2008). Maturation of iron-sulfur proteins in eukaryotes: mechanisms, connected processes, and diseases. **Annu. Rev. Biochem**. 77:669–700.

Long S., Vávrová Z., Lukeš J. (2008). The import and function of diatom and plant frataxins in the mitochondrion of Trypanosoma brucei. **Mol. Biochem. Parasitol**. 162:100-104.

Lukeš J., Hashimi H., Zíková A. (2005). Unexplained complexity of the mitochondrial genome and transcriptome in kinetoplastid flagellates. **Curr. Genet**. 48:277-299.

Lutz T., Westermann B., Neupert W., Herrmann J.M. (2001). The mitochondrial proteins Ssq1 and Jac1 are required for the assembly of iron sulfur clusters in mitochondria. **J. Mol. Biol**. 307:815-23.

Malkin R. And Rabinowitz J.C. (1966). The reconstitution of clostridial ferredoxin. **Biochem. Biophys. Res. Commun.** 23:822-827.

Matouschek A., Pfanner N., Voos W. (2000). Protein unfolding by mitochondria. The Hsp70 import motor. **EMBO Rep**. 1:404-10.

Mayer M.P., Bukau B. (2005). Hsp70 chaperones: cellular functions and molecular mechanism. **Cell Mol. Life Sci.** 62:670-84.

Mayer M.P., Rüdiger S., Bukau B. (2000). Molecular basis for interactions of the DnaK chaperone with substrates. **Biol. Chem.** 381:877-85.

Moro F., Fernández V., Muga A. (2003). Interdomain interaction through helices A and B of DnaK peptide binding domain. **FEBS Lett**. 533:119-23.

Mühlenhoff U., Gerber J., Richhardt N., Lill R. (2003). Components involved in assembly and dislocation of iron–sulfur clusters on the scaffold protein Isu1p. **EMBO J.** 22:4815–25.

Mühlenhoff, U., Gerl M. J., Flauger B., Pirner H. M., Balser S., Richhardt N., Lill R., Stolz J. (2007). The Fe/S assembly proteins Isa1 and Isa2 are required for the function but not for the de novo synthesis of the Fe/S clusters of biotin synthase in Saccharomyces cerevisiae. **Eukaryot. Cell.** 6:191–206.

Netz D.J., Pierik A.J., Stümpfig M., Mühlenhoff U., Lill R. (2007). The Cfd1-Nbp35 complex acts as a scaffold for iron-sulfur protein assembly in the yeast cytosol. **Nat. Chem. Biol.** 3:278–86.

Novotná L. (2010). Functional analysis of subunit MRB3010 of the mitochondrial binding complex 1 in Trypanosoma brucei. Master Thesis, Faculty of Science, University of South Bohemia, Czech Republic

Panigrahi A.K., Zíková A., Dalley R.A., Acestor N., Ogata Y., Anupama A., Myler P.J., Stuart K.D. (2008). Mitochondrial complexes in *Trypanosoma brucei*: a novel complex and a unique oxidoreductase complex. **Mol. Cell. Proteomics.** 7:534-45.

Panigrahi AK, Zíková A, Dalley RA, Acestor N, Ogata Y, Anupama A, Myler PJ, Stuart KD (2008). Mitochondrial complexes in Trypanosoma brucei: a novel complex and a unique oxidoreductase complex. **Mol. Cell. Proteomics**. 3:534-45.

Patzer S. and Hantke K. (1999). SufS is a NifS-like protein, and SufD is necessary for stability of the [2FE-2S] FhuF protein in Escherichia coli**. J.Bacteriol**. 181:3307-09.

Pays E. and Vanhollebeke B. (2008). Mutual self-defense: the Trypanolytic factor story. **Microbes Infect.** 10:985-9.

Pfaffl M.W. (2001). A new mathematical model for relative quantification in real-time RT-PCR. **Nucleic Acids Res**. 29:45.

Räz B., Iten M., Grether-Bühler Y., Kaminsky R., Brun R. (1997). The Alamar Blue assay to determine drug sensitivity od African trypanosomes (T.b. rhodesiense and T.b. gambiense) in vitro. **Acta Trop.** 68:139-147.

Roberts L. and Janovy J. (2004). Foundations of Parasitology, Seventh Edition. McGraw-Hill New York, USA.

Rouault T. A. and Tong W. H. (2008). Iron-sulfur cluster biogenesis and human disease. **Trends Genet**. 24:398–407.

Rubio L.M., Ludden P.W. (2005). Maturation of nitrogenase: a biochemical puzzle. **J. Bacteriol.** 187:405–14.

Schilke B., Forster J., Davis J., James P., Walter W., Laloraya S., Johnson J., Miao B., Craig E. (1996). The cold sensitivity of a mutant of Saccharomyces cerevisiae lacking a mitochondrial heat shock protein 70 is suppressed by loss of mitochondrial DNA. J. **Cell. Biol**. 134:603-13.

Schilke B., Voisine C., Beinert H., Craig E. (1999). Evidence for a conserved system for iron metabolism in the mitochondria of Saccharomyces cerevisiae. Proc**. Natl. Acad. Sci. USA** 96:10206-11

Schilke B., Williams B., Knieszner H., Pukszta S., D'Silva P., Craig E.A., Marszalek J. (2006). Evolution of mitochondrial chaperones utilized in Fe-S cluster biogenesis. **Curr. Biol**. 16:1660–65.

Schilke B., Williams B., Knieszner H., Pukszta S., D'Silva P., Craig E.A., Marszalek J. (2006). Evolution of mitochondrial chaperones utilized in Fe-S cluster biogenesis. **Curr. Biol**. 16:1660-5

Sichting M., Mokranjac D., Azem A., Neupert W., Hell K. (2005) Maintenance of structure and function of mitochondrial Hsp70 chaperones requires the chaperone Hep1. **EMBO J**. 24:1046-56.

Strub A., Lim J.H., Pfanner N., Voos W. (2000). The mitochondrial protein import motor. **Biol. Chem.** 381:943-9.

Swain J.F., Dinler G., Sivendran R., Montgomery D.L., Stotz M., Gierasch L.M. (2007). Hsp70 chaperone ligands control domain association via an allosteric mechanism mediated by the interdomain linker. **Mol. Cell**. 26:27-39.

Takahashi Y., Tokumoto U. (2002). A third bacterial system for the assembly of iron-sulfur clusters with homologs in archaea and plastids. **J. Biol. Chem**. 277:28380–83.

Tielens A.G.M., van Hellemond J.J. (2009). Surprising variety in energy metabolism within Trypanosomatidae. **Trends Parasitol** 25: 482-490.

Vickerman K.(1985). Development cycles and biology of pathogenic trypanosomes. **Med. Bull**. 41: 105-114.

Vickery L. E. and Cupp-Vickery J. R. (2007). Molecular chaperones HscA/Ssq1 and HscB/Jac1 and their roles in iron-sulfur protein maturation. Crit. Rev. Biochem. **Mol. Biol**. 42:95-111.

Voisine C., Cheng Y.C., Ohlson M., Schilke B., Hoff K., Beinert H., Marszalek J., Craig E.A. (2001). Jac1, a mitochondrial J-type chaperone, is involved in the biogenesis of Fe/S clusters in Saccharomyces cerevisiae. **Proc. Natl. Acad. Sci. USA** 98:1483-8.

Vondrusková E, van den Burg J, Zíková A, Ernst NL, Stuart K, Benne R, Lukes J. (2005). RNA interference analyses suggest a transcript-specific regulatory role for mitochondrial RNA-binding proteins MRP1 and MRP2 in RNA editing and other RNA processing in Trypanosoma brucei**. J Biol Chem**. 280:2429-38.

Wächtershauser G. (2007). On the chemistry and evolution of the pioneer organism. **Chem. Biodivers.** 4:584–602.

Waller J.C., Alvarez S., Naponelli V., Lara-Nuñez A., Blaby I.K., Da Silva V., Ziemak M.J., Vickers T.J., Beverley S.M., Edison A.S., Rocca J.R., Gregory J.F. 3rd, de Crécy-Lagard V., Hanson A.D. (2010). A role for tetrahydrofolates in the metabolism of iron-sulfur clusters in all domains of life. **Proc. Natl. Acad. Sci. USA**. 107:10412-7.

Westermann B., Prip-Buus C., Neupert W., Schwarz E. (1995). The role of the GrpE homologue, Mge1p, in mediating protein import and protein folding in mitochondria. **EMBO J**. 14:3452-60.

Wickstead B., Ersfeld K. and Gull K. (2002). Targeting of a tetracycline-inducible expression system to the transcriptionally silent minichromosomes of Trypanosoma brucei. **Mol Biochem Parasitol.** 125:211-6.

Xu X. M. and Moller S. G. (2008). Iron-sulfur cluster biogenesis systems and their crosstalk. **Chem.Bio.Chem**. 9:2355–2362.

Zhao Y., Wang W., Qian L. (2007). Hsp70 may protect cardiomyocytes from stress-induced

injury by inhibiting Fas-mediated apoptosis. **Cell Stress Chaperones**. 12:83-95.

Zheng L., Cash V.L., Flint D.H., Dean D.R. (1998). Assembly of iron-sulfur clusters. Identification of an iscSUA-hscBA-fdx gene cluster from Azotobacter vinelandii. **J. Biol. Chem**. 273:13264–72.

Zheng L., White R.H., Cash V.L., Dean D.R. (1994) Mechanism for the desulfurization of L-cysteine catalyzed by the NifS gene-product. **Biochemistry** 33:4714-20.

Zhu X., Zhao X., Burkholder W.F., Gragerov A., Ogata C.M., Gottesman M.E., Hendrickson W.A. (1996). Structural analysis of substrate binding by the molecular chaperone DnaK. **Science**. 272:1606-14.

6 List of abbreviations

Ak	akinetoplastid
ATP	adenosine triphosphate
BS	bloodstream stage of *T. brucei*
Dk	dyskinetoplastid
dsRNA	double-stranded RNA
etOH	ethanol
FBS	fetal bovine serum
G	neomycin
H	hygromycin
Hsp	heatshock protein
HAT	Human African trypanosomiasis
kDNA	kinetoplast DNA
MM	mastermix
mt	mitochondrial
mtDNA	mitochondrial DNA
nt	nucleotide
P	phleomycin
PBD	peptide binding domain
PCR	polymerase chain reaction
PS	procyclic stage of *T. brucei*
qPCR	quantitative Real-Time PCR
RNAi	RNA interference
RPM	rotate per minute
ROS	reactive oxygen species
RT	reverse transcription

tet	tetracyclin
tet-	non-induced cells
tet+	induced cells
U	unit
WT	wild type

7 Appendix

7.1 Stage-specific requirement for Isa1 and Isa2 proteins in the mitochondrion of Trypanosoma brucei and heterologous rescue by human and Blastocystis orthologues (Long S., Changmai P., Tsaouis A.D., Skalický T., Verner Z., Wen Y., Roger J.R., Lukeš J.)

Stage-specific requirement for Isa1 and Isa2 proteins in the mitochondrion of Trypanosoma brucei and heterologous rescue by human and Blastocystis orthologues

Shaojun Long[1,#], Piya Changmai [1,2], Anastasios D. Tsaousis[3], Tomáš Skalický[1,2], Zdeněk Verner[1,2], Yan-Zi Wen[1,+], Andrew J. Roger[3]

and Julius Lukeš[1,2,*]

[1]*Biology Centre, Institute of Parasitology, Czech Academy of Sciences, České Budějovice (Budweis), Czech Republic;*

[2]*Faculty of Sciences, University of South Bohemia, České Budějovice (Budweis), Czech Republic;*

[3]*Centre for Comparative Genomics and Evolutionary Bioinformatics, Department of Biochemistry and Molecular Biology, Dalhousie University, Halifax, Canada*

Present addresses: [#] Institute for Cell and Molecular Biosciences, Faculty of Medical Science, Newcastle University, U.K.

[+] School of Life Sciences, Sun Yat-Sen (Zhongshan) University, Guangzhou, China

[*]Corresponding author. Mailing address: Biology Centre, Branišovská 31, 37005 České Budějovice, Czech Republic. Phone: (+420) 387775416. Fax: (+420) 385310388. E-mail: jula@paru.cas.cz;

Summary

IscA/Isa proteins were proposed to function as alternative scaffolds for the assembly of Fe-S clusters and/or provide iron for their assembly in both prokaryotes and eukaryotes. Isa are usually non-essential and in most organisms seem to be confined to the mitochondrion. We have studied the function of TbIsa1 and TbIsa2 in *Trypanosoma brucei*, where the requirement for both of these mitochondrial proteins to sustain cell growth depends on the life-cycle stage of this kinetoplastid parasite. The TbIsa proteins are abundant in the procyclic form, which contains an active organelle. Both proteins are indispensable for cell growth, as they are required for the assembly of Fe-S clusters in mitochondrial aconitase, fumarase and succinate dehydrogenase. Free radical oxygen species but not iron accumulate in the procyclic mitochondrion upon ablation of the TbIsa proteins and their depletion does not influence the assembly of Fe-S clusters in cytosolic proteins. Importantly, in the bloodstream form of *T. brucei*, in which the mitochondrion is devoid of respiratory complexes, the TbIsa proteins are non-essential. Depletion of Iba57, an interacting partner of the Isa proteins, resulted in the destabilization of TbIsa1 as well as aconitase, and made the procyclic form sensitive to oxidative stress. The Isa2 orthologue of the anaerobic protistan parasite *Blastocystis* rescued the activities and growth of a TbIsa1/2 double knock-down. Rescues of single knock-downs as well as heterologous rescues with human orthologues recovered the activities of aconitase to varying extents, while the rescues of fumarase were significantly more efficient. These results show that the Isa1 and Isa2 proteins of diverse eukaryotes have overlapping functions.

Introduction

Iron-sulfur (Fe-S) proteins are present in all domains of life. Most of them are essential and it is estimated that in a typical eukaryotic cell over 100 proteins containing Fe-S clusters are involved in electron transport, catalysis, sensing and DNA/RNA metabolism. However, this is likely an underestimate because numerous other Fe-S cluster-dependent functions are continuously being elucidated and more proteins than previously appreciated have been shown to possess the evolutionarily ancient Fe-S cofactors (Fontecave, 2006; Lill, 2009; Lill and Mühlenhoff, 2005).

The current paradigm holds that most, if not all, Fe-S clusters in eukaryotes are synthesized within their mitochondria by the highly conserved iron-sulfur cluster (ISC) assembly machinery that originated from this organelle's prokaryotic endosymbiont ancestor. While a substantial fraction of the clusters formed *de novo* are integrated into organellar proteins, some of them are exported into the cytosol and the nucleus, where they are incorporated into the target proteins via a eukaryote-specific cytosolic Fe-S cluster pathway (=CIA) (Katoh *et al.*, 2002; Lill and Mühlenhoff , 2008). Key components of the ISC system are: i/ cysteine desulfurase (Nfs/IscS) that catalyzes desulfurization of L-cysteine into alanine providing sulfur (Zheng *et al*., 1993), ii/ frataxin (Yfh), which is proposed to deliver iron, although its exact function remains to be established (Lill and Mühlenhoff , 2008; Long *et al*., 2008a), iii/ ferredoxin (Yah1) that provides electrons for the reduction of sulfur to sulfide in the clusters (Nakamura et al., 1999), and iv/ a metallochaperone (IscU/Isu1), on which the Fe-S cofactors are transiently assembled (Mühlenhoff *et al*., 2003; Nishio and Nakai, 2000). However, the list of conserved and essential components of the Fe-S cluster assembly pathway is steadily growing and currently includes approximately two dozen proteins (Lill, 2009).

With the exception of the CIA pathway, all dedicated machineries for Fe-S cluster assembly contain the A-type scaffold component (Lill, 2009). In eukaryotic genomes, the homologue(s) of prokaryotic IscA are the Isa proteins (Rouault and Tong, 2005; Zheng *et al*., 1998)In the yeast *Saccharomyces cerevisiae*, as well as in numerous other eukaryotes, two Isa homologues labelled

Isa1 and Isa2 were recently shown to have an additional binding partner Iba57, also involved in Fe-S cluster assembly (Gelling *et al*., 2008). Isa1 is found in all multicellular model organisms, while it may be poorly conserved or even missing in protists with reduced mitochondria or mitosomes, such as *Encephalitozoon cuniculi*, *Cryptosporidium parvum*, *Entamoeba histolytica* and *Trichomonas vaginalis* (Lill and Mühlenhoff 2005; Vinella *et al*., 2009).

It was proposed that the rather small IscA and SufA (member of the bacterial SUF operon) proteins serve in prokaryotic Fe-S cluster synthesis as alternative scaffold proteins (Krebs *et al*., 2001; Ollagnier-de-Choudens *et al*., 2001; Wollenberg *et al*., 2003) and a similar function was also suggested for their eukaryotic homologues (Wu *et al*., 2002). Furthermore, IscA may provide iron for the Fe-S cluster assembly in *E. coli*, especially under limited iron conditions (Ding *et al*., 2004), a role consistent with its very strong iron-binding affinity (Ding and Clark, 2004). These features were recently demonstrated also for the human Isa1 (hIsa1) (Lu *et al.*, 2010). Deletion of IscA or SufA causes only a minor growth phenotype in *E. coli* (Djman *et al*., 2004), while the simultaneous elimination of both proteins is lethal (Tan *et al*., 2009) and can be partially rescued by hIsa1 (Lu *et al.*, 2010).

Two independent crystallographic studies of the *E. coli* IscA revealed a monodimeric or monotetrameric form with a novel fold and a pocket that can accommodate an iron atom or a Fe-S cluster (Bilder *et al*., 2004; Cupp-Vickery *et al*., 2004). Moreover, Mossbauer spectroscopical analysis was instrumental in showing that IscA can bind both [2Fe-2S] and [4Fe-4S] clusters, although it remains to be established whether the former cluster type is an intermediate step in the construction of [4Fe-4S] clusters, or a derivative thereof (Ollagnier-de-Choudens *et al*., 2004).

Although IscA/Isa proteins are widely distributed across the tree of Life, they do not seem to be essential, since elimination of the protein in *E. coli* leads to only a mild phenotype (Djman *et al*., 2004; Tokumoto and Takahashi, 2001). Two different explanations for this result have been put forward: i/ IscA/Isa proteins from different Fe-S cluster machineries can, to some extent, complement each other, or, ii/ they are essential only under specific growth conditions (Fontecave and Ollagnier-de-Choudens, 2008). The latter possibility gained some support from the observation that IscA in *E. coli* is indispensable in the presence of high concentrations of oxygen (Johnson *et al*., 2006) but is non-essential under anaerobic conditions (Wang *et al*., 2010). The Isa proteins are also non-essential in *S. cerevisiae* (Jensen and Culotta, 2000; Pelzer *et al*., 2000), where they function as substrate-specific assembly factors required for proper function of biotin and lipoic acid synthases, as well as in the maturation of mitochondrial aconitase (Gelling *et al*., 2008; Mühlenhoff *et al*., 2007). The hIsa1 protein is expressed in multiple tissues (Córaz *et al*., 2004) and was recently shown to have dual localization in human cells (Song *et al*., 2009). Even though the majority of the protein in HeLa cells was localized in the mitochondrial matrix, a fraction was also consistently found in the cytosol and it was proposed that hIsa1 might serve as a scaffold for delivery of Fe-S clusters to aconitases in both cellular compartments (Song *et al*., 2009). In any case, the Isa1 deficiency in yeast was rescued by its human orthologue (Córaz *et al*., 2004), while hIsa1 can rescue the IscA and SufA mutant in *E. coli* (Lu *et al*., 2010). Furthermore, a large-scale computational analysis uncovered a strong co-expression between the Isa1 and Isa2 proteins and the synthesis of heme (Nilssen *et al*., 2009). Still, too little is currently known about the potential cross talk between Fe-S cluster and heme biosynthetic processes (Wingert *et al*., 2005) to draw further conclusions.

In order to further clarify the function of the Isa proteins, we undertook their functional analysis in *Trypanosoma brucei*, a parasitic protist responsible for the highly pathogenic African sleeping sickness and other diseases. As trypanosomatids are evolutionarily distant from other eukaryotes that have been well studied, trypanosome Isa proteins may have retained function(s) that are, in some respects, ancestral to the mitochondrial endosymbiont in which these proteins first entered the eukaryotic cell. Moreover, trypanosomes represent very interesting model organisms, in which the

fully active mitochondrion of the procyclic stage transforms into a down-regulated organelle that retains only basic functions in the bloodstream stage (Lukeš *et al*., 2005). We reasoned that functional analyses in these two different forms of mitochondria in trypanosomes may shed additional light on the still rather enigmatic function of the Isa proteins in the eukaryotic cell.

Results

Identification and phylogenetic analyses of Isa1, Isa2 and Iba57

The available kinetoplastid genomes were searched for homologues of the yeast Isa1 and Isa2 proteins. A BLAST search identified two homologues in the *T. brucei* genome, here labelled TbIsa1 and TbIsa2. We identified similar Isa orthologues in the *Trypanosoma cruzi*, *Leishmania major, L. braziliensis* and *L. infantum* genomes (Fig. 1). Alignment of their deduced amino acid sequences with numerous prokaryotic and eukaryotic homologues revealed high conservation of both proteins among kinetoplastid flagellates, including the three cysteine residues predicted to be involved in the ligation of Fe or Fe-S cluster complexes. From the sequence alignment it is apparent that the characteristic architecture of the *E. coli* IscA protein, composed of two α-helices and seven β-sheets (Bilder *et al*., 2004), is likely conserved in its *T. brucei* homologues, and this prediction was confirmed by structural modelling (data not shown). The TbIsa1 (Tb927.8.5540) and TbIsa2 genes (Tb927.5.1030) code for 272 and 173 amino acids-long proteins with calculated molecular weights of 29.5 kDa and 19.0 kDa, respectively, and their overall identity is 23% at the amino acid level. Both proteins are predicted to contain a cleavable mitochondrial import signal, with probability 0.3733 and 0.9748 for TbIsa1 and TbIsa2, respectively (MitoProtII) and similarly high probabilities predicted by pSORT.

To investigate the phylogenetic distribution of the Isa1 and Isa2 proteins (ISA1/2) we used a previously published alignment from a genome wide search on these proteins (Vinella *et al*., 2009). To this alignment, we added the sequences of Isa1 and Isa2 from all available identified homologues but also some additional eukaryotic sequences recently available from genomic and transcriptomic projects. Maximum likelihood and Bayesian phylogenetic analyses of these proteins demonstrated that Isa1 and Isa2 sequences form two independent clades both of which group α-proteobacterial isoforms with their eukaryote orthologues, although the relevant branches have weak bootstrap support and posterior probabilities. Interestingly, while most eukaryotes have both isoforms, all homologues from parasites such as *Trichomonas vaginalis* and *Giardia lamblia* cluster within the Isa2 clade, while the diatom *Thalassiosira pseudonana* homologues group within the Isa1 cluster. The genome of another parasite, *Entamoeba histolytica*, appears to be completely devoid of either Isa homologue (Fig. 1 and data not shown).

A genome-wide search was also performed in order to identify the presence of Iba57 genes within eukaryotic genomes. In addition to the trypanosomatid sequences, homologues were identified in representatives of a wide variety of eukaryote groups including the Fungi, animals, Plantae, ciliates, and a brown alga. Curiously, however, a clear homologue of this protein was absent in many recently sequenced protistan genomes including *Encephalitozoon cuniculi, G. lamblia, E. histolytica, T. vaginalis, T. pseudonana, Phaeodactylum tricornutum, Phytophthora infestans,* and *Blastocystis* sp. Nevertheless, maximum likelihood and Bayesian phylogenetic analyses of this protein showed a phylogeny that did not strongly conflict with expected eukaryote groupings (Suppl. Fig. 6). This suggests that the genomes that apparently lack Iba57 either do in fact have homologues that are too divergent to be picked up by bioinformatic methods used here, or they have been secondarily lost through reductive evolution. Overall, the phylogenetic analyses from the

Isa1/2 and Iba57 proteins suggest a widespread distribution of this machinery within eukaryotes and potentially the presence of these proteins in the ancient machinery of the α-proteobacterium that gave rise to the mitochondrion.

Expression, subcellular localization and interaction of TbIsa

In order to establish the subcellular localization, and to follow the sedimentation properties and depletion of the TbIsa proteins, we have separately over-expressed the full-size Isa1 protein in *E. coli*, from which the abundantly expressed insoluble protein has been purified (data not shown). Specific polyclonal antibodies generated against TbIsa1 in a rat were used for further experiments. The polyclonal antibodies against TbIsa2 were generated against a synthetic oligopeptide derived from the *T. brucei* protein (see Materials and Methods). In order to verify the predicted mitochondrial localization of both proteins, we have obtained cytosolic and mitochondrial fractions from the PF 29-13 cells. The purity of both fractions, obtained by digitonin fractionation, was confirmed by compartment-specific cytosolic and mitochondrial markers enolase and mitochondrial RNA binding protein (MRP) 2, respectively. As shown in Fig. 2A, all detectable TbIsa1 and TbIsa2 proteins are indeed confined to the organelle.

Based on the crystal structure of IscA it was predicted that in *E. coli* this protein forms one of the two alternative tetrameric oligomers (Bilder *et al*., 2004). Since two Isa paralogs are present in the trypanosome and most other eukaryotic genomes (Fig. 1), we have tested their possible interaction first by sedimentation in glycerol gradients containing mitochondrial lysates from *T. brucei* PF cells. Probing the gradient fractions with anti-TbIsa1 and anti-TbIsa2 antibodies revealed that both proteins co-sediment in fractions 4 and 6, with TbIsa1 also present in fraction 8 (Suppl. Fig. 1). Sedimentation of the control mitochondrial proteins TbRGG1 and KREL1 was in agreement with previously reported data (Hashimi *et al*., 2008). Elsewhere it was shown that under identical conditions protein complexes of about 100 kDa sediment in the fractions 3 through 7 (Vondrušková *et al*., 2005). This result therefore suggests that TbIsa1 and TbIsa2 do not exist as monomers, but form either homo- or hetero-oligomers.

To distinguish between these two possibilities, we performed co- immunoprecipitation experiments using the cell lysates and mitochondrial fractions obtained with digitonin fractionation from the *T. brucei* PF cells. In co-immunoprecipitations, the anti-TbIsa1 rat antibodies were used both in physiological salt and high salt conditions. Western blot analysis of the eluate with the specific anti-TbIsa2 antibody revealed that TbIsa1 does not bind TbIsa2 (Fig. 2B). The experiment under high salt condition confirmed the lack of protein-protein interaction between TbIsa1 and TbIsa2, since TbIsa1 did not pull TbIsa2 down (Fig. 2C). To further confirm the lack of interaction between these two proteins and potential binding with other proteins, cells overexpressing TAP-tagged TbIsa1 and TbIsa2 were generated, lysates from these cells were subjected to tandem-affinity purification following conditions described elsewhere (Panigrahi *et al*., 2009) and the co-purifying proteins were analyzed by mass spectrometry. In agreement with the co-immunoprecipitation experiment, the tagged TbIsa1 did not bind TbIsa2 and vice versa (A. Zíková, pers. commun.). Moreover, no other binding partners were identified by TAP-copurification and mass spectrometry, indicating that the sedimentation of the TbIsa proteins in glycerol gradient could reflect weak interactions with other proteins, such as Iba57, same as in yeast (Gelling *et al*., 2008).

Expression of both TbIsa genes is essential in PF cells

In order to assess the function of individual Isa proteins in the PF (=insect) of *T. brucei*, we used RNAi to selectively down-regulate the mRNA levels of TbIsa1 and/or TbIsa2. A fragment of the TbIsa1 gene or the entire TbIsa2 gene was cloned into the p2T7-177 vector containing opposing tetracycline-regulatable promoters. Moreover, another cell line was transfected with a *Not*I-linearized p2T7-177 vector containing fragments of the TbIsa1 and TbIsa2 genes cloned in tandem, which allowed their parallel ablation. For each construct, several clonal cell lines have been obtained by limiting dilution using phleomycin as a selectable marker. In representative clones RNAi was induced by the addition of 1 μg/ml tetracycline to the medium and the growth was monitored using cell counter. Upon RNAi induction, the growth of the TbIsa knock-downs was identical with the non-induced cells until day 3. Thereafter, the growth of the RNAi-induced TbIsa1 and TbIsa2 cells slowed significantly down (Figs. 3A and B). A cumulative effect occurred in the induced double knock-down cells, which virtually stopped dividing on day 4 post-induction (Fig. 3C), and did not recover even after 12 days . The depletion of the target proteins was monitored by western blot analysis using specific antibodies. In cells in which the TbIsa1 mRNA was targeted, a very strong decrease of the TbIsa1 protein occurred already by day 2 of RNAi induction (Fig. 3D). While more than 90% of the protein was eliminated at this early time point, residual TbIsa1 protein remained present at a stable level even by day 4.

In the TbIsa2 knock-downs, the anti-TbIsa2 antibody allowed observing the virtual disappearance of the target protein by day 2 (Fig. 3D). In both cell lines, western analysis was instrumental to show that both antibodies and RNAi knock-downs are specific for their targets, as the levels of the non-interfered TbIsa protein remained unaltered even after four days of RNAi induction. Western analysis with the anti-TbIsa1/Isa2 antibodies confirmed a very efficient elimination of both proteins in the double knock-downs (Fig. 3D) and the lack of their mutual interaction.

TbIsa are required for the assembly of mitochondrial Fe-S clusters only

While early studies implicated the yeast Isa proteins with the assembly of both cytosolic and mitochondrial Fe-S clusters (Jensen *et al*., 2000; Pelzer *et al*., 2000), according to more recent data their function is associated only with the mitochondrion (Mühlenhoff *et al*., 2007). We have tested the effect of individual and parallel depletion of the TbIsa proteins on selected enzymes in both cellular compartments of procyclic trypanosomes. The Fe-S cluster-containing aconitase (encoded by one gene) and fumarase (encoded by two different genes) have dual localization in trypanosome cells, with 30 and 50% of aconitase and fumarase activities in the mitochondrion, respectively (Saas *et al*., 2000; Coustou *et al*., 2006), allowing us to measure their activities separately in the mitochondrion and cytosol (Figs. 4A and B). The purity of each compartment fraction was assessed by western blot analysis using antibodies against mitochondrial MRP2 and cytosolic enolase (Fig. 4E). As shown in Fig. 4A, in all three RNAi knock-downs, 2 days upon the addition of tetracycline into the medium the mitochondrial aconitase activity dropped by 40 to 60%. Following additional 48 hrs, only about 25% of the activity persisted (Fig. 4A). The depletion of any of the TbIsa proteins had an even more dramatic effect on mitochondrial fumarase, which on day 2 decreased by between 50 to 75%, while on day 4 only 10 to 25% residual activity remained (Fig. 4B). The activity of succinate dehydrogenase (complex II), an Fe-S cluster containing enzyme that is exclusively mitochondrial, followed a pattern very similar to both above-mentioned enzymes. Its activity dropped most in the double knock-downs, with only 15% of its activity remaining after 4 days of RNAi induction (Fig. 4C). The activity of threonine dehydrogenase, an enzyme lacking Fe-S clusters, was used as a control; its activity was unaffected in both the non-induced and in the RNAi-induced cells (Fig. 4D).

In order to evaluate possible associations of the TbIsa proteins with other components of the

mitochondrial Fe-S cluster assembly machinery, we have followed the levels of the cysteine desulfurase Nfs, metallochaperone IscU and frataxin in the interfered cells 2, 4 and 6 days of RNAi induction. However, in both the single and double knock-downs the abundance of all of these proteins remained unaltered (Suppl. Fig. 2). Measurement of aconitase and fumarase activities in pure cytosolic fractions obtained from the non-induced and RNAi-induced TbIsa knock-downs revealed that neither of these activities is decreased.

Mitochondrial ROS are elevated but iron content remains constant upon depletion of TbIsa

We were interested to determine if the disturbance of mitochondrial Fe-S cluster-containing enzymes had a more general impact on functions of the organelle. Mitochondrial membrane potential was quantified using flow cytometry and the uptake of the dye TMRE. Indeed, in cells where RNAi was used to ablate any of the TbIsa proteins, the membrane potential decreased (Suppl. Fig. 3A). Next, the accumulation of ROS in the mitochondrion of the non-induced and RNAi-induced cells was measured using dihydroethidium. In RNAi double knockdown we detected a substantial increase in ROS, although this phenotype was much weaker in the other cell lines (Fig. 5A; Suppl. Fig. 3B). In yeast, disruptions of the ISC pathway, such as the depletion of the Isa proteins, frequently leads to iron accumulation in the mitochondrion. We wondered whether same effect will also occurs in the trypanosome cells. The concentration of iron was followed in mitochondrial fractions by the ferene method, which detects all intracellular iron except that bound by heme (Pieroni *et al*., 2001). The measurement revealed an unaltered iron level in the organelle of RNAi-induced double knock-downs when compared with the non-induced cells (Fig. 5B).

Both TbIsa are non-essential in BF cells

Since the depletion of TbIsa's exhibited an effect on the mitochondrial Fe-S cluster-containing proteins in the PF cells, we also generated RNAi knock-downs in the BF cells, which are known to have a largely down-regulated organelle, as compared to the PF cells (Lukeš *et al*., 2005; Schneider, 2001; Tielens and van Hellemond, 1998). First, we checked the levels of the TbIsa proteins in total lysates of BF cells obtained from rat blood. Using the anti-TbIsa1 antibodies, we detected lower amount of the protein as compared to the PF cells (Fig. 6A). Next, the TbIsa1, TbIsa2 and TbIsa1/2 RNAi constructs used to deplete the target proteins in the PF cells were electroporated into the *T. brucei* 920 BF cells. The growth of phleomycin-resistant non-induced and RNAi-induced clones was then followed for one week, with cells diluted on a daily basis. Unexpectedly, no or only a very weak growth phenotype was observed in either of the transfectants (Fig. 6B and Suppl. Fig. 4A and 4B). Since the target TbIsa transcripts were undetectable in the BF cells assayed by northern blotting, the only proof that RNAi was working was the appearance of the double stranded RNA in the induced cells (Fig. 6C). However, western analysis with anti-TbIsa1 antibody confirmed substantial depletion of the protein upon RNAi induction (Fig. 6D).

Functional rescues with human Isa homologues

While human Isa1 has been intensely studied and can rescue *E. coli* (Lu *et al*., 2010) and yeast cells depleted for its homologues (Córaz-Castellano *et al*., 2004), nothing is known about the function of human Isa2. Here we have attempted to use the trypanosome model to study the human Isa proteins

using a complementation assay. Based on our observation that TbIsa1 can to some extent substitute for TbIsa2, and vice versa, since both proteins have similar biochemical phenotypes, we prepared various rescue combinations with the human Isa genes. To this end, the following rescue cell lines were generated: i/ TbIsa1 + hIsa1; ii/ TbIsa2 + hIsa2; iii/ TbIsa1 + hIsa2; iv/ TbIsa2 + hIsa1; v/ TbIsa1/2 + hIsa1; vi/ TbIsa1/2 + hIsa1/2; vii/ TbIsa1/2 + hIsa2.

In both the human and *T. brucei* cells, most mitochondrion-targeted proteins are synthesized as precursors that are, upon import, proteolytically matured by mitochondrial processing peptidase. We have shown recently that the signal peptide on the human frataxin will efficiently target the downstream protein into the trypanosome organelle (Long *et al*., 2008b). Therefore, the coding sequence for the human frataxin signal peptide (1-54 residues) was introduced to replace the predicted signal peptide (1-13 residues) of hIsa1gene obtained from the human cDNA library, after an attempt with full-length hIsa1 failed due to the lack of its import into the *T. brucei* mitochondrion (data not shown). The full-length hIsa2 with its genuine import signal inserted in the pFC4 vector was used in all rescue experiments with this protein. Import of these heterologous proteins was followed using antibody against the HA_3-tag attached to the C-termini of hIsa1 protein and with a specific antibody against hIsa2. As shown in Fig. 7A, all tagged hIsa1 was imported into the single mitochondrion of PF cells, while the situation was more complex in the case of hIsa2, which was equipped with its genuine import signal. Western analysis detected two forms, apparently representing the pre-processed (arrow) and processed (arrowhead) hIsa2, while no signal was detected in cell lines lacking this protein (Fig. 7C). Therefore we resorted to western analysis of cellular fractions from the TbIsa2 + hIsa2 cells. As expected, the resulting mitochondria contained only the shorter processed form of hIsa2, whereas the most abundant species in the cytosol was the pre-processed protein. In the total cell lysate, the processed hIsa2 protein predominated, although the processing of this alien protein was apparently less efficient relative to the genuine trypanosome mitochondrial proteins (Fig. 7B).

Next, we measured the activities of aconitase and fumarase in the mitochondrion, as activities of these proteins in the cytosol were not influenced by the status of the TbIsa proteins (Fig. 4). Comparative measurement of these activities in the above-described PF cell lines, as well as in cells with ablated TbIsa2 and TbIsa1/2 showed that both activities are, to some extent, rescued in all cases (Fig. 8). Particularly efficient is the rescue of TbIsa2 by hIsa2, while the other combinations resulted in less efficient rescues, especially when aconitase is considered (Fig. 8B). The activity of fumarase was restored to almost wild type levels even in both cross-rescues (TbIsa1 + hIsa2 and TbIsa2 + hIsa1) (Fig. 8A; panels F and G), strongly indicating that the functions of the human Isa proteins are overlapping in *T. brucei*.

Rescue with Blastocystis *Isa2*

We decided to attempt another rescue using the BhIsa2 protein derived from the anaerobic organelle from *Blastocystis* sp. that displays features of both mitochondria and hydrogenosomes (Stechmann *et al.*, 2008). The full-length BhIsa2 gene amplified from a cDNA molecule was cloned into the pABPURO vector and introduced into the PF *T. brucei* inducible for RNAi against the *T. brucei* Isa1/2 double knockdown. The empty pABPURO vector and TbIsa1/2 RNAi knockdown were used as controls (Fig. 9; Suppl. Fig. 6). The growth phenotype triggered by the depletion of TbIsa1/2 was partially rescued by the expression of BhIsa2 (Suppl. Fig. 6). Morever, the activities of mitochondrial fumarase (Fig. 9A), aconitase (Fig. 9B), as well as succinate dehydrogenase (Fig. 9C), were almost identical with those in wild type cells.

Iba57 is needed for stability of TbIsa1 and aconitase

Since Iba57 was recently shown to interact with Isa1 and Isa2 in yeast (Gelling *et al*., 2008), we decided to investigate its function and relationship with the Isa proteins in *T. brucei*. The RNAi knock-down of Iba57 resulted in different outcomes in the PF and BF cells. While a growth phenotype became apparent in PF cells 4 days after RNAi induction (Suppl. Fig. 4C), BF cells depleted for Iba57 grew at the same rate as wild type and non-induced trypanosomes (Suppl. Fig. 4D), correlating well with the impact of TbIsa depletion in this life stage (Figs. 3 and 6). The Iba57 mRNA was undetectable in both PF and BF cells by Northern blot analysis, but the appearance of a strong band of specific double stranded RNA in the induced cells is indirect evidence of functional RNAi (Suppl. Fig. 4E). Moreover, the down-regulation of the target mRNA was confirmed by qPCR (data not shown).

Next, we addressed possible interaction between Iba57 and the TbIsa proteins. Since Iba57 was not among proteins pulled down with TAP-tagged TbIsa1 and TbIsa2 (A. Zíková, pers. Commun.), it is unlikely that there is a strong interaction between these proteins and Iba57. However, a decrease of TbIsa1 followed ablation of Iba57 (Fig. 10A), indicating that a weak or indirect interaction exists between these proteins in *T. brucei*. Furthermore, aconitase was destabilized in the absence of Iba57 (Fig. 10B), indicating possible interaction of Iba57 with mitochondrial aconitase during execution of its function. Finally, paraquat treatment revealed that cells deficient in Iba57 were up to 60x more sensitive to this drug, as compared to the non-induced cells (Fig. 10C). This result likely reflects the increased sensitivity of Iba57-depleted cells to ROS.

Discussion

T. brucei and related flagellates are responsible for devastating diseases of humans and other vertebrates in most tropical regions. These parasites are also the most genetically tractable excavate protists, and as a consequence, they are the only representatives of this eukaryotic super-group, in which functional studies are routinely made. We are interested in investigating how Fe-S clusters are generated in this deeply-divergent and medically highly relevant protist.

So far, we have demonstrated that several key components of the pathway are present in *T. brucei* and their function seems to be conserved with respect to the well-studied eukaryotes, such as *S. cerevisiae*, *Arabidopsis thaliana* and humans. A preliminary search for genes encoding members of the ISC and CIA pathways in the *T. brucei* genome revealed not only the presence of all conserved components but in a few cases even the existence of several homologues of otherwise single-copy genes (S.L. and J.L., unpubl. results). Therefore, it is reasonable to assume that the complexity of the Fe-S cluster assembly in this unicellular eukaryote will be similar to that of the sophisticated machinery emerging from the studies of multicellular organisms.

Proper assembly of the Fe-S clusters in trypanosomes clearly requires the function of cysteine desulfurase Nfs, its interaction partner Isd11 and the metallochaperone IscU, the bulk of which is localized in the single reticulated mitochondrion (Paris *et al*., 2010; Smid *et al*., 2006). More recently we have shown that, although undetectable by western analysis, a tiny amount of Nfs is also present in the cytosol/nucleus and the same seems to apply for selenocysteine lyase, which has overlapping functions with the above-mentioned protein (Poliak *et al*., 2010). Furthermore, the *T. brucei* Nfs is indispensable for the thiolation of tRNAs in both mitochondrial and cytosolic compartments (Wohlgamuth-Benedum *et al*., 2009). Another core ISC component, frataxin, is essential for clusters incorporated not only into the mitochondrial proteins, but also the cytosolic

ones, although for survival of the trypanosome, mitochondrial localization of frataxin is mandatory (Long *et al*., 2008a,b).

Here we have focused on the role of the eukaryotic Isa proteins, functionally studied so far mostly in *S. cerevisiae*. Until recently, they were affiliated with the Fe-S cluster assembly of mitochondrial proteins such as aconitase and biotin synthase (Pelzer *et al*., 2000; Mühlenhoff *et al*., 2007). This view was, however, recently challenged, as human Isa1 was proposed to play an important role in both mitochondrial and cytosolic Fe-S cluster assembly in HeLa cells (Song *et al*., 2009). We have therefore inspected activities of the Fe-S cluster-containing fumarase and aconitase, which have a dual localization in the PF trypanosomes (Coustou *et al*., 2006; Saas *et al*., 2000) and are thus particularly suitable for assessing the impact on different cellular compartments. Whereas activities of both enzymes invariably dropped in both the mitochondrion and cytosol of the PF cells upon the depletion of Nfs, IscU, Isd11 or frataxin (Smid *et al*., 2006; Paris *et al*., 2010; Long *et al*., 2008a), the consequence of depletion of the Isa proteins was different, as it impacts only on the organellar Fe-S cluster-containing enzymes. Moreover, the activity of succinate dehydrogenase was strongly depleted in all TbIsa knock-downs, a phenomenon which went unnoticed in other eukaryotes (Gelling *et al*., 2008; Jensen and Culotta, 2000; Kaut *et al*., 2000; Mühlenhoff *et al*., 2007; Pelzer *et al*., 2000).

It is likely that this drop in activities of all three inspected mitochondrial Fe-S proteins is responsible for the lethal phenotype we observed. Moreover, the ablation of the TbIsa proteins caused a dramatic increase of ROS in all tested cell lines, particularly in the double knock-down. We attribute this effect to the disruption of the respiratory chain due to the shortage of Fe-S clusters needed for its components, not to Fenton reaction since iron did not accumulate in the TbIsa-depleted organelle. Particularly telling is the apparent unimportance of TbIsa in the BF cells, in which both proteins can be ablated with no impact on cell growth. It is well known that the BF mitochondrion is considerably reduced and lacks respiratory complexes, yet it still efficiently imports proteins, maintains membrane potential, and replicates and transcribes its mitochondrial DNA, the transcripts of which are properly edited and translated (Hashimi *et al*., 2010; Schneider, 2001). This organelle lacks most if not all Fe-S cluster-containing proteins such as respiratory complexes I thru IV (Besteiro *et al*., 2005; Lukeš *et al*., 2005; Tielens and van Hellemond, 1998), fumarase (Saas, *et al*., 2000) and aconitase (P.C. and J.L., unpubl. results). The only currently known [2Fe-2S] cluster-containing mitochondrial protein in the BF *T. brucei* - monothiol glutaredoxin-1 is, however, non-essential (Comini *et al*., 2008). Our results provide indirect, but rather strong evidence that except of very low amount of aconitase, no other proteins containing the [4Fe-4S] clusters are made in this down-regulated organelle, rendering the two TbIsa proteins fully dispensable for this life stage. Still, the low amount of TbIsa in BF cells may reflect the existence of as yet unidentified [4Fe-4S] proteins in their mitochondrion.

Recently, Song *et al.* (2009) showed that in HeLa cells the majority of hIsa1 is located in the mitochondrion, while a miniscule but functionally important amount of this protein is also present in the cytosol. Although we cannot entirely rule out a similar situation in the studied flagellates, two lines of evidence presented in this study -- the lack of an effect of TbIsa ablation on the cytosolic Fe-S cluster proteins and the non-essentiality of these proteins in the BF cells -- indicate that the TbIsa proteins only have a functional role in the mitochondrion of *T. brucei*. In *E. coli* IscA was shown to be required for maturation of the [4Fe-4S] enzymes (Tan et al., 2009). The non-essentiality of TbIsa for cytosolic Fe-S proteins indicates that ferredoxin, an [2Fe-2S] protein and electron donor for the ISC machinery (Lill and Mühlenhoff 2008) indeed remains unaffected by the lack of the TbIsa proteins in the organelle. It thus appears that in *T. brucei* the Isa proteins specifically function for mitochondrial [4Fe-4S] proteins, such as fumarase, aconitase, and succinate dehydrogenase. However, the cofactor of IscA/Isa proteins, whether it is iron (Ding *et al*., 2004; Ding and Clark, 2004; Lu *et al*., 2010) or Fe-S cluster (Ollagnier-de-Choudens *et al*., 2004),

remains elusive. Our attempts to identify the cofactor in TbIsa failed due to low expression of the His-tagged protein.

It is also worth noting that heme is not synthesized in trypanosomes (Kořený et al., 2010), so the association of Isa1 with heme synthesis, supported by the data obtained in mouse and zebra fish (Nilsson *et al*., 2009) is certainly not contributing to its essentiality in trypanosomes. Furthermore, the [4Fe-4S] cluster-carrying biotin synthase, which requires for the synthesis of biotin in the *S. cerevisiae* mitochondria the assistance of Isa (Mühlenhoff *et al*., 2007), is not encoded in the *T. brucei* genome and thus cannot contribute to the observed growth phenotype. We have also inspected the function of Iba57, the interacting partner of Isa in yeast (Gelling *et al*., 2008). In this case data obtained from PF *T. brucei* is consistent with a weak interaction, as well as with the impact of Iba57 depletion on aconitase and ROS build-up, which is in good correlation with hypersensitivity of Iba57 knock-outs to oxidative stress (Walter *et al*., 2010).

We have demonstrated that TbIsa1 and TbIsa2 have a similar function in mitochondrion-confined Fe-S cluster assembly, the essentiality of which is particularly visible in PF RNAi double knock-downs, a situation unlike yeast (Jensen *et al*., 2000; Pelzer *et al*., 2000). It was shown recently that human Isa1 was able to partially rescue the growth of the *E. coli* IscA and SufA double knock-out, but no characterization of the rescues was provided (Lu, *et al*., 2010). Here we demonstrate the capacity of hIsa1 and/or hIsa2 to (partially) cross-rescue the activities of mitochondrial aconitase and fumarase in both single and double TbIsa1 and/or TbIsa2 knock-downs, proving their overlapping function. Ablation of TbIsa2 and hIsa2 seems to have a stronger effect on mitochondrial Fe-S proteins than that of their counterparts. However, in none of the various rescue combinations cell growth was fully recovered, indicating that hIsa failed to replace an as yet unknown activity of the TbIsa proteins. The same conclusion applies for the rescue with Isa2 from *Blastocystis* sp.

The fact that both TbIsa proteins are essential components of the mitoproteome of PF *T. brucei*, their function being conserved as confirmed by rescue with orthologues from evolutionarily very distantly related anaerobic unicellular and aerobic multicellular eukaryotes, testifies to the unique and indispensable role of the Isa proteins in the Fe-S cluster assembly.

Experimental Procedures

Phylogenetic analysis

For Isa1/2 sequences, multiple sequence alignments were created using MAFFT (Katoh *et al*., 2002) based on a seed alignment of ATC sequences kindly provided by Celine Brochier-Armanet (Vinella *et al.*, 2009). The complete multiple sequence alignment was trimmed using MANUEL (Blouin *et al*., 2009) and phylogenetic trees were estimated from alignments by using RAxML 7.04 (Stamatakis *et al*., 2005) with the LG+F model of amino acid substitution and a γ model of rate heterogeneity. Bayesian phylogenetic analysis was carried out using MrBayes with the same model settings.

For Iba57 sequences, BLASTP and TBLASTN searches were performed in complete eukaryotic genomes to identify homologues of this protein. Sequence alignments were created using MAFFT and the alignment was subsequently trimmed using MANUEL. To reduce potential alignment errors and phylogenetic artifacts, some extremely divergent and partial sequences (e.g. *Babesia bovis*, *Theileria parva*) were not included in the multiple alignment or phylogenetic analysis. Phylogenetic trees were estimated from an alignment of 71 taxa and 296 positions by

using the same programs and model settings as described for the Isa1/2 sequences above.

RNAi constructs, transfections, cloning, RNAi induction and cultivation

To down-regulate the Isa1 and Isa2 mRNAs by RNAi, 530-nt and 522-nt long fragments of the Isa1 and Isa2 genes were amplified using primer pairs Isa1-FP and Isa1-RP, and Isa2-FP and Isa2-RP (Suppl. Table 1), respectively, from total genomic DNA of the *T. brucei* strain 29-13. Both amplicons were separately cloned into the p2T7-177 vector, which was, upon *Not*I-mediated linearization, introduced into procyclic (PF) *T. brucei* 29-13 cells using a BTX electroporator and selected as described elsewhere (Vondrušková et al., 2005). RNAi was induced by the addition of 1 μg/ml tetracycline to the SDM-79 medium. The double knock-down was prepared by cloning the same fragment of the Isa2 gene, into the p2T7-177+Isa1 construct, which was stably integrated into the *T. brucei* 29-13 PF cells as described above. The cell density of all three lines was measured every 24 hrs using the Beckman Z2 Coulter counter over a period of 12 days after the induction of double stranded RNA synthesis. All three RNAi constructs were introduced into the 427 bloodstream (BF) *T. brucei* cells using the Amaxa Nucleofector II electroporator, with transfectants kept in the HMI-9 medium and selected following a protocol described elsewhere (Hashimi *et al*., 2008).

To study protein-protein interactions, a construct inducibly expressing C-terminally TAP-tagged TbIsa1 protein was created by PCR amplification of the full-size gene and subsequent cloning into the pLew-79-MHTAP plasmid. Similarly, in order to obtain cells expressing TAP-tagged TbIsa2 protein, the full-size gene was PCR-amplified as described above. The *Not*I-linearized constructs were electroporated into the *T. brucei* 29-13 cells, which were selected using phleomycine (Vondrušková et al., 2005). For ablation of Iba57, 446-nt long fragment of the gene amplified using primers Iba-F and Iba-R (Suppl. Table 1) was cloned into p2T7-177 and electroporated into 29-13 PF and 427 BF cells as described above.

Northern blot analysis

Approximately 10 μg/lane of total RNA isolated using Trizol (Sigma) from the BF cell lines, was loaded on a 1% agarose-formaldehyde gel and transferred to a nitrocellulose membrane that was subsequently UV cross-linked. Hybridization was performed in NaPi solution using probes labeled by random priming with [α-^{32}P] dATP (MP Biomedicals) overnight at 55 ^{o}C. Membranes were washed and the radioactive signal was detected as described previously (Hashimi *et al*., 2008).

Expression of recombinant TbIsa1 and digitonin fractionation

The full-size TbIsa1 gene was amplified by PCR with primers Isa1-FP/O and Isa1-RP/O (containing the stop codon) (Suppl. Table 1). The amplicon was gel-purified and cloned into the pET/100D expression vector (Invitrogen). The resulting expression plasmid encoding His_6-tagged TbIsa1 was transformed into the E. coli strain BL21 (star DE3) (Novagen). Insoluble protein was obtained from induced bacterial cells (incubation at 37^{o}C for 3 hrs, and induced with 1 mM IPTG) under denaturing conditions using ProBond Ni-chelating resin (Invitrogen). Digitonin fractionation of T. brucei PF cells was performed following a protocol described elsewhere (Smid *et al*., 2006).

Preparation of antibodies and Western blot analyses

Polyclonal antibody against the TbIsa1 protein was prepared by immunizing a rat at two-week intervals with the purified recombinant Isa1 protein by Cocalico Biologicals Inc. (Reamstown, PA). In the case of TbIsa2, a synthetic oligopeptide (QPKSQELRTVAEGEC) corresponding to amino acids 97-110 of the *T. brucei* protein was used to raise polyclonal antibodies in a rabbit, which were subsequently affinity-purified by GeneScript©. Cell lysates corresponding to 5 x 10^6 cells/lane of the PF cells, or 1.5 x 10^7 cells of the BF cells were separated on a 15% SDS-polyacrylamide gel, transferred to membranes and probed. The anti-TbIsa1 polyclonal rat antibodies and the anti-TbIsa2 rabbit antibodies were used at 1:1,000 and 1:100 dilutions, respectively. The polyclonal rabbit antibodies against MRP2 (Vondrušková *et al*., 2005), frataxin (Long *et al*., 2008a), IscS and IscU (Smid *et al*., 2006) prohibitin(Týč *et al*., 2010), enolase (provided by P.A.M. Michels), aconitase (provided by M. Boshart), and human Isa2 (provided by H. Puccio) were used at 1: 1,000, 1: 1,500, 1:500, 1:1,000, 1:1,000, 1:200,000, 1:500, and 1:1,000 dilutions, respectively. Antibodies against TbRGG1 and KREL1 were used as described elsewhere (Hashimi *et al*., 2008). The HA_3- or TAP-tagged *in vivo* expressed TbIsa proteins were determined by western blot analysis using corresponding polyclonal antibodies (Hashimi *et al*., 2008; Long *et al*., 2008a).

Immunoprecipitation

Immunomagnetic beads (Dynabeads M-280; Invitrogen) coated with sheep anti-rat IgG were coupled with rat anti-TbIsa1 antibody either in physiological TET100 buffer or high salt TET400 buffer (100mM or 400mM NaCl, 20mM Tris-HCl, 0.1% Triton X-100, 0.1% BSA and protease inhibitor cocktail) for 1 hr at 4 ^oC with bidirectional mixing. Total cell lysate or mitochondrial lysate obtained by digitonin fractionation were prepared from 5 x 10^8 PF cells in TET100 or TET400 buffer containing 0.1% Triton, spun at 13200 rpm for 10 min at 4 ^oC, and the obtained supernatants were mixed with pre-incubated and primary antibody-coupled magnetic beads. After incubation for 1 hr at 4 ^oC, coupled proteins in the beads were washed 5x with either TET100 and TET400 buffer, and then eluted with 1x SDS-sample buffer. The eluted proteins were separated by SDS-PAGE on a 15% SDS-PAGE gel and detected by anti-TbIsa1 and TbIsa2 antibodies.

Measurement of intracellular iron

Cytosolic and mitochondrial fractions were prepared by digitonin fractionation as described above. After protein concentration was estimated with the Bradford reagent (BioRad), the volume of the fractions was decreased using a vacuum centrifuge, but the protein pellet was kept wet. Iron content was quantified by the ferene method (Hennesy and Reid, 1984; Pieroni *et al*., 2001). Briefly, 3-5 mg protein/sample was resuspended in 100 µl of phosphate buffered saline, treated with 50 µl concentrated HCl in 100^{o}C for 15 min, the sample was centrifuged and supernatant was transferred to a new tube. 50 µl of the supernatant was mixed with 0.3 ml 1M acetic acid-sodium acetate buffer (pH 5.5), then briefly treated with 5 µl thioglycolic acid with subsequent addition of 10 µl 6.25 mM ferene-S (Sigma). The reaction was incubated for 1 hr at room temperature, and the absorbance was measured at 593 nm using a Tecan Spectrometre. To calculate the number of moles of iron bound to the protein, the molar extinction coefficient for ferene-S of 33,850 L cm/mol was used. A standard

iron solution was used as a control.

Measurement of mitochondrial membrane potential, ROS and oxygen stress

After centrifugation, exponentially growing PF cells were resuspended in 1 ml of fresh SDM-79 medium (at a concentration 5 x 10^6 cells/ml) and mitochondrial inner membrane potential and ROS were measured by the uptake of 0.4% tetramethylrodamine ethyl ester (TMRE) (Molecular Probes) or oxidation of dihydroethidium (Sigma) in the time frame of 20 min at 27 ^oC. After staining, the cells were resuspended in Iso-flow buffer and instantly measured by flow cytometry using an Epics XL flow cytometer (Coulter).

The sensitivity of cells to oxidative stress was measured by exposing them to paraquat added to the cultivation medium in a wide range of concentrations, ranging from 4^{-10} to 40 mM. After 44 hrs of incubation, resazurin was added to each culture and after 4 hrs the viability of cells was established by measurement of fluorescence. Obtained data was analysed by GraphPad Prism software using nonlinear regression (curve fit) with a sigmoidal dose-response analysis, and the EC_{50} was calculated.

Measurement of enzymatic activities

The activities of fumarase, aconitase and threonine dehydrogenase were measured in cytosolic and mitochondrial fractions obtained with digitonin fractionation, the purity of which were controlled by compartment-specific antibodies against MRP2 and enolase using Western blot analysis. The activities of fumarase and aconitase were determined spectrophotometrically at 240 nm as the rate of production of fumarate and cis-aconitate respectively. The activity of threonine dehydrogenase was established at 340 nm as the rate of NAD^+ reduction as described elsewhere (Saas *et al*., 2000). The activity of succinate dehydrogenase was measured in crude mitochondrial membrane extract as described elsewhere (Horváth *et al*., 2005).

Rescue with human Isa

A 390 nt-long full-length cDNA of the human Isa1 (hIsa1) gene fragment (AAH02675) with the stop codon (or without the stop codon in case of tagging) were amplified from a commercial human liver cDNA library (Invitrogen) using primers hFxn-hIsa1, hFxn-hIsa1-M and hIsa1-R-RP or hIsa1-HA_3, and cloned into the pABPURO vector with or without HA_3 tag in their 3' end, respectively, following a strategy described previously (Long *et al*., 2008b). Next, the mitochondrial targeting peptide (1-13 amino acids) of hIsa1 predicted by MitoProt II (0.9807) was replaced with mitochondrial targeting peptide of human frataxin (amino acids 1-55), which is known to efficiently import proteins in the *T. brucei* organelle (29), using primers hFxn-hIsa1 and hIsa1-R-RP or hIsa1-HA_3 (Suppl. Table 1). A 465-nt long full-length cDNA (AAH15771) was amplified from a commercial hIsa2 construct (NITE Biological Resource Center) using primers hIsa2-R-FP and hIsa2-R-RP, and cloned into the pFC4 vector with blasticidin resistance, producing pFC4-hIsa2. All constructs were verified by sequencing. pABPURO- and pFC4-based constructs were linearized with *BstXI* and *NotI*, respectively, and used for transfection of the PF cells, in which RNAi against TbIsa1, TbIsa2 and TbIsa1+2 can be induced. In these cells, the activities of mitochondrial fumarase and aconitase were measured as described above.

Rescue with Blastocystis *Isa*

A partial sequence of the Isa2 gene was identified among the expressed sequence tags of *Blastocystis* sp. (Stechmann *et al.*, 2008). The full-length sequence of this gene was obtained using RACE techniques as described previously (Stechmann *et al.*, 2008). The 498 nt-long full-length cDNA of the *Blastocystis* Isa2 (BhIsa2) gene was cloned into the pABPURO vector (using primers BhIsa-F and BhIsa-R; Suppl. Table 1), following the cloning strategy described above for hIsa. A putative mitochondrial targeting peptide of the *Blastocystis* Isa2 protein, predicted by MitoProt II with high probability (>0.99), was retained in the construct for the rescue experiments. The linearized construct was introduced into the inducible knock-downs PF cells for TbIsa1 and TbIsa2. In the obtained cell lines, the activities of fumarase, aconitase, succinate dehydrogenase and threonine dehydrogenase were measured in total cell lysates, as well as in subcellular fractions as described above.

Acknowledgements

We thank members of our laboratories for discussions, Gabriela Ridvanová for technical assistance, Helene Puccio (Université de Strasbourg) and Michael Boshart (Ludwig-Maximilians-Universität Műnchen) for the donation of anti-hIsa2 and anti-aconitase antibodies, respectively, Alena Zíková (Biology Centre, České Budějovice) for sharing unpublished data, and André Schneider (University of Berne) for providing the pFC4 vector. This work was supported by the Grant Agency of the Czech Republic 204/09/1667, the Ministry of Education of the Czech Republic (LC07032, 2B06129 and 6007665801) and the Praemium Academiae award to J.L. A.D.T. was supported by an EMBO fellowship and travel grant from the Canadian Institute for Advanced Research to visit Czech Republic.

References

Besteiro, S., Barrett, M.P., Rivière, L., and Bringaud, F. (2005) Energy generation in insect stages of *Trypanosoma brucei*: Metabolism in flux. *Trends Parasitol* **21**: 185-191.

Bilder, P.W., Ding, H., and Newcomer, M.E. (2004) Crystal structure of the ancient Fe-S scaffold IscA reveals a novel protein fold. *Biochemistry* **43**: 133-139.

Blouin, C., Perry, S., Lavell, A., Susko, E., and Roger, A.J. (2009). Reproducing the manual annotation of multiple sequence alignments using a SVM classifier. *Bioinformatics* **25**: 3093-3098.

Córaz-Castellano, I., del Valle Machargo, M., Trujillo, E., Arteaga, M.F., González, T., Martín-Vasallo, P., and Avila, J. (2004). hIscA: a protein implicated in the biogenesis of iron-sulfur clusters. *Biochim Biophys Acta* **1700**: 179-188.

Comini, M.A., Retting, J., Dirdjaja, N., Hanschmann, E.M., Berndt, C., Krauth- Siegel, R.L. (2008) Monothiol glutaredoxin-1 is an essential iron-sulfur protein in the mitochondrion of

African trypanosomes. *J Biol Chem* 283: 27785-27798.

Coustou, V., Biran, M., Besteiro, S., Rivière, L., Baltz, T., Franconi, J.M., and Bringaud, F. (2006). Fumarate is an essential intermediary metabolite produced by the procyclic *Trypanosoma brucei*. *J Biol Chem* **281**: 26832-26846.

Cupp-Vickery, J.R., Silberg, J.J., Ta, D.T., and Vickery, L.E. (2004) Crystal structure of IscA, an iron-sulfur cluster assembly protein from *Escherichia coli*. *J Mol Biol* **16**: 127-137.

Djaman, O., Outten, F.W., and Imlay, J.A. (2004) Repair of oxidized iron-sulfur clusters in *Escherichia coli*. *J Biol Chem* **279**: 44590-44599.

Ding, H., Clark, R.J., and Ding, B. (2004) IscA mediates iron delivery for assembly of iron-suflur clusters in IscU under the limited accessible free iron conditions. *J Biol Chem* **279**: 37499-37504.

Ding, H., and Clark, R.J. (2004) Characterization of iron binding in IscA, an ancient iron-sulfur cluster assembly protein. *Biochem J* **379**: 433-440.

Fontecave, M. (2006). Iron-sulfur clusters: ever-expanding roles. *Nature Chem Biol* **2**: 171-174.

Fontecave, M., and Ollagnier-de-Choudens, S. (2008). Iron-sulfur cluster biosynthesis in bacteria: Mechanisms of cluster assembly and transfer. *Arch Biochem Biophys* **474**: 226-237.

Gelling, C., Dawes, I.W., Richhardt, N., Lill, R., and Mühlenhoff, U. (2008) Mitochondrial Iba57 is required for Fe-S cluster formation on aconitase and activation of radical SAM enzyme. *Mol Cell Biol* **28**: 1851-1861.

Goldberg, A.V., Molik, S., Tsaousis, A.D., Neumann, K., Kuhnke, G., Delbac, F., *et al.* (2008) Localization and functionality of microsporidian iron-sulfur cluster assembly. *Nature* **452**: 624-U7.

Hashimi, H., Zíková, A., Panigrahi, A.K., Stuart, K.D., and Lukeš, J. (2008) TbRGG1, a component of a novel multiprotein complex involved in kinetoplastid RNA editing. *RNA* **14**: 970-980.

Hashimi, H., Benkovičová, V., Čermáková, P., Lai, D.-H., Horváth, A., and Lukeš, J. (2010) The assembly of F_1F_0-ATP synthase is disrupted upon interference of RNA editing in *Trypanosoma brucei*. *Int J Parasitol* **40**:45-54.

Hennesy, J.D., and Reid, R.G. (1984) Ferene - a new spectrophotometric reagent for iron. *Can J Chem* **62**: 721-724.

Horváth, A., Horáková, E., Dunajčíková, P., Verner, Z., Pravdová, E., Šlapetová, I., *et al.* (2005) Down-regulation of the nuclear-encoded subunits of the complexes III and IV disrupts their respective complexes but not complex I in procyclic *Trypanosoma brucei*. *Mol Microbiol* **58**: 116-130.

Jensen, L.T., and Culotta, V.C. (2000) Role of *S. cerevisiae* ISA1 and ISA2 in iron homeostasis. *Mol Cell Biol* **20**: 3918-3927.

Johnson, D.C., Dean, D.R., Smith, A.D., and Johnson, M.K. (2005) Structure, function, and formation of biological iron-sulfur clusters. *Annu Rev Biochem* **74:** 247-281.

Johnson, D.C., Unciuleac, M.C., and Dean, D.R. (2006) Controlled expression of nif and isc iron-sulfur protein maturation components reveals target specificity and limited functional replacement between the two systems. *J Bacteriol* **188**: 7551-7561.

Katoh, K., Misawa, K., Kuma, K., and Miyata, T. (2002) MAFFT: a novel method for rapid multiple sequence alignment based on fast Fourier transform. *Nucleic Acids Res* **30**: 3059-

3066.

Kaut, A., Lange, H., Diekert, K., Kispal, G., and Lill, R. (2000) Isa1p is a komponent of the mitochondrial machinery for maturation of cellular iron-sulfur proteins and requires conserved cysteine residuem for function. *J Biol Chem* **275**: 15955-15961.

Kořený, L., Lukeš, J., and Oborník, M. (2010) Evolution of the heme synthetic pathway in kinetoplastid flagellates: An essential pathway that is not essential after all? *Int J Parasitol* **40**: 149-156.

Krebs, C., Agar, J.N., Smith, A.D., Frazzon, J., Dean, D.R., Huynh, B.H., and Johnson, M.K. (2001) IscA, an alternate scaffold for Fe-S cluster biosynthesis. *Biochemistry* **40**: 14069-14080.

Lill R (2009) Function and biogenesis of iron-sulfur proteins. *Nature* **460**: 831-838.

Lill, R., and Mühlenhoff, U.(2005) Iron-sulfur-protein biogenesis in eukaryotes. *Trends Biochem Sci* **30**: 133-141.

Lill, R., and Mühlenhoff, U. (2008) Maturation of iron-sulfur proteins in eukaryotes: Mechanisms, connected processes and diseases. *Annu Rev Biochem* **77**: 669-700.

Long, S., Jirků, M., Mach, J., Ginger, M.L., Sutak, R., Richardson, D., *et al.* **(**2008a) Ancestral roles of eukaryotic frataxin: mitochondrial frataxin function and heterologous expression of hydrogenosomal *Trichomonas* homologs in trypanosomes. *Mol Microbiol* **69**: 94-109.

Long, S., Jirků, M., Ayala, F.J., and Lukeš, J. (2008b) Mitochondrial localization but not processing of human frataxin is essential for a rescue of frataxin deficiency in the excavate flagellate *Trypanosoma brucei*. *Proc Natl Acad Sci USA* **105**: 13468-13473.

Lu, J., Yang, J., Tan, G., and Ding, H. (2008) Complementary roles of SufA and IscA in the biogenesis of iron-sulfur clusters in *Escherichia coli*. *Biochem J* **409**: 535-543.

Lu, J., Bitoun, P.J., Tan, G., Wang, W., Min, W., and Ding, H. (2010) Iron-binding activity of human iron-sulfur cluster assembly protein hIscA1. *Biochem J* **428**: 125-131.

Lukeš, J., Hashimi, H., and Zíková, A. (2005) Unexplained complexity of the mitochondrial genome and transcriptome in kinetoplastid flagellates. *Curr Genet* **48**: 277-299.

Mühlenhoff, U., Gerber, J., Richhardt, N., and Lill, R. (2003) Components involved in assembly and dislocation of iron-sulfur clusters on the scaffold protein Isu1p. *EMBO J* **22**: 4815-4825.

Mühlenhoff, U., Gerl, M.J., Flauger, B., Pirner, H.M., Balser, S., Richhardt, N., *et al.* **(**2007) The ISC proteins Isa1 and Isa2 are required for the function but not for the de novo synthesi of Fe/S cluster sof biotin synthase in *Saccharomyces cerevisiae*. *Eukaryot Cell* **6**: 495-504.

Nakamura, M., Saeki, K., and Takahashi, Y. (1999) Hyperproduction of recombinant ferredoxins in *Escherichia coli* by coexpression of the ORF1-ORF2-iscS-iscU-iscA-hscB-hscA-fdx-ORF3 gene cluster. *J Biochem* **126**: 10-18.

Nilsson, R., Schultz, I.J., Pierce, E.L., Soltis, K.A., Naranuntarat, A., Ward, D.M. *et al*., (2009) Discovery of genes essential for heme biosynthesis through large-scale gene expression analysis. *Cell Metabol* **10**: 119-130.

Nishio, K., and Nakai, M. (2000) Transfer of iron-sulfur cluster from NifU to apoferredoxin. *J Biol Chem* **275**: 22615-22618.

Ollagnier-de-Choudens, S., Mattioli, T., Tagahashi, Y., and Fontecave, M. (2001) Iron-sulfur cluster assembly – Characterization of IscA and evidence for a specific and functional

complex with ferredoxin. *J Biol Chem* **276**: 22604-22607.

Ollagnier-de-Choudens, S., Sanakis, Y., and Fontecave, M. (2004) SufA/IscA: reactivity studies of a class of scaffold proteins involved in [Fe-S] cluster assembly. *J Biol Inorg Chem* **9**: 828-838.

Panigrahi, A.K., Ogata, Y., Zíková, A., Anupama, A., Dalley, R.A., Acestor, N., *et al.* (2009) A comprehensive analysis of *Trypanosoma brucei* mitochondrial proteome. *Proteomics* **9**: 434-450.

Paris, Z., Changmai, P., Rubio, M.A.T., Zíková, A., Stuart, K.D., Alfonzo, J.D., and Lukeš, J. (2010) The Fe/S cluster assembly protein Isd11 is essential for tRNA thiolation in *Trypanosoma brucei*. *J Biol Chem* **285**: 22394-22402.

Pelzer, W., Mühlenhoff, U., Diekert, K., Siegmund, K., Kispal, G., and Lill, R. (2000) Mitochondrial Isa2p plays a crucial role in the maturation of cellular iron-sulfur proteins. *FEBS Lett* **476**: 134-139.

Pieroni, L., Khalil, L., Charlotte, F., Poynard, T., Piton, A., Hainque, B., and Imbert-Bismut, F. (2001) Comparison of bathophenanthroline sulfonate and ferene as chromogens in colorimetric measurement of low hepatic iron concentration. *Clin Chem* **47**: 2059-2061.

Poliak, P., Van Hoewyk, D., Oborník, M., Zíková, A., Stuart, K.D., Tachezy, J., *et al.* **(**2010) Functions and cellular localization of cysteine desulfurase and selenocysteine lyase in *Trypanosoma brucei*. *FEBS J* **277**: 383-393.

Rouault, T.A., and Tong, W.H. (2005) Iron-sulfur cluster biogenesis and mitochondrial iron homeostasis. *Nat Rev Mol Cell Biol* **6**: 345-351.

Saas, J., Ziegelbauer, K., von Haeseler, A., Fast, B., and Boshart, M. (2000) A developmentally regulated aconitase related to iron-regulatory protein-1 is localized in the cytoplasm and in the mitochondrion of *Trypanosoma brucei*. *J Biol Chem* **275**: 2745-2755.

Schneider, A. (2001) Unique aspects of mitochondrial biogenesi in trypanosomatids. *Int J Parasitol* **31**: 1403-1415.

Smid, O., Horáková, E., Vilímová, V., Hrdý, I., Cammack, R., Horváth, A., *et al.* **(**2006) Knock-downs of mitochondrial iron-sulfur cluster assembly proteins IscS and IscU down-regulate the active mitochondrion of procyclic *Trypanosoma brucei*. *J Biol Chem* **281**: 28679-28686.

Song, D., Tu, Z., and Lee, F.S. (2009) Human ISCA1 interacts with IOP1/NARFL and functions in both cytosolic and mitochondrial iron-sulfur protein biogenesis. *J Biol Chem* **284**: 35297-35307.

Stamatakis, A., Ludwig, T., and Meier, H. (2005) RAxML-III: a fast program for maximum likelihood-based inference of large phylogenetic trees. *Bioinformatics* **21**: 456-463.

Stechmann, A., Hamblin, K., Perez-Brocal, V., Gaston, D., Richmond, G.S., van der Giezen, M., *et al.* (2008) Organelles in *Blastocystis* that blur the distinction between mitochondria and hydrogenosomes. *Curr Biol* **18**: 580-585.

Tan, G., Lu, J., Bitou, J.P., Huang, H., and Ding, H. **(**2009) ISA/SufA paralogs are required for the [4Fe-4S] cluster assembly in enzyme sof multiple physiological pathways in *Escherichia coli* under aerobic growth conditions. *Biochem J* **420**: 463-472.

Tielens, A.G.M., and van Hellemond, J.J. (1998) Differences in energy metabolism between Trypanosomatidae. *Parasitol Today* **14**: 265-271.

Tokumoto, U., and Takahashi, Y. (2001) Genetic analysis of the isc operon in *Escherichia coli*

involved in the biogenesis of cellular iron-sulfur proteins. *J Biochem* **130**: 63-71.

Týč, J., Faktorová, D., Kriegová, E., Jirků, M., Vávrová, Z., Maslov, D.A., and Lukeš, J. (2010) Probing for primary functions of prohibitin in *Trypanosoma brucei*. *Int J Parasitol* **40**: 73-83.

Vinella, D., Brochier-Armanet, C., Loiseau, L., Talla, E., and Barras, F. (2009). Iron-sulfur (Fe/S) protein biogenesis: phylogenomic and genetic studies of A-type carriers. *PLoS Genet* **5**:e1000497.

Vondrušková, E., van den Burg, J., Zíková, A., Ernst, N.L., Stuart, K., Benne, R., and Lukeš, J. (2005) RNA interference analyses suggest a transcript-specific regulatory role for MRP1 and MRP2 in RNA editing and other RNA processing in *Trypanosoma brucei*. *J Biol Chem* **280**: 2429-2438.

Walter, J.C., Alvarez, S., Naponelli, V., Lara-Nunez, A., Blaby, I.K., Da Silva, V., *et al.* **(**2010) A role for tetrahydrofolates in the metabolism of iron-sulfur clusters in all domains of life. *Proc Natl Acad Sci USA* **107**: 10412-10417.

Wang, W., Huang, H., Tan, G., Si, F., Liu, M., Landry, P.A., *et al.* (2010) In vivo evidence for the iron binding activity of an iron-sulfur cluster assembly protein ISA in *Escherichia coli*. *Biochem J* (in press).

Wingert, R.A., Galloway, J.L., Barut, B., Foott, H., Fraenkel, P., Axe, J.L., *et al.* (2005) Deficiency of glutaredoxin 5 reveals Fe-S clusters are required for vertebrate haem synthesis. *Nature* **436**: 1035-1039.

Wohlgamuth-Benedum, J.M., Rubio, M.A.T., Paris, Z., Long, S., Poliak, P., Lukeš, J., and Alfonzo, J.D. (2009) Thiolation controls cytoplasmic tRNA stability and acts as a negative determinant for tRNA editing in mitochondria**.** *J Biol Chem* **284**: 23947-23953.

Wollenberg, M., Berndt, C., Bill, E., Schwenn, J.D., and Seidler, A. (2003) A dimer of the FeS cluster biosynthesis protein IscA from cyanobacteria binds a [2Fe2S] cluster between two protomers and transfers it to [2Fe2S] and [4Fe4S] apo proteins. *Eur J Biochem* **270**: 1662-1671.

Wu, G., Mansy, S.S., Hemann, C., Hille, R., Surerus, K.K., and Cowan, J.A. (2002) Iron-sulfur cluster biosynthesis: characterization of *Schizosaccharomyces pombe* Isa1. *J Biol Inorg Chem* **7**: 526-532.

Zheng, L., White, R.H., Cash, V.L., Jack, R.F., and Dean, D.R. (1993) Cysteine desulfurase activity indicates a role for NIFS in metallocluster biosynthesis. *Proc Natl Acad Sci USA* **90**: 2754-2758.

Zheng, L., Cash, V.L., Flint, D.H., and Dean, D.R. (1998) Assembly of iron-sulfur clusters. Identification of an iscSUA-hscBA-fdx gene cluster from *Azotobacter vinelandii*. *J Biol Chem* **273**: 13264-13272.

Figure Legends

Fig. 1. **Phylogenetic analysis of the Isa1/2 proteins**. Phylogenetic tree of a selection of 88 of Isa1 and Isa2 sequences representing their diversity. The tree shown was estimated from 108 aligned amino acids using the LG+G+F model with RAxML and MrBayes. Only bipartitions that received >50% ML bootstrap support are labelled with support values.

Fig. 2. Expression and localization of TbIsa proteins in procyclic *T. brucei*.

(**A**) Western blot analysis of TbIsa1 and TbIsa2 in total lysates (T) and purified mitochondrial (M) and cytosolic fractions (C). Mitochondrial RNA binding protein 2 (MRP2) and enolase were used as mitochondrial and cytosolic markers, respectively.

(**B, C**) Co-immunoprecipitation of TbIsa1 and TbIsa2. Mitochondrial fractions (M) obtained with digitonin fractionation were immunoprecipitated with affinity-purified rat polyclonal antibodies specific for TbIsa1 under physiological salt (**B**) or high salt conditions (C) (see Experimental procedures). Antibodies were coated on sheep anti-rat IgG immunomagnetic beads, and proteins in the collected immunoprecipitates were identified by Western blot analysis using affinity-purified antibodies specific for TbIsa1 and TbIsa2. Su represents the supernatant after binding with the immunomagnetic beads during procedures, and IP indicates the protein eluate from the immunomagetic beads. Protein size marker positions are indicated.

Fig. 3. TbIsa proteins are essential for growth of PF *T. brucei* and RNAi is specific for target TbIsa.

Growth inhibition following RNAi induction against TbIsa1 (**A**), TbIsa2 (**B**) and TbIsa1/2 (**C**). Cell numbers were measured using cell counter. The numbers of non-induced cells (squares; black line) and those after RNAi induction (diamonds; grey line) are indicated. The *y* axis is labeled by a log scale and represents the product of cell densities measured and total dilution. The curves are representatives of three cell lines from three rounds of experiments.

(**D**) TbIsa1 and TbIsa2 protein levels were analyzed by Western blot analysis in whole-cell extracts from wild types (WT) PF cells, non-induced (-) and RNAi induced single and double knock-downs 2 and 4 days of induction. Anti-enolase antibody was used as a loading control. Left and middle panels represent single TbIsa1 and TbIsa2 knock-down cells. Right panel represents the TbIsa1/2 double knock-down cells. Protein size marker positions are indicated.

Fig. 4. Biochemical consequences of RNAi-mediated down-regulation of TbIsa proteins in PF *T. brucei*. (**A**) The effect of RNAi against TbIsa1, TbIsa2 and TbIsa1/2 on the activity of the Fe-S cluster-containing cytosolic (left panel) and mitochondrial (right panel) aconitase. Enzymatic activities were measured in non-induced cells (grey columns) and cells 2 and 4 days of RNAi induction (black columns). Specific activities are shown as percentage of activities in non-induced cells; the mean and the SD values represent the average of three experiments.

(**B**) Enzymatic activities of Fe-S cluster-containing fumarase are shown same as in (A).

(**C**) Enzymatic activities of Fe-S cluster-containing mitochondrial succinate dehydrogenase (=complex II) are shown same as in (A).

(**D**) Enzymatic activities of Fe-S cluster lacking threonine dehydrogenase are shown same as in (A).

(**E**) The purity of cellular fractions (cyto – cytosolic; mito – mitochondrial) obtained from non-induced (-) cells, as well as from TbIsa1, TbIsa2 and TbIsa1/2 knock-downs 2 and 4 days upon RNAi induction was verified by enolase and MRP2, which served as cytosolic and mitochondrial markers, respectively.

Fig. 5. ROS is elevated but iron is not in mitochondria of PF *T. brucei* with down-regulated TbIsa1/2.

(**A**) Radical oxygen species (ROS) accumulate in the TbIsa1/2 double knock-downs 4 days of RNAi induction (black line), as compared to the respective non-induced cells (grey line). The

measurement was done by incubating the cells in the presence of 5 μg/ml dihydroethidium for 30 min, followed by analysis by flow cytometry. Representative data from three independent experiments are shown.

(**B**) The concentration of iron was quantified by the ferene method (see Experimental procedures) in the mitochondrion of the non-induced cells (Tet-) and cells, in which TbIsa1/2 were ablated (4 days of RNAi induction) (Tet+). Representative data from three independent inductions are shown.

Fig. 6. TbIsa proteins are non-essential for BF *T. brucei*.

(**A**) TbIsa1 is much less abundant in BF 920 cells (BF) than in the PF 29-13 cells (PF), as shown by Western blot analysis with the α-TbIsa1 antibodies. Cytosolic enolase was used as a loading control.

(**B**) Growth curves of TbIsa1/2 double knock-down cells over 7 days showed that RNAi silencing altered only very weekly the growth of the BF cells. Cells were diluted every 24 hours to a density of 10^5 cells/ml and their numbers were measured using cell counter. The numbers of non-induced cells (squares; black line) and those after RNAi induction by the addition of 1 μg/ml tetracycline (diamonds; grey line) are indicated. The *y* axis is labeled by a log scale and represents the product of cell densities measured and total dilution.

(**C**) Northern blot analysis of total RNA extracted from non-induced (-) cells, and from TbIsa2 knock-down cells 48 hours of RNAi induction (+). TbIsa2 gene was used as a probe. The position of specific double stranded RNA is indicated. As a control, the gel was stained with ethidium bromide to visualize rRNA bands (lower panel).

(**D**) Western blot analysis of total protein extracted from non-induced (-) cells, and from TbIsa1 knock-down cells 4 days of RNAi induction (+). The anti-TbIsa1 antibody followed the target protein, the anti-enolase antibody was used as a loading control.

Fig. 7. Human Isa proteins are expressed, processed and efficiently targeted into the mitochondrion of PF *T. brucei*.

(**A**) Western blot analysis of the expression and targeting of the HA_3-tagged human frataxin signal peptide lead hIsa1. Total cell lysate (T), and mitochondrial (M) and cytosolic (C) fractions isolated by digitonin fractionation were probed with antibody against the HA_3 tag. Anti-MRP2 and anti-enolase antibodies were used as mitochondrial and cytosol-specific markers, respectively.

(**B**) Western blot analysis of the expression, processing and targeting of hIsa2. Total cell lysate (T), and mitochondrial (M) and cytosolic (C) fractions isolated by digitonin fractionation were probed with antibody against human Isa2. Anti-MRP2 and anti-enolase antibodies were used as mitochondrial and cytosol-specific markers, respectively. The pre-processed and processed forms of hIsa2 are indicated with an arrow and arrowhead, respectively.

(**C**) Western blot analysis of the expression and processing of hIsa2 in various PF cell lines. Total cell lysate was obtained from 29-13 PF cells (A), TbIsa1 knock-downs (B), TbIsa2 knock-downs (C), TbIsa1 knock-downs transfected with pFC4-hIsa2 (D), TbIsa2 knock-down transfected with pABPURO-hIsa1 (E), TbIsa2 knock-down transfected with pFC4-hIsa2 (F), TbIsa1/2 double knock-down transfected with pABPURO-hIsa1 (G), TbIsa1/2 double knock-down transfected with pFC4-hIsa2 (H), TbIsa1/2 double knock-down transfected with both pABPURO-hIsa1 and pFC4-hIsa2-HA (I). The pre-processed and processed forms of hIsa2 are indicated with an arrow and arrowhead, respectively. The HA_3-tagged hIsa2 appears as a heavy band labeled with an asterisk. Anti-enolase antibody was used as loading control.

Fig. 8. Biochemical consequences of TbIsa knock-downs (cross) rescued with human Isa proteins in PF *T. brucei*.

(**A**) Enzymatic activity of aconitase was measured in mitochondrial fractions obtained with digitonin fractionation. Its activity in 29-13 PF cells represents 100% (white column), its activities are depleted in TbIsa2 (A) and TbIsa1/2 double knock-downs (B) 2 and 4 days upon RNAi inductions (gray columns). Activity in the following cells is shown in black columns: TbIsa2 knock-downs transfected with pFC4-hIsa2 (C), TbIsa1/2 double knock-down transfected with pFC4-hIsa2 (D), TbIsa1/2 double knock-down transfected with pABPURO-hIsa1 and pFC4-hIsa2 (E), TbIsa1 knock-down transfected with pFC4-hIsa2 (F), TbIsa2 knock-down transfected with pABPURO-hIsa1 (G), TbIsa1 knock-down transfected with pABPURO-hIsa1+HA_3 (H); the mean and the SD values represent the average of three measurements.

(**B**) Enzymatic activity of Fe-S cluster-containing mitochondrial fumarase. Cell lines are same as in (A).

Fig. 9. Biochemical consequences of TbIsa1/2 double knock-down rescued with *B. hominis* Isa2 proteins in PF *T. brucei*.

Enzymatic activities of fumarase (**A**), aconitase (**B**), and succinate dehydrogenase (**C**) were measured in the digitonin isolated mitochondria. A given activity in 29-13 PF cells represents 100% (white column). Activity in non-induced TbIsa1/2 cells (1/2-) and the same cell transfected with BhIsa2 (Bh-) is shown in grey columns. Activity in RNAi-induced TbIsa1/2 (1/2+), TbIsa1/2 with an empty pABPURO vector (V+), and those transfected with BhIsa2 (Bh+) after 4 days of RNAi induction is shown in black columns; the mean and the SD values represent the average of three measurements.

Fig. 10. Consequences of Iba57 ablation on TbIsa1, aconitase and sensitivity to oxidative stress of PF *T. brucei*.

(**A**) Western blot analysis of TbIsa1 in mitochondrial extracts from wild type (WT) PF, non-induced (-) and RNAi-induced Iba57 knock-downs (+) (6 days of induction) reveals destabilization of TbIsa1 upon the ablation of Iba57. Mitochondrial MRP1 was used as loading control.

(**B**) Western blot analysis of Tbaconitase in mitochondrial extracts from wild type (WT) PF, non-induced (-) and RNAi-induced Iba57 knock-downs (+) (6 days of induction) reveals destabilization of Tbaconitase upon the ablation of Iba57. MRP2 was used as loading control.

(**C**) Altered sensitivity to oxidative stress upon depletion of Iba57. Non-induced cells and those 6 days of RNAi induction were exposed to various concentrations of paraquat (in the range from 4^{-10} to 40 mM). After 44 hrs of incubation, resazurin was added to each culture and after 4 hrs fluorescence was measured to determine cell viability. Obtained data was analysed by GraphPad Prism software using nonlinear regression (curve fit) with sigmoidal dose-response analysis, and the EC_{50} was calculated. Depletion of Iba57 leads to 62x higher sensitivity to paraquat (EC_{50} = 17.93 μM) as compared to the non-induced cells (EC_{50} = 1.13 mM). The values shown are the means from two independent inductions.

Supplementary Figures

Suppl. Fig. 1. TbIsa1 and TbIsa2 cosediment in glycerol gradient.

Cleared lyzates from mitochondria hypotonically isolated from wild type cells were separated by sedimentation in 10 to 30% glycerol gradient. Even fractions from the gradients were run on SDS-PAGE gels, blotted and immunodecorated with polyclonal antibodies against TbIsa1, TbIsa2 and mitochondrial marker protein TbRGG1, and monoclonal antibodies against subunit KREL1 of the mitochondrial editosome.

Suppl. Fig. 2. Effect of TbIsa RNAi on other Fe-S cluster assembly proteins.

Expression level of cysteine desulfurase (Nfs1), metallochaperone (IscU) and frataxin were determined by Western blot analysis of whole cell lysates of the parental 29-13 cell line (WT), non-induced cells (-) and TbIsa1/2 double knock-down cells 2, 4 and 6 days of RNAi induction. Enolase was used as a loading control.

Suppl. Fig. 5. Mitochondrial membrane potential was alightlyaltered., and ROS is elevated in mitochondria of PF T. brucei with down-regulated TbIsa1 or TbIsa2. A. Inner membrane potential was measured by flow cytometry following incubation of non-induced (grey line) and RNAi-induced cells (black line) with TMRE (see Experimental procedures). B. Radical oxygen species (ROS) accumulate in the TbIsa1 and TbIsa2 single knock-downs 4 days of RNAi induction (black line), as compared to the respective non-induced cells (grey line). The measurement by flow cytometry was done by incubating the cells in the presence of dihydroethidium (see Experimental procedures). Representative data from three independent experiments are shown.).

Suppl. Fig. 4. TbIsa1, TbIsa2 and TbIba57 are non-essential for BF *T. brucei*, and TbIba57 has slight effect on cell growth upon depletion

(**A and B** Growth curves of TbIsa1(A) and TbIsa2 (B) single knock-down cells over 7 days showed that RNAi silencing did not alter the growth of the BF cells. Cells were diluted every 24 hours to a density of 10^5 cells/ml and their numbers were measured using cell counter. The numbers of non-induced cells (squares; black line) and those after RNAi induction (diamonds; grey line) are indicated. The *y* axis is labeled by a log scale and represents the product of cell densities measured and total dilution.

(C) Growth curves of non-induced and RNAi-induced PF cells. **(D)** Growth curves of non-induced and RNAi-induced BF cells. **(E)** Northern blot analysis of the PF (left panel) and BF cells (right panel). Total RNA was extracted from parental 29-13 PF cells (WT) (or 920 BF cells), non-induced (-) as well as cells 48 hrs of RNAi induction (+). The position of double stranded RNA synthesized following RNA induction is indicated by a arrow. As a loading control, the gel was stained with ethidium bromide to visualize rRNA bands (lower panels).

Suppl. Fig. 5. Growth of PF *T. brucei* TbIsa knock-downs expressing human Isa proteins is not rescued.

(**A**) Growth curve of TbIsa2 knock-down expressing human Isa2. (**B**) Growth curve of TbIsa1/2 double knock-down expressing human Isa1 and Isa2. (**C**) Growth curve of TbIsa1/2 double knock-down expressing human Isa2. (**D**) Growth curve of TbIsa1 knock-down expressing human Isa2. (**E**) Growth curve of TbIsa2 knock-down expressing human Isa1. The numbers of non-induced cells (squares; black line) and those after RNAi induction (diamonds; grey line) are indicated. The cells were cultivated as described in Fig 3. The *y* axis is labeled by a log scale and represents the product of cell densities measured and total dilution.

Suppl. Fig. 6. Growth of PF *T. brucei* TbIsa knock-downs expressing *Blastocystis* sp. Isa2 protein is partly rescued.

Growth curves of two genetically modified TbIsa1/2 double knock-down cell lines. Non-induced cells (full diamonds, black line) and RNAi-induced cells (full circles, grey line) are compared with RNAi-induced cells bearing empty pABPURO vector (empty diamonds, black and dotted line) or same cells bearing a vector constitutively expressing BhIscA2 (empty circles, grey and dotted line). The cells were cultivated as described in Fig. 3. The *y* axis is labeled by a log scale and represents the product of cell densities measured and total dilution.

Suppl. Fig. 7. Phylogenetic tree of Iba57. Distribution of the iba57 homologues among eukaryotic lineages. The tree shown was estimated from 296 aligned amino acids (71 taxa) using the LG+G+F model with RAxML. Support values are shown next to branches as maximum likelihood bootstrap support (LG+G+F model, RAxML)/posterior probability (LG+G+F model, MrBayes). Only bipartitions that received >50% ML bootstrap support are labelled with support values.

Suppl. Table 1. Sequences of used oligonucleotides.

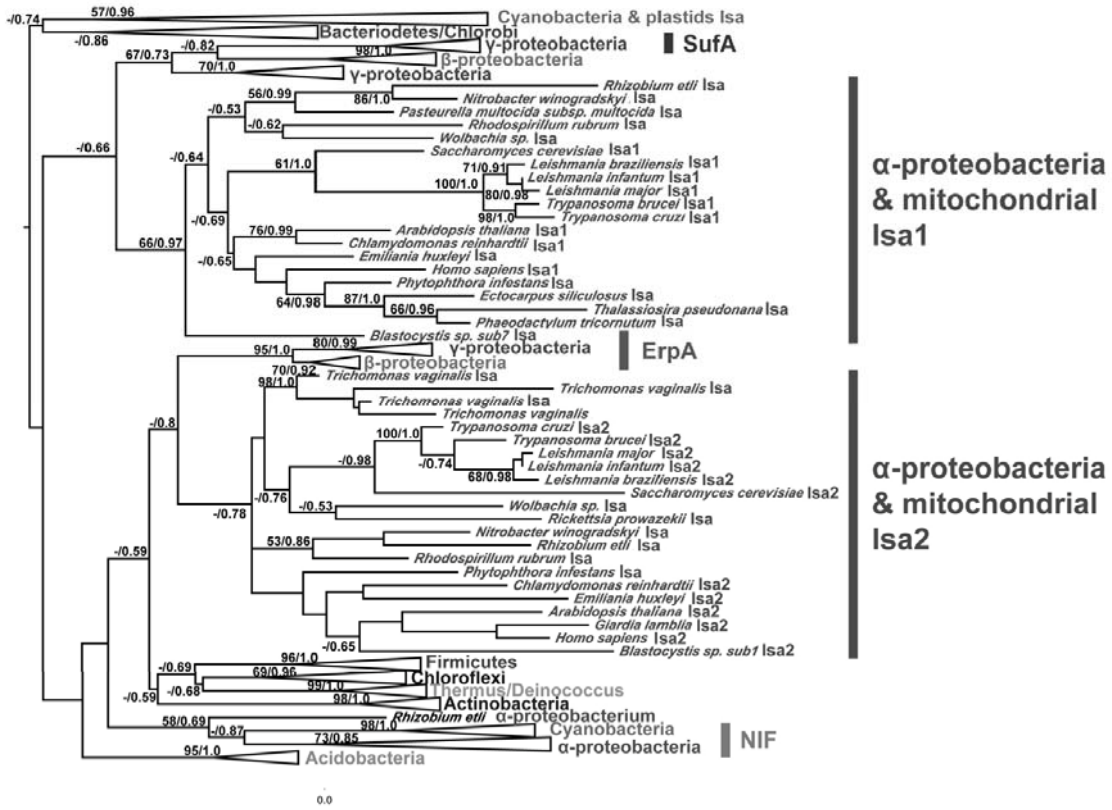

Fig. 1

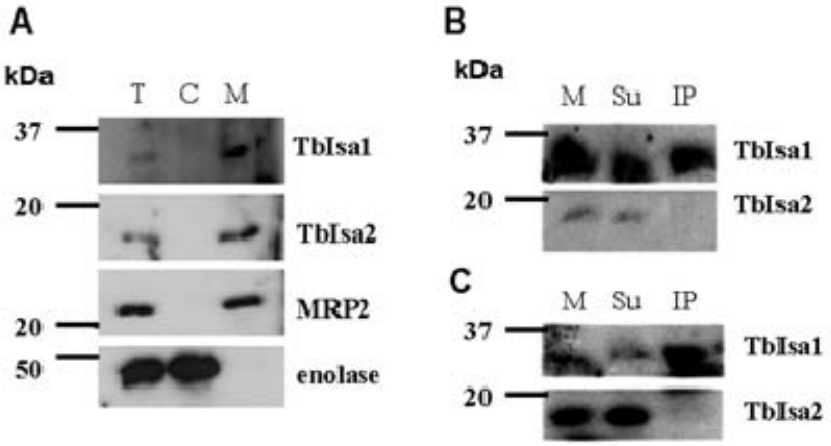
A
kDa
T C M
37
TbIsa1
20
TbIsa2
20
MRP2
50
enolase
B
kDa
M Su IP
37
TbIsa1
20
TbIsa2
C
M Su IP
37
TbIsa1
20
TbIsa2

Fig. 2

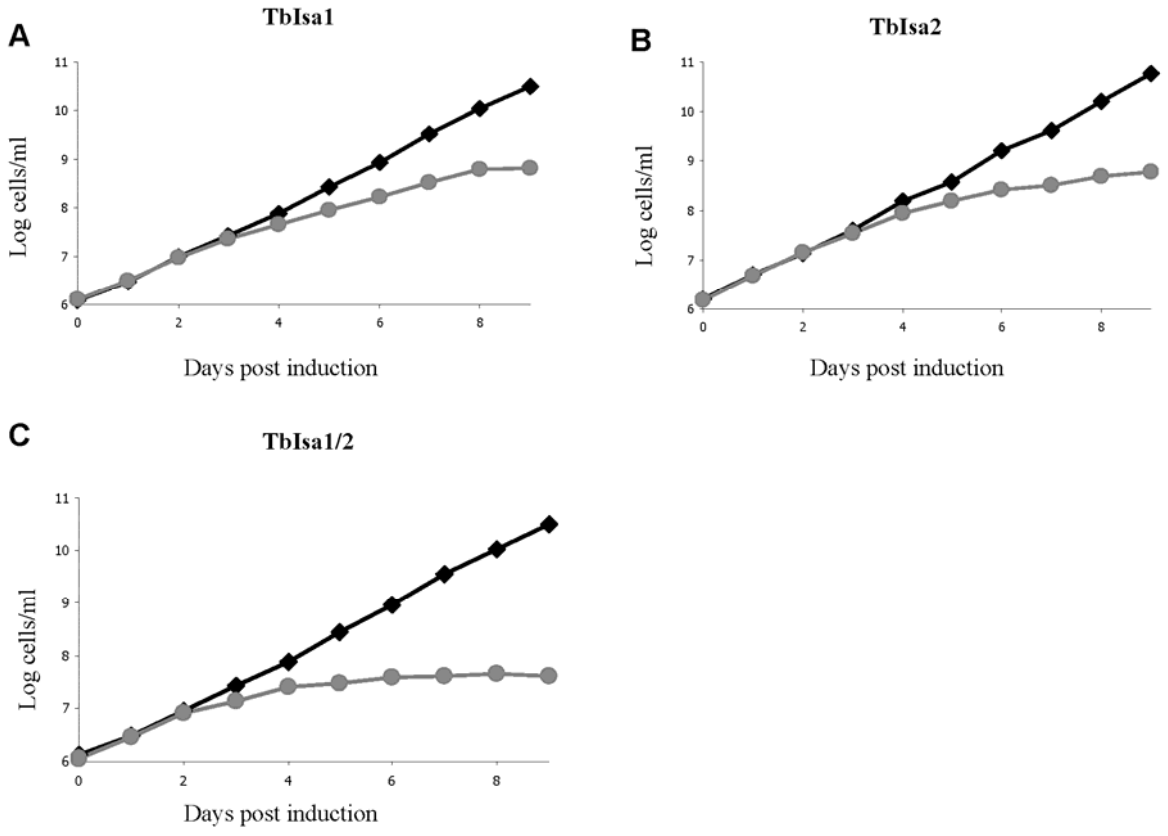
A
TbIsa1
Log cells/ml
Days post induction
B
TbIsa2
Log cells/ml
Days post induction
C
TbIsa1/2
Log cells/ml
Days post induction

Fig. 3

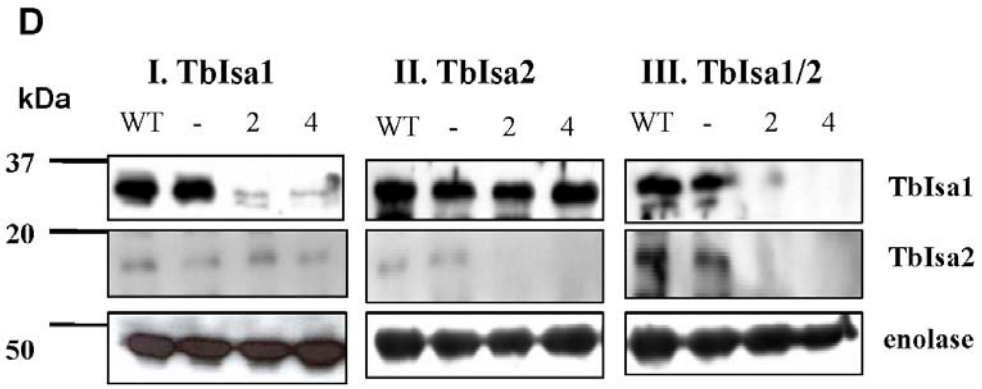
D
I. TbIsa1
II. TbIsa2
III. TbIsa1/2
kDa
WT - 2 4
WT - 2 4
WT - 2 4
37
20
50
TbIsa1
TbIsa2
enolase

Fig. 3

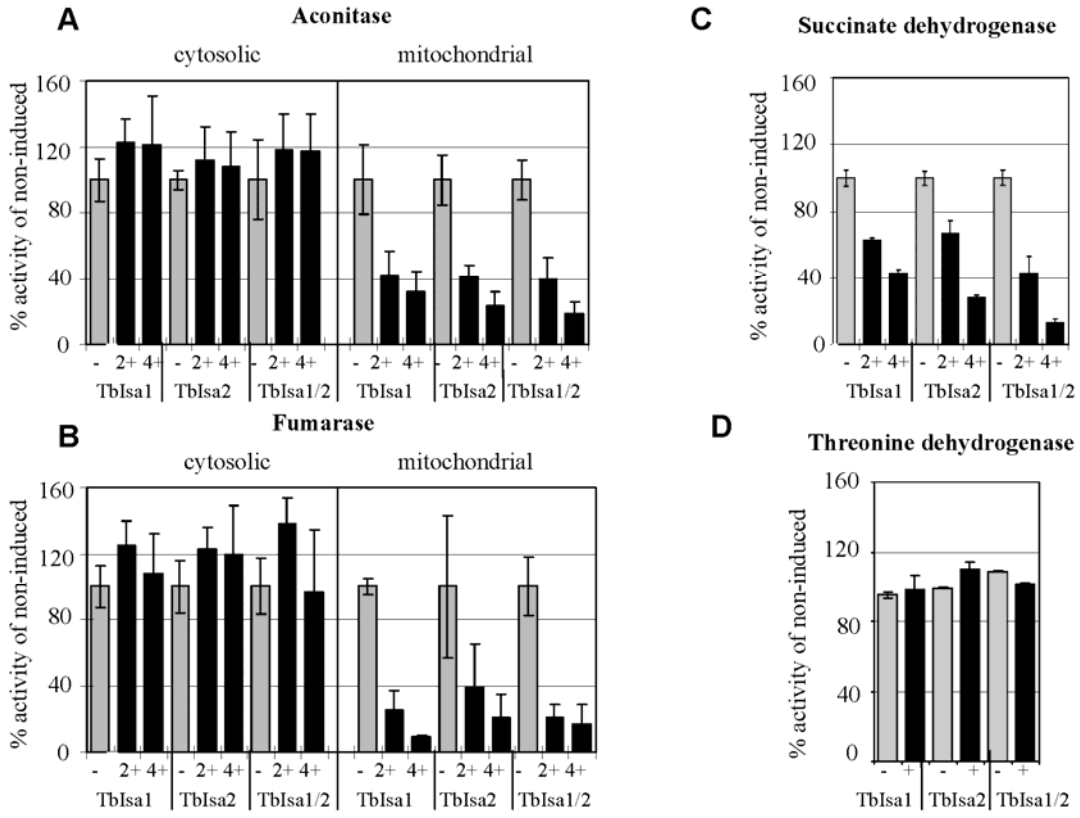
A
Aconitase
cytosolic
mitochondrial
% activity of non-induced
160
120
80
40
0
- 2+ 4+
TbIsa1
TbIsa2
TbIsa1/2
B
Fumarase
C
Succinate dehydrogenase
D
Threonine dehydrogenase
- +

Fig. 4

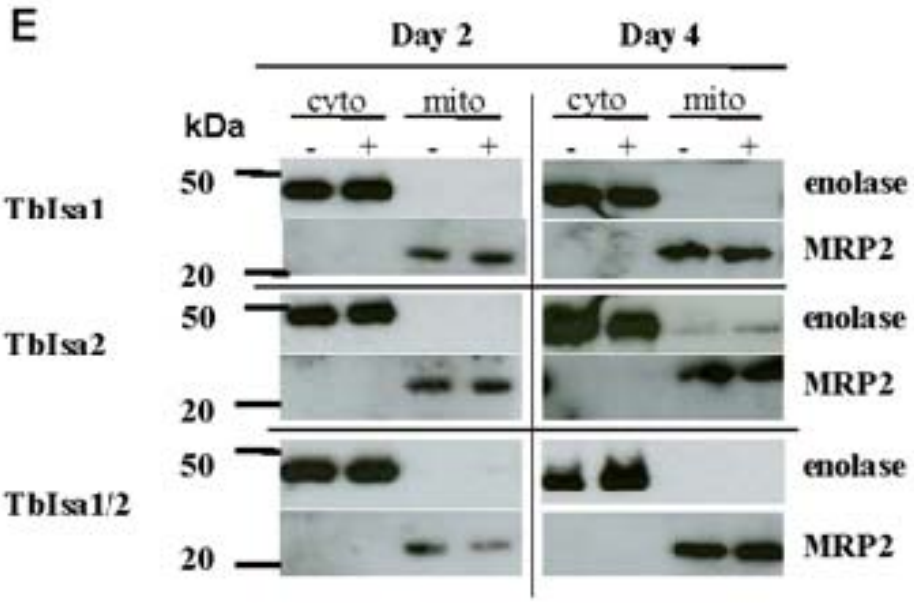
E
Day 2
Day 4
cyto
mito
cyto
mito
kDa
- + - + - + - +
TbIsa1
50
20
enolase
MRP2
TbIsa2
50
20
enolase
MRP2
TbIsa1/2
50
20
enolase
MRP2

Fig. 4

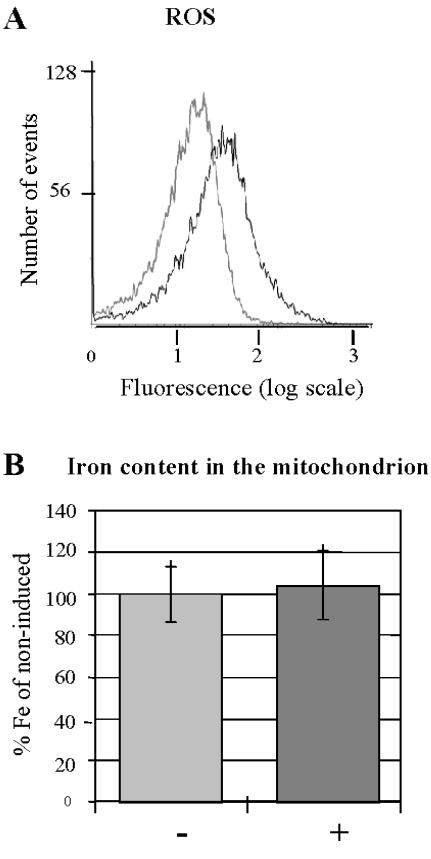
A
ROS
128
56
Number of events
0
1
2
3
Fluorescence (log scale)
B
Iron content in the mitochondrion
140
120
100
80
60
40
20
0
% Fe of non-induced
-
+

Fig. 5

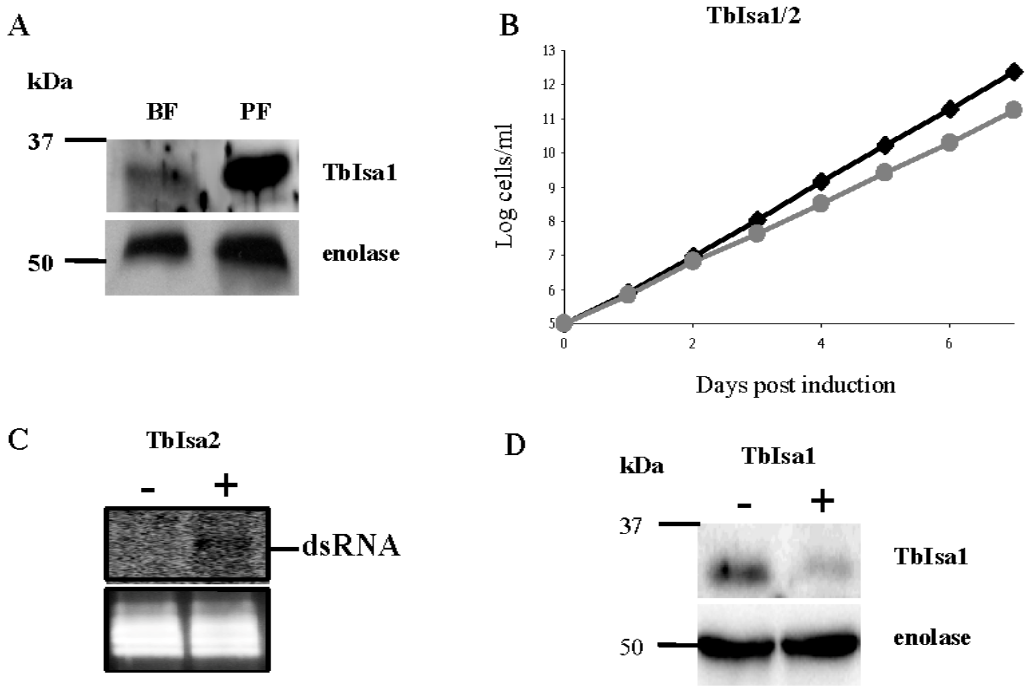
A
kDa
BF
PF
37
TbIsa1
50
enolase
B
TbIsa1/2
Log cells/ml
Days post induction
C
TbIsa2
-
+
dsRNA
D
kDa
TbIsa1
-
+
37
TbIsa1
50
enolase

Fig. 6

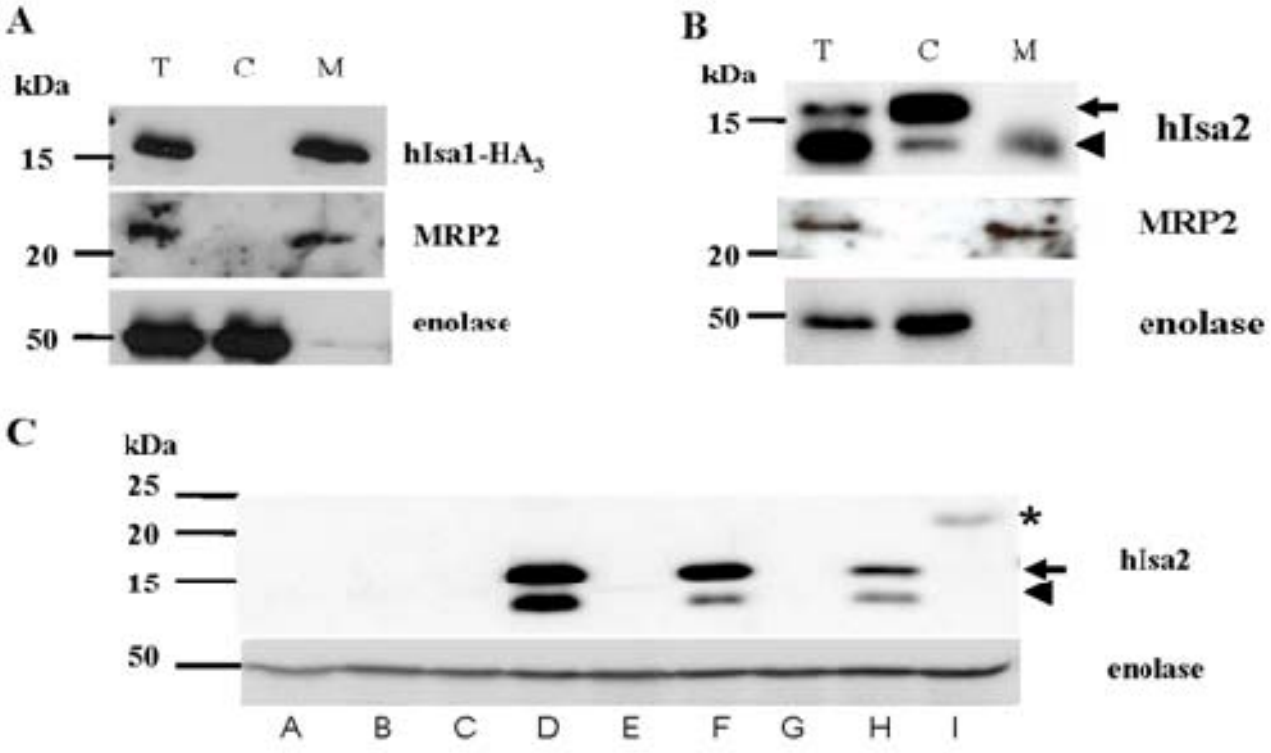
A
kDa
T
C
M
15
hIsa1-HA3
20
MRP2
50
enolase
B
kDa
T
C
M
15
hIsa2
20
MRP2
50
enolase
C
kDa
25
20
15
50
*
hIsa2
enolase
A
B
C
D
E
F
G
H
I

Fig. 7

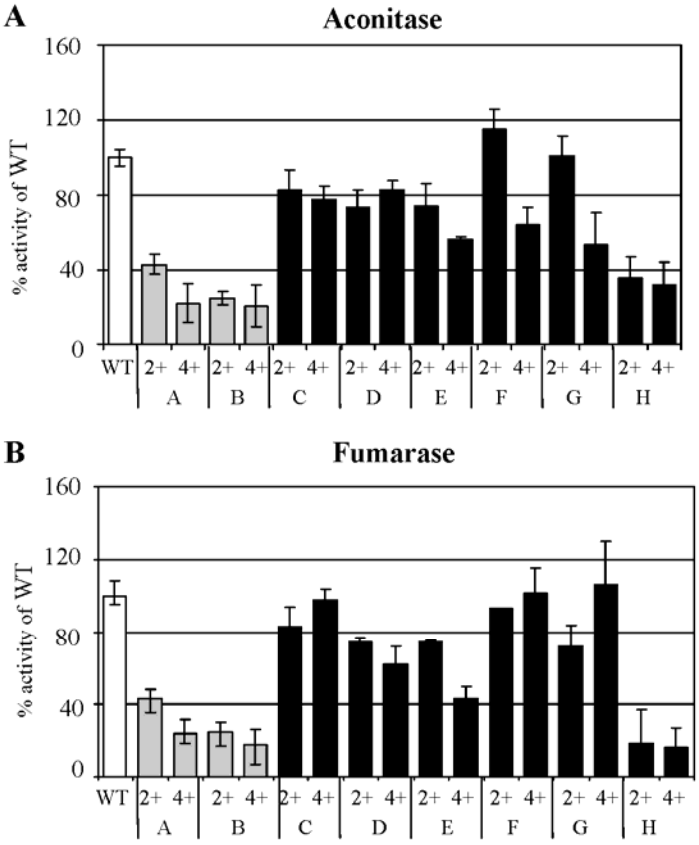
A
Aconitase
160
120
80
40
0
% activity of WT
WT
2+ 4+
A
B
C
D
E
F
G
H
B
Fumarase
160
120
80
40
0
% activity of WT

Fig. 8

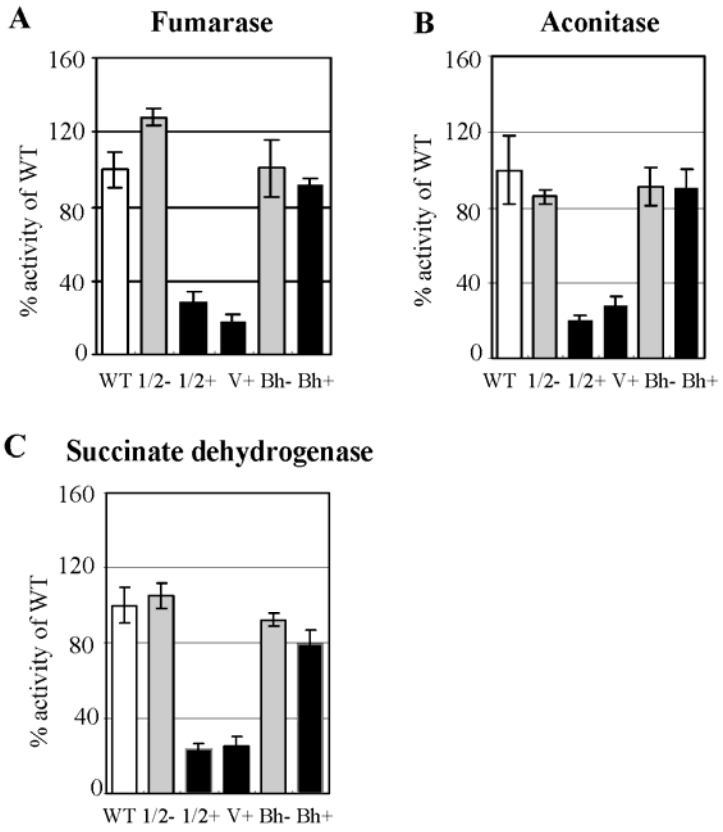
A
Fumarase
160
120
80
40
0
% activity of WT
WT 1/2- 1/2+ V+ Bh- Bh+
B
Aconitase
160
120
80
40
0
% activity of WT
WT 1/2- 1/2+ V+ Bh- Bh+
C
Succinate dehydrogenase
160
120
80
40
0
% activity of WT
WT 1/2- 1/2+ V+ Bh- Bh+

Fig. 9

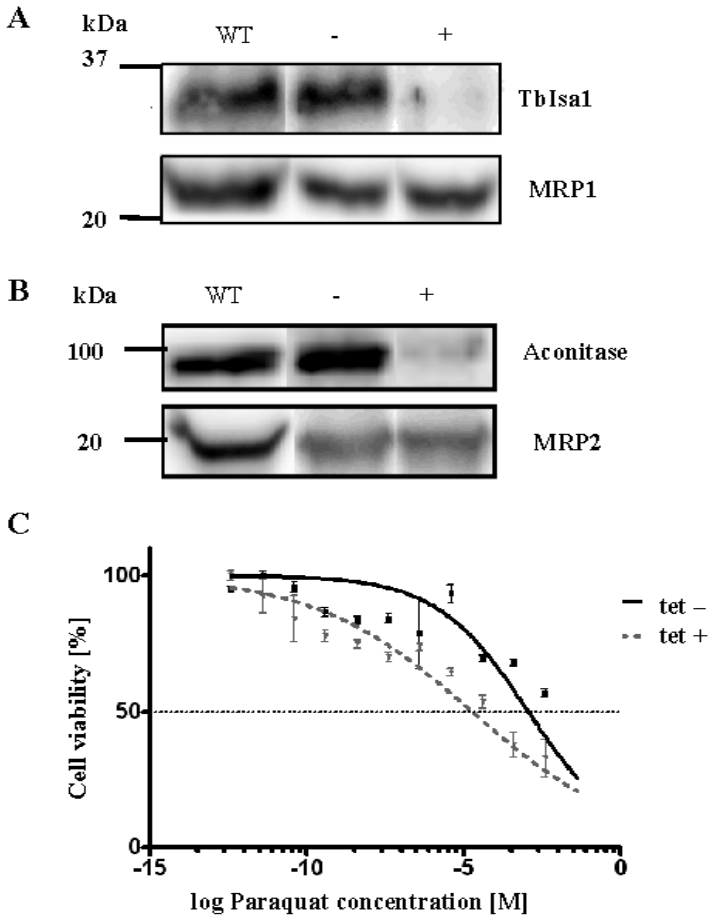

Fig. 10

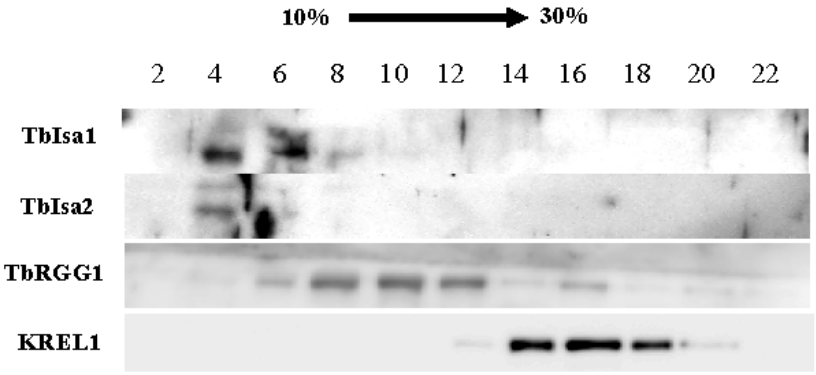

Suppl. Fig. 1

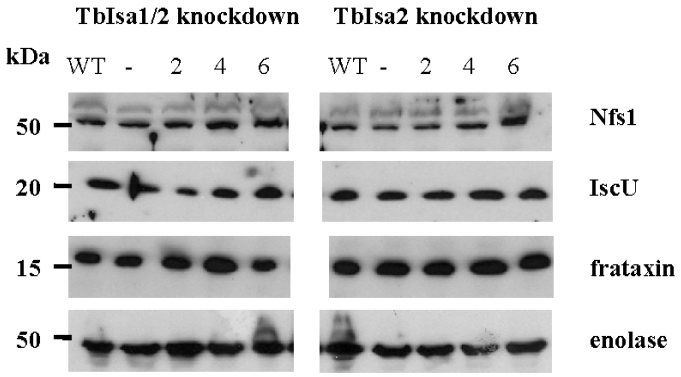

Suppl. Fig. 2

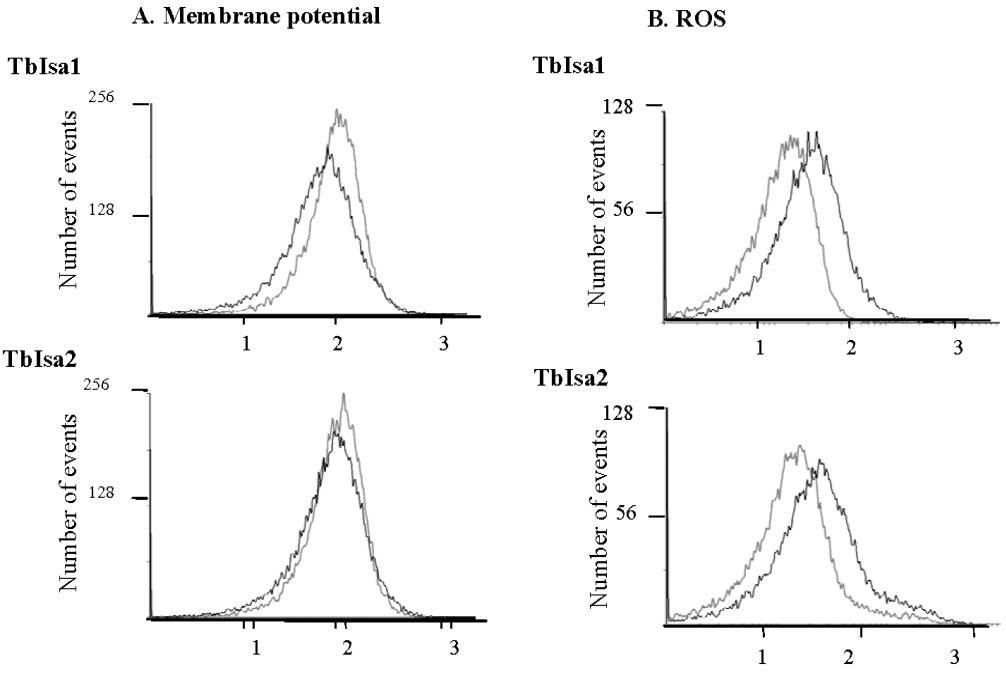

Suppl. Fig. 3

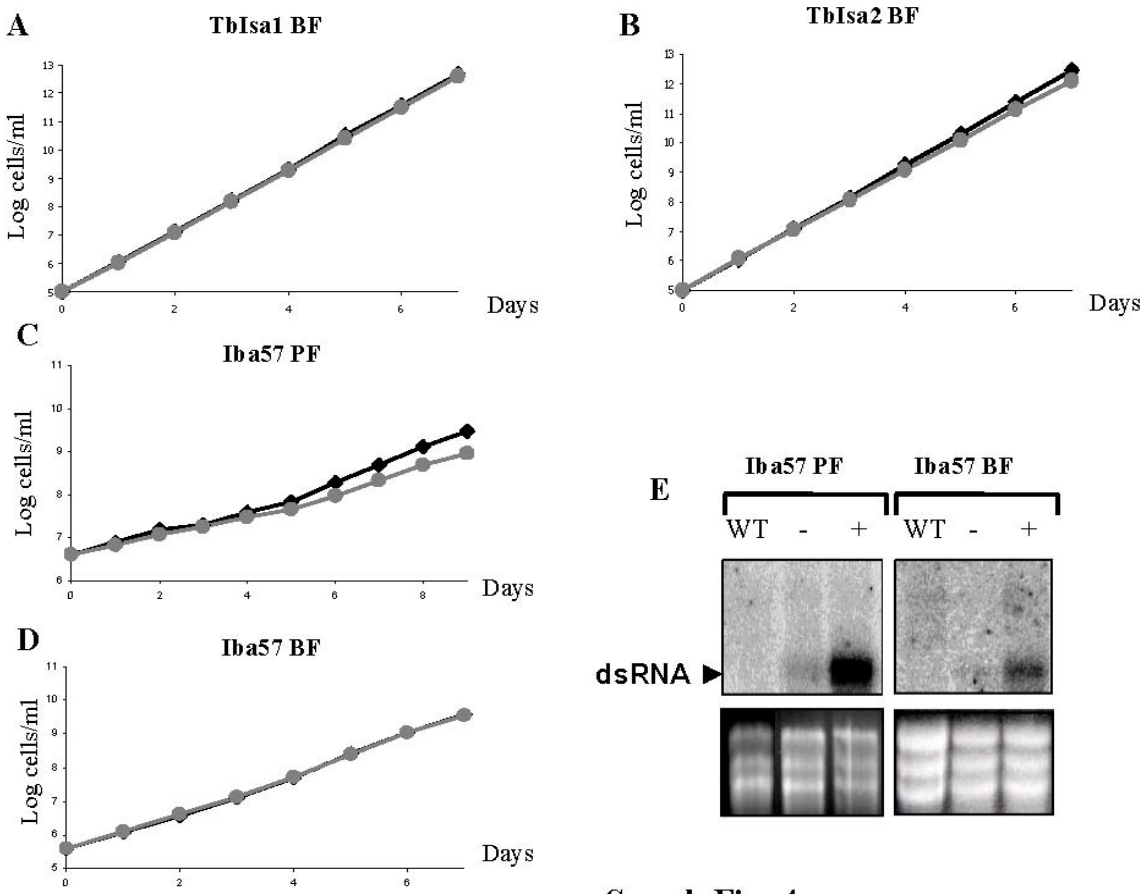

Suppl. Fig. 4

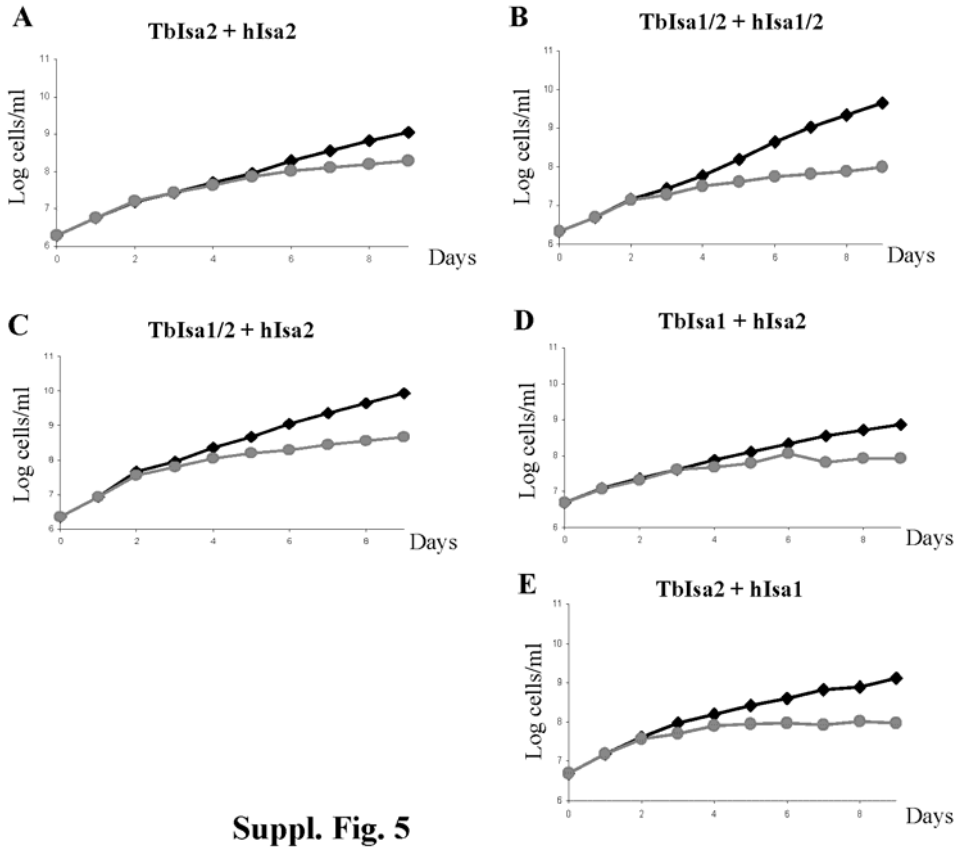

Suppl. Fig. 5

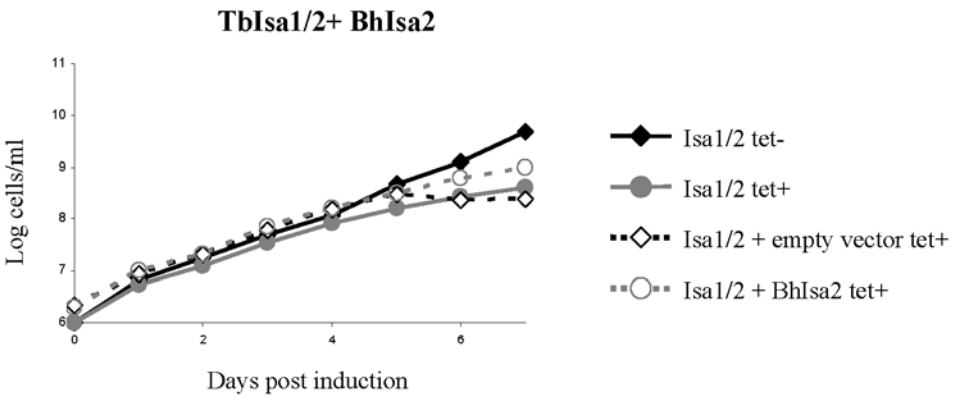

Suppl. Fig. 6

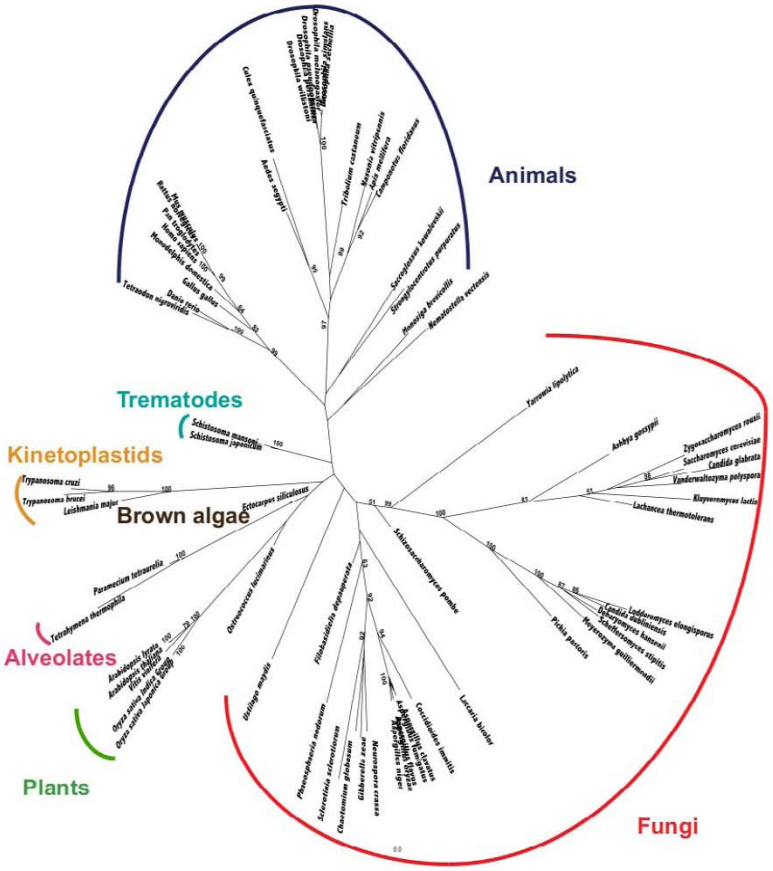

Suppl. Fig. 7

Table 1.

Oligonucleotides	Sequences (5' – 3') and used restriction sites	
Tblsa1-FP	gaagcttATGATGCGCTTCTTCGTATG	*HindIII*
Tblsa1-RP	gACTAGTGCCAGTTTCGTCACCTTTGC	*SpeI*
Tblsa2-FP	gctcgagATGCTGCGCACTTCCCTGTT	*XhoI*
Tblsa2-RP	gACTAGTTCACACCTTTTGCTGCTGCT	*SpeI*
Double-RP	gaagcttTCACACCTTTTG CTGCTGCT	*HindIII*
Tblsa1-FP/O	CACCATGCGCTTCTTCGTATG	
Tblsa1-RP/O	TCAAAGCTGCTCGTCAGCG	
hlsa1-R-FP	gGCTAGCatgtcggctt ccttagtccg	*NheI*
hFxn-hlsa2	GATATCatgtggactc tcgggcgccg	*EcoRV*
hFxn-hlsa2-M	tgcagcttcctcttgctcactgcgcggcggggcgtgcagg	
hlsa1-R-RP	gGGATCCtcaaatattaaagctttctc	*BamHI*
hlsa1-HA_3	gGGATCCaatattaaagctttctc	*BamHI*
hlsa2-R-FP	gAAGCTTatggctgccg cctgggggtc	*HindIII*
hlsa2-R-RP	gGGATCCtcaaagtttgatagagaaa	*BamHI*
BhlscA-F	CCCGGGCCATGGATGTTCCGCTTTTCTTCTGCGCTTG	*NcoI*
BhlscA-R	CGCGCGAAGCTTTTATTCGTAGGGGTTCGACGTCTTCG	*HindIII*
Tblba-F	CCTCGAGATGCGCAAGAAGTTAG	*XhoI*
Tblba-R	CGGATCCATGAGTACGGTGAG	*BamHI*